

1 Evolution of gene regulatory network topology and dorsal-ventral axis specification in  
2 early development of sea urchins (Echinoidea)

3

4 Short Title: Evolution of gene regulatory network topology in sea urchins

5

6 Eric M. Erkenbrack<sup>1\*,#a</sup>

7

8 <sup>1</sup>Division of Biology and Biological Engineering, California Institute of Technology,

9 Pasadena, California, United States of America

10 <sup>#a</sup>Current address: Department of Ecology and Evolutionary Biology, Yale University,

11 West Haven, Connecticut, United States of America

12

13 \* Corresponding Author

14 Email: [erkenbra@caltech.edu](mailto:erkenbra@caltech.edu) (EME), [eric.erkenbrack@yale.edu](mailto:eric.erkenbrack@yale.edu) (EME)

15

## 1 **Abstract**

2 Developmental gene regulatory networks (dGRNs) are assemblages of interacting  
3 regulatory factors that direct ontogeny of animal body plans. The hierarchical topology  
4 of these networks predicts that their nodes will evolve at different rates and  
5 consequently will bias the trajectories of embryonic evolution. To test this, detailed,  
6 comparative analyses of dGRNs that specify early, global embryonic domains are  
7 required. The most extensively detailed dGRNs have been documented for one of the  
8 two subclasses of extant sea urchins, the euechinoids. Remarkably, euechinoid dGRNs  
9 operating in early development show little appreciable change even though they  
10 diverged approximately 90 million years ago (mya). Therefore, to better understand the  
11 evolutionary dynamics of dGRNs, comparative microdissection must be undertaken for  
12 sea urchins that diverged deeper in geological time. Recent studies of cidaroids, the  
13 sister clade of euechinoid sea urchins, suggest that comparative analyses of their  
14 embryonic domain specification may prove insightful for understanding the evolutionary  
15 dynamics of dGRNs. Here, I report the spatiotemporal dynamics of 19 regulatory factors  
16 involved in dorsal-ventral patterning of non-skeletogenic mesodermal and ectodermal  
17 domains in the early development of *Eucidaris tribuloides*, a cidaroid sea urchin.  
18 Multiple lines of evidence indicate that deployment of ectodermal regulatory factors is  
19 more impervious to change than mesodermal regulatory factors in the sea urchin  
20 lineage and are supported by multiple lines of experimental evidence. Additionally,  
21 endogenous spatiotemporal expression data, intra-class reporter microinjections, and  
22 perturbation analyses of Nodal and Notch signaling allow the enumeration of numerous  
23 alterations to regulatory factor deployment since the divergence of echinoids. These

1 results provide a global view of early embryonic developmental processes in two clades  
2 that diverged at least 268.8 mya and show that the dGRNs controlling embryonic  
3 specification exhibit differential lability, supporting the hypothesis that the topologies of  
4 dGRNs bias rates of evolutionary change and alter the developmental evolutionary  
5 trajectories of embryogenesis.

## 6 **Author Summary**

7 Early in the development of an embryo, networks of genes are initiated to differentiate  
8 the rapidly dividing cells into distinct territories that will later serve specific functions.  
9 Sea urchins have revealed much about how this process unfolds. Recent studies have  
10 focused on one of the two modern lineages of sea urchins and have shown that these  
11 processes have not appreciably changed over the past 90 million years. I sought to  
12 determine if this trend extends over even larger evolutionary distances by investigating  
13 similar processes in a sea urchin from the second modern lineage, which is removed by  
14 268 million years of evolution. By revealing where and when these genes are expressed  
15 and interfering with common mechanisms of development in a distantly related sea  
16 urchin, I show that changes to these networks of genes have occurred at all levels of  
17 the network. Additionally, I present data that suggests that changes to these networks of  
18 genes occur disproportionately in certain embryonic territories, which may be true for  
19 early development for other groups of organisms as well.

## 20 **Introduction**

21 From egg to embryo, early bilaterian development is the transformation of a  
22 single cell, the fertilized egg, into a dynamic gastrulating embryo with multiple cell types

1 and embryonic domains. Integral to early development of a triploblastic bilaterian is the  
2 delineation of embryonic domains—endoderm, ectoderm, mesoderm—and their  
3 subdomains—dorsal, ventral, anterior, posterior, mesenchymal, etc. This partitioning  
4 sets the stage for specification of morphological features of the larva and/or adult.  
5 Asymmetrically distributed RNA and proteins in the egg provide the initial inputs into this  
6 process and thereby determine the spatial coordinates of domain formation [1, 2]. In the  
7 context of these maternal factors, zygotic transcription is initiated, and the interplay  
8 between the genomically encoded regulatory program and its output of regulatory  
9 factors, e.g. transcription factors and cell signaling pathways, delineates embryonic  
10 domains [3]. The deployment of evolutionarily conserved cohorts of transcription factors,  
11 or regulatory states, is the spatial readout of developmental gene regulatory networks  
12 (dGRNs) and provides each embryonic domain with its molecularly distinct and  
13 functional identity [4, 5].

14 The trajectories of change that can occur to developmental programs during  
15 evolution are affected both by the sequential unfolding of embryonic development and  
16 the hierarchical structure or topology of GRNs [6]. For example that certain nodes in  
17 GRNs will evolve at different rates would seem to follow from their inherent hierarchical  
18 architecture and would provide a powerful mechanistic explanation as to why constraint  
19 occurs in some developmental processes and evolutionary change has occurred in  
20 others [7]. However, despite the overt importance of the structure of developmental  
21 GRNs to effect change in developmental evolution in predictable ways, illustrative  
22 examples are scant in the literature. To address questions of the frequency and nature  
23 of change to dGRNs, the taxa sampled must be phylogenetically diverged enough to

1 have undergone significant change to dGRNs and phylogenetically close enough so  
2 that similarity of developmental programs will afford meaningful comparisons. Due to  
3 the cascading nature of early specification events and the rapid establishment of  
4 embryonic domains, early development is attractive in so far that it promises to provide  
5 fundamental insight into both its lineage-specific evolution and hierarchical change in  
6 developmental GRNs.

7         Sea urchins (class Echinodea) provide an excellent model system to study  
8 mechanisms of evolutionary change in early development. Specification of cell lineages  
9 and embryonic domains in sea urchin embryos depends on the canonical cleavage  
10 positions of their blastomeres [8, 9], thereby facilitating interpretation of mechanisms of  
11 spatial change. Also, a well-studied fossil record constrains the dating of evolutionary  
12 events [10] and has established that the sister subclasses of sea urchins—cidaroids  
13 and euechinoids—diverged from one another at least 268.8 million years ago (mya)  
14 [11]. And yet, relative to their conspicuously diverged adult body plans, early embryonic  
15 development in these two clades is strikingly similar [12]. This geologically ancient  
16 expanse combined with copious change of life history strategies in multiple sea urchin  
17 lineages provide a convenient framework, with experimental replicates, to investigate  
18 evolution and mechanisms of developmental programs [13]. For indirect developing sea  
19 urchins (taxa with feeding larval forms), morphological and developmental  
20 heterochronies exhibited by cidaroids and euechinoids have long been a topic of  
21 interest, but only recently have become the subject of molecular research [14-20].  
22 Research on the early development of euechinoids has brought into high resolution the  
23 players and molecular logic directing the global embryonic developmental GRN that

1 encompasses the varied embryonic domains and subdomains of the purple sea urchin  
2 *Strongylocentrotus purpuratus* [21-32]. Additionally, abundant comparative evidence  
3 exists for other euechinoid taxa, including *Lytechinus variegatus* [33-39] and  
4 *Paracentrotus lividus* [40-44]. Remarkably, although these three indirect-development  
5 euechinoid sea urchins diverged from one another approximately 90 mya [10, 45], very  
6 little appreciable change to developmental GRNs has been observed in their early  
7 development [46-48]. Two questions arise from this observation: (1) how deep in  
8 geological time does this early developmental constraint extend, and (2) does this  
9 apparent calcification of GRN circuitry extend to specification of all embryonic domains  
10 or merely to some? Answers to these questions would obtain fundamental insight into  
11 the lability and evolutionary dynamics of GRN topology and whether certain embryonic  
12 domains or subdomains have a greater propensity to change in early development than  
13 others. Such an analysis might also reveal the precise locations of and frequency in  
14 changes to GRN architecture over evolutionary time and would yield a more thorough  
15 understanding of the interplay of constraint and evolvability of early developmental  
16 programs.

17       Recently, studies of the cidaroid sea urchin *Eucidaris tribuloides* revealed that  
18 mesoderm specification in this clade is markedly different from that observed in  
19 euechinoids [12, 20, 49]. Spatiotemporal and perturbation analyses of endomesodermal  
20 formation in *E. tribuloides* arrived at the conclusion that deployment of mesodermal  
21 regulatory factors has diverged more than deployment of endodermal regulatory factors  
22 since the cidaroid-euechinoid divergence. These studies provide insight into  
23 developmental process at the vegetal pole and bring within reach a global embryonic

1 perspective that would afford a glimpse into rates of change to whole apparatus of  
2 developmental GRN throughout the early embryo. Here, I surveyed spatial and temporal  
3 expression patterns of non-skeletogenic mesodermal (NSM) and ectodermal regulatory  
4 factors in the cidaroid sea urchin *E. tribuloides* (Table 1). This study focused on dorsal-  
5 ventral (D-V; also called Aboral-Oral) patterning, which has consequences for both  
6 ectoderm and mesoderm. D-V axis specification is a well-documented process in the  
7 euechinoid GRN [48] and is a highly conserved developmental mechanism in  
8 deuterostomes [50, 51]. I present evidence that deployment of the primary regulatory  
9 factors specifying the sea urchin mesoderm have diverged substantially in indirect-  
10 developing echinoids. These alterations are overrepresented in specification of  
11 mesodermal SM and NSM subdomains. However ectodermal and endodermal domains  
12 and subdomains show a high degree of constraint relative to mesodermal domains.  
13 Spatiotemporal dynamics of regulatory factors involved in *E. tribuloides* D-V axis  
14 specification are essentially congruent with that of euechinoids, suggesting constraint  
15 on deployment of these factors for sea urchin taxa with indirect-developing, feeding  
16 larval life strategies. Thus, I argue that in early development of indirect-developing sea  
17 urchins unequal rates of change exist at specific nodes of early developmental GRNs. I  
18 enumerate specific examples of these changes at every level of GRN architecture. The  
19 lability of developmental GRNs supports the notion that change can occur at all levels of  
20 their hierarchy in early development and offers an in principle mechanistic explanation  
21 for observations of rapid change to nearly all components of developmental process in  
22 the development of direct developing, nonfeeding sea urchins [52-55]. These results  
23 suggest that, while early development is dependent on and constrained by cascading,

1 sequential specification events, deployment of early developmental GRNs in bilaterian  
 2 lineages may be biased towards alterations to specific embryonic domains or  
 3 developmental programs.

4 **Table 1. Regulatory factors examined in this study and their spatiotemporal**  
 5 **expression in *Eucidaris tribuloides*.**

Gene	Maternal/ zygotic	Onset of zygotic activation	Embryonic domain/spatial expression
<i>bra</i>	zygotic	early blastula	broad in early endomesoderm, then endodermal; perianal ectoderm and ventral ectoderm by mid-gastrula
<i>chordin</i>	zygotic	hatching blastula	center of presumptive ventral ectoderm, then expanding slightly to most of presumptive ventral ectoderm
<i>ese</i>	zygotic	64-cell	broad in anterior/animal ectoderm early; then by early gastrula broadly in NSM and restricted to presumptive ANE; later restricted in archenteron by mesenchyme gastrula and in ANE
<i>foxq2</i>	maternal	16-cell	broadly in anterior/animal ectoderm early; subsequently restricted to ANE/lateral ectoderm by late blastula
<i>gatac</i>	zygotic	swimming blastula	in SM by late blastula and later in NSM as well; later asymmetrical in NSM by gastrula stage
<i>gatae</i>	zygotic	early blastula	first broadly in endomesoderm, then cleared from SM; later in endoderm and asymmetrical in NSM by gastrula stage
<i>gcm</i>	zygotic	early blastula	first in SM; then in NSM and cleared from SM; later asymmetrical in NSM by early gastrula; presumptive dorsal
<i>gsc</i>	zygotic	hatching blastula	early spatial not observed; presumptive ventral ectoderm from late blastula onwards
<i>irxa</i>	zygotic	late blastula	in dorsal ectoderm extending from border of ANE to blastopore; by gastrula stage excluded only from ventral ectoderm and pre-oral ANE
<i>lefty</i>	zygotic	64-cell	early blastula distribution not observed; presumptive ventral ectoderm by late blastula and onwards
<i>msx</i>	zygotic	late blastula	pregastrular distribution not observed; dorsal lateral ectoderm by early gastrula
<i>nodal</i>	zygotic	64-cell	early blastula distribution not observed; center of presumptive ventral ectoderm at SB, expanding slightly to most of ventral ectoderm by gastrula stage
<i>not</i>	zygotic	early blastula	early blastula distribution not observed; presumptive ventral ectoderm, then also in presumptive ventral mesoderm by mesenchyme gastrula
<i>onecut</i>	maternal	64-cell	early blastula pattern not observed, by early gastrula in post-oral ventral ectoderm and expanding anteriorly in a band encompassing ventral ectoderm
<i>prox</i>	zygotic	hatching blastula	SM early and subsequently in NSM; broadly in mesoderm by mid-gastrula
<i>scl</i>	zygotic	swimming blastula	SM early and subsequently in NSM; partially restricted in mesoderm by mesenchyme gastrula
<i>tbx2/3</i>	maternal	64-cell	early blastula distribution not observed; presumptive dorsal ectoderm by late blastula; later in dorsal lateral ectoderm as well as dorsal archenteron



1

## 2 **Results**

### 3 **Dynamics of ectodermal D-V axis regulatory states in the** 4 **cidaroid *E. tribuloides***

5         In euechinoids, numerous regulatory factors direct segregation of ectoderm into a  
6 diverse set of regulatory states [48, 56, 57]. *Nodal*, a member of the activin subfamily of  
7 the transforming growth factor- $\beta$  (TGF- $\beta$ ) family of signaling molecules, is a critical  
8 factor in establishing dorsal-ventral (D-V) polarity in sea urchins [37, 40]. *Nodal* directly  
9 regulates, among others, *nodal* (itself), *not*, *lefty* and *chordin* [42, 58]. In *E. tribuloides*,  
10 zygotic transcription of *nodal*, *not* and *lefty* begins by early blastula stage (Figure 1A, 1B,  
11 1C). In contrast, transcriptional activation of *chordin* is delayed by at least 5 hours from  
12 this initial cohort, indicative of an intermediate regulator between *nodal* and *chordin* in *E.*  
13 *tribuloides* (Figure 1A, 1E). From 17 hpf to 40 hpf, spatial expression of *nodal* is  
14 observed in a well-defined region in the ventral ectoderm (VE) that expands slightly as  
15 gastrulation proceeds (Figure 1A1-1A4, Figure S1). Unlike *nodal*, the spatial distribution  
16 of its targets is not solely restricted to a small field of cells in the VE. *Lefty* (also known  
17 as Antivin), an antagonist of *nodal*, exhibits a broader pattern of expression that, by 50  
18 hpf, expands into the ventral side of the archenteron (Figure 1B1-1B4, Figure S1).  
19 Similarly, *chordin* transcripts are detected in VE throughout early *E. tribuloides*  
20 development (Figure 1E1-1E4, Figure S1). The homeobox gene *not*, known to play a  
21 role directly downstream of *nodal* in euechinoid D-V ectodermal and mesodermal  
22 polarization [29, 59], was observed spatially in VE during gastrulation, and later extends

1 vegetally towards the perianal ectoderm and is observed in the archenteron (Figure  
2 1C1-1C4, Figure S1). While I do not present the spatial distribution of the critical Nodal-  
3 responsive regulatory factor *bmp2/4* here, qPCR timecourse data indicate that *bmp2/4*  
4 is upregulated with the *nodal-not-lefty* cohort (Figure S2). In euechinoids, the *bmp2/4*  
5 ligand is a direct target of Nodal and is translocated across the embryo to the dorsal  
6 side, where it upregulates dorsal ectoderm (DE) specification genes such as *tbx2/3* [40,  
7 60, 61]. In *E. tribuloides*, *tbx2/3* is transcriptionally active very early with the *nodal-not-*  
8 *lefty* cohort. *Tbx2/3* exhibits spatial expression from late blastula stage onwards that is  
9 complementary to VE genes (Figure 1D1-1D4). By mid-gastrula stage, *tbx2/3* is also  
10 expressed in the archenteron and much later, by 70 hpf, is expressed in the bilateral  
11 clusters of cells synthesizing the larval skeleton (Figure S1), which is similar to the  
12 spatial expression in two euechinoids with notably interesting heterochronic differences  
13 [62, 63]. Lastly, the Forkhead family transcription factor *foxq2* is sequentially restricted  
14 to and specifically expressed in embryonic anterior neural ectoderm (ANE) territory in  
15 deuterostomes [64]. In euechinoids, *foxq2* restriction to ANE is a crucial component of  
16 D-V axis specification, setting the anterior boundary of VE by restricting expression of  
17 *nodal* [25, 57]. In *E. tribuloides*, *foxq2* exhibited an expression pattern consistent with  
18 observations in euechinoids and other deuterostomes, suggesting conserved roles for  
19 this gene in ANE and D-V specification (Figure 1F, Figure S1).

20

21 **Fig 1. Spatiotemporal dynamics of six regulatory factors in *E. tribuloides* suggest**  
22 **conserved deployment of ectodermal dorsal-ventral embryonic domains in**  
23 **echinoids.** Visualization of mRNA transcripts revealed by whole mount in situ

1 hybridization, and estimates of absolute mRNA transcript abundance determined by  
2 qPCR during first 35 hours post fertilization (hpf). Individual data points are light grey.  
3 Blue data points represent the mean at that particular timepoint. (A1) Temporal  
4 dynamics of *nodal*. (A2-A5) *Nodal* spatial distribution is restricted to a small field of cells  
5 in the ventral ectoderm (VE) up to early-mid gastrula stage. (B1) Temporal dynamics of  
6 *lefty*. (B2-B5) *Lefty* spatial distribution is restricted to a small field of cells in VE. (C1)  
7 Temporal dynamics of *not*. (C2-C5) *Not* spatial distribution is first detected in a similar  
8 field of cells as *nodal* and *lefty*; however, the domain of *not* subsequently expands by 28  
9 hpf where it is seen in the ventral side of the archenteron, where non-skeletogenic  
10 mesoderm (NSM) and endoderm are being segregated. By 40 hpf, the spatial domain of  
11 *not* extends from anterior neural ectoderm to the perianal ectoderm, is clearly seen in  
12 NSM, and was not detected in endodermal lineages. (D1) Temporal dynamics of *tbx2/3*.  
13 (D2-D5) Spatial distribution of *tbx2/3* at 17 hpf is detected broadly in dorsal ectoderm  
14 and later extends from the perianal ectoderm to lateral AE, but not past the embryonic  
15 equator. (E1) Temporal dynamics of *chordin*. (E2-E5) Spatial distribution of *chordin* is  
16 first observed in a few cells in VE at 17 hpf and subsequently expands to extend from  
17 the perianal ectoderm to ANE. (F1) Temporal dynamics of *foxq2*. (F2-F5) *Foxq2* spatial  
18 distribution is detected very early in development and is spatially restricted to anterior  
19 ectoderm by 17 hpf.

20

21 **Fig S1. Spatial expression of regulatory factors involved in dorsal-ventral (D-V)**  
22 **axis formation in *E. tribuloides*, including the dorsal ectoderm transcription factor**  
23 ***msx*.** Additional whole mount in situ hybridization images of selected timepoints for (A1-

1 A6) *bra*, (B1-B8) *chordin*, (C1-C8) *foxq2*, (D1-D6) *lefty*, (E1-E4) *msx*, (F1-F3) *nodal*,  
2 (G1) *not*, and (H1-H4) *tbx2/3*.

3

4 **Fig S2. Temporal expression dynamics of four ectodermal regulatory factors in *E.***

5 ***tribuloides*.** qPCR timecourses of (A) *bmp2/4*, (B) *emx*, (C) *hesC* and (D) *msx*.

6

7 **Dynamics of ciliated band regulatory states in the cidaroid *E.***

8 ***tribuloides***

9 Free-feeding, indirect-developing sea urchins possess a single neurogenic  
10 ciliated band (CB) early in development that circumnavigates the larval ventral face and  
11 facilitates feeding and locomotion [65]. This structure has undergone frequent  
12 modification in the lineages leading to modern sea urchins, viz. in planktotrophic larvae  
13 [66]. In euechinoids *gooseoid* (*gsc*), *onecut* and *irxa* contribute to the geometric  
14 patterning of CB formation [30, 42, 67]. In euechinoids, *gsc* is expressed in VE and is  
15 directly downstream of *nodal* signaling on the ventral side of the embryo [42]. *onecut*  
16 (also known as *hnf6*) is a ubiquitous, maternally deposited factor that is restricted to the  
17 boundary of VE and DE, at which lies progenitor CB territory; and *irxa* is expressed  
18 exclusively in DE downstream of *tbx2/3* [42, 68]. In the cidaroid *E. tribuloides*, *gsc* is  
19 zygotically expressed with the *nodal-not-lefty* cohort by 12 hpf and is specifically  
20 expressed in VE (Figure 2A, Figure S3). *Onecut* is also a maternally deposited factor in  
21 *E. tribuloides*; early *onecut* spatial expression was difficult to interpret, as staining was  
22 only observed much later in development in a restricted band of cells encircling the VE.  
23 The spatial dynamics of *onecut* in *E. tribuloides* is quite remarkable, however, insofar

1 that whole-mount *in situ* hybridization (WMISH) timecourse revealed that its activation  
2 unfolds slowly and in a sequential manner that begins in the progenitor field of post oral  
3 CB and subsequently extends in a narrow band of 4-8 cell diameters towards progenitor  
4 pre oral CB (Figure 2B, Figure S3). This observation is in stark contrast to that in  
5 euechinoids, in which *onecut* is observed to be ubiquitously expressed early and later  
6 delimited to the CB territory by transcriptional repressors in the VE and DE [30, 69]. *Irx*  
7 initiates zygotic expression at mid-blastula stage (~14 hpf) in *E. tribuloides*, and by 28  
8 hpf is observed broadly in DE (Fig 2C). Unlike in euechinoids, *irxa* is broadly distributed  
9 in DE—much more so than *tbx2/3*—indicating that it is likely broadly activated in the  
10 ectoderm and repressed in VE and ANE. The spatial distributions of *gsc*, *onecut* and  
11 *irxa* are highly suggestive of a conserved regulatory apparatus that spatially restricts CB  
12 to the boundary of VE and DE. To test for this conservation, I assayed a series of  
13 endogenous and site-directed mutagenesis *onecut* BACs from *S. purpuratus* by  
14 microinjection [67]. Remarkably, a BAC that has been shown to recapitulate the  
15 endogenous *S. purpuratus onecut* expression pattern faithfully expressed reporter GFP  
16 in the CB of *E. tribuloides* (Figure S4). Further, a BAC harboring mutated repressor  
17 sites for the ventral repressor *gsc* repeatedly exhibited ectopic expression in VE of *E.*  
18 *tribuloides* (Figure S4). Taken together, the early specification of CB regulatory factors  
19 suggests divergence of initial activation and spatial distributions of *onecut* and *irxa* and  
20 is consistent with conserved circuitry of *gsc*. Later, *E. tribuloides* CB patterning exhibits  
21 congruence with spatial expression patterns and circuitry observed in euechinoids,  
22 suggesting stage-specific constraint during larval morphogenesis.  
23

1 **Fig 2. Spatiotemporal dynamics of three regulatory factors in *E. tribuloides***  
2 **suggest conserved spatial distribution of ciliary band embryonic domain in**  
3 **euechinoids.** Visualization of mRNA transcripts revealed by whole mount in situ  
4 hybridization, and estimates of absolute mRNA transcript abundance determined by  
5 qPCR during first 35 hours post fertilization (hpf). Individual data points are light grey.  
6 Blue data points represent the mean at that particular timepoint. (A1) Temporal  
7 dynamics of *gooseoid* (*gsc*). (A2,A3) Spatial distribution of *gsc* at 22 hpf to 32 hpf is  
8 observed exclusively in ventral ectoderm (VE). (B1) Temporal dynamics of *onecut*.  
9 (B2,B3) By 40 hpf *onecut* is detected in the future post oral ciliary band and is initiated  
10 in a band moving from the posterior to the anterior. (C1) Temporal dynamics of *irxa*.  
11 (C2,C3) At 28 hpf, *irxa* is detected in dorsal ectoderm (DE) and extends from the  
12 vegetal endodermal domains to anterior neural ectoderm. By 40 hpf *irxa* is seen  
13 extending anteriorly at the boundary of DE and VE.

14

15 **Fig S3. Spatial expression in *E. tribuloides* of regulatory factors involved in**  
16 **euechinoid ciliary band restriction.** Additional whole mount in situ hybridization  
17 images of selected timepoints for (A1-A9) *gsc*, (B1-B9) *onecut*, and (C1-C5) *irxa*.

18

19 **Fig S4. Expression dynamics in *E. tribuloides* of GFP reporter BACs harboring**  
20 **the regulatory locus of *S. purpuratus onecut* suggest conservation of geometric**  
21 **positioning circuitry of ciliary band in echinoids .** (A) Table showing reporter  
22 analysis of spatial expression of five different *S. purpuratus* GFP BACs in *E. tribuloides*.  
23 The BACs were previously utilized to analyze the *cis*-regulatory dynamics of *onecut*

1 spatial distribution in *S. purpuratus* (Barsi and Davidson, 2016). (B) BAC reporter 1,  
2 which harbors mutations to all known *cis*-regulatory modules (CRMs), showed an  
3 absolute reduction of all reporter expression. (C, D) BAC reporters 2 and 3, which  
4 harbor mutated enhancer CRMs, showed reduced reporter expression both in terms of  
5 percent embryos exhibiting reporter activity and in the number of cells with reporter. (E)  
6 BAC Reporter 4, which harbors mutations to the dorsal and ventral ectodermal  
7 repression CRMs, increases the percent of embryos that show reporter expression in  
8 the ventral ectoderm, as well as normal reporter expression in the ciliary band. (F) BAC  
9 Reporter 5, which harbors the unperturbed, wild-type locus of *S. purpuratus onecut*,  
10 faithfully exhibits reporter GFP in the ciliary band domain of *E. tribuloides*.

11

## 12 **Dynamics of non-skeletogenic mesoderm regulatory states** 13 **in the cidaroid *E. tribuloides***

14 Non-skeletogenic mesoderm (NSM) in euechinoids arises at the vegetal plate  
15 from early cleavage endomesodermal precursors and gives rise to four different cell  
16 types: blastocoelar cells, pigment cells, circumesophageal cells and coelomic pouch  
17 cells [70]. Experimental observations indicate that euechinoids completely rely on  
18 presentation of Delta ligand in the adjacent SM to upregulate NSM regulatory factors in  
19 veg2 endomesodermal cells [34, 71, 72]. As gastrulation begins, euechinoid NSM has  
20 already become segregated into dorsal NSM and ventral NSM in response to Nodal  
21 signaling from VE [29, 73]. Mesodermal patterning in *E. tribuloides* also depends on  
22 Notch signaling, though by restricting SM fate to the micromere-descendants and,  
23 strikingly, not affecting the early expression of *gcm*, a regulatory factor involved in NSM

1 segregation and pigment cell specification [20]. In *E. tribuloides*, *ese* and *gcm* are early  
2 euechinoid NSM regulatory factors that are zygotically activated at late cleavage/early  
3 blastula stage (Figure 3A, 3D). In contrast to *S. purpuratus* spatial distribution, *ese* in *E.*  
4 *tribuloides* is observed both in the ANE and the NSM simultaneously (Figure 3A1-3A4,  
5 Figure S5) [74]. Indeed, very early in development *ese* is exclusively in animal  
6 blastomeres and later becomes zygotically expressed in NSM progenitors at the vegetal  
7 pole (Figure S5). In NSM, *ese* expression first occurs broadly just prior to the onset of  
8 gastrulation and is subsequently restricted to one side of the archenteron (Figure 3A1-  
9 3A4). After gastrulation begins, *gcm* is expressed transiently in ventral and dorsal NSM,  
10 and by 28 hpf is restricted to a cluster of cells just below the tip of the archenteron  
11 (Figure 3D1-3D4). Later this expression is seen solely on one side of the archenteron  
12 as *gcm*-positive cells ingress rapidly into the blastocoel at 36 hpf (Figure S5). In contrast  
13 to its spatial expression in euechinoids and similar to its expression in asteroids [75, 76],  
14 *gcm* in *E. tribuloides* is upregulated in the ectoderm at late blastula/early gastrula stage  
15 (Figure S5). While I cannot definitively preclude the possibility that these *gcm*-positive  
16 cells are mesodermal in origin, all observations of and experimental data on *E.*  
17 *tribuloides* supports the notion that SM is the first mesodermal lineage to ingress at 28  
18 hpf. The data presented here are at least 6 hours prior to this initial ingression event  
19 and are highly supportive of the hypothesis that *gcm* is activated in the ectoderm at the  
20 onset of gastrulation. Directly downstream of *gcm* in euechinoids is *gatae* [29]. In *S.*  
21 *purpuratus*, *gatae* is observed in endomesoderm early in development [77]. In *E.*  
22 *tribuloides* NSM, *gatae* is expressed throughout the endomesoderm at the time of SM  
23 ingression (~28 hpf) and later is observed restricted to one side near the tip of the



1 archenteron, as well as in the second wave of ingressing mesenchyme (Figure 3C1-  
2 3C4). *Gatac* (*gata1/2/3*), *prox* and *scl*, all of which are ventral NSM genes in  
3 euechinoids [29], come off the baseline at similar times in *E. tribuloides* and are  
4 detectable in a few cells at the base of the vegetal pole by 18 hpf by WMISH (Figure  
5 S5). Of these three genes, *scl* was the first to show D-V NSM polarity followed by *gatac*  
6 (Figure 3B1-3B4, 3F1-3F4). Surprisingly, by 36 hpf *prox* did not exhibit an expression  
7 pattern that clearly indicated D-V polarity (Figure 3E1-3E4; Figure S5), suggesting that  
8 either *prox* is a general mesodermal regulatory factor in *E. tribuloides* or it is spatially  
9 restricted later in its development.

10

11 **Fig 3. Spatiotemporal dynamics of six regulatory factors in *E. tribuloides* suggest**

12 **divergent deployment and specification of non-skeletogenic mesoderm domains**

13 **in echinoids.** Visualization of mRNA transcripts revealed by whole mount in situ

14 hybridization, and estimates of absolute mRNA transcript abundance determined by

15 qPCR during first 35 hours post fertilization (hpf). Individual data points are light grey.

16 Blue data points represent the mean at that particular timepoint. (A1) Temporal

17 dynamics of *ese*. (A2-A5) *Ese* is detected primarily in non-skeletogenic mesoderm

18 (NSM) but also in anterior neural ectoderm. By 28 hpf, *ese* is observed at the tip of the

19 archenteron and is asymmetrically polarized in NSM. (B1) Temporal dynamics of *gatac*.

20 (B2-B5) At 28 hpf *gatac* is expressed throughout the mesoderm and does not show

21 polarity. By 36 hpf, *gatac* is detected in ingressing cells and is polarized at the tip of the

22 archenteron. (C1) Temporal dynamics of *gatae*. (C2-C5) *Gatae* is detected throughout

23 the endomesoderm at 28 hpf. Later at 36 hpf *gatae* is cleared from progenitor foregut

1 endodermal domains and is expressed at the blastopore, in ingressing mesenchymal  
2 cells and at the tip of the archenteron, where it is polarized. (D1) Temporal dynamics of  
3 *gcm*. (D2-D5) As gastrulation begins *gcm* is expressed broadly in NSM; however by 28  
4 hpf it exhibits stark polarity in a field of cells that resides basal to the tip of the  
5 archenteron. *Gcm* is also observed in a few ectodermal cells at the time of primary  
6 mesenchymal ingression. (E1) Temporal dynamics of *prox*. (E2-E5) *Prox* spatial  
7 distribution is observed throughout NSM at 28 hpf. By 36 hpf it is expressed in  
8 ingressing mesenchymal cells and polarity is not yet observed. (F1) Temporal dynamics  
9 of *scl*. (F2-F5) Spatial distribution of *scl* is observed throughout NSM at 22 hpf. At 28 hpf  
10 it is expressed in ingressing mesenchyme and throughout NSM, where it is polarized.  
11 Orange asterisks denote position of archenteron.

12

13 **Fig S5. Spatial expression of euechinoid non-skeletogenic mesodermal**  
14 **regulatory factors in *E. tribuloides*, including pregastrular timepoints.** Additional  
15 whole mount in situ hybridization (WMISH) images of selected timepoints for (A1-A12)  
16 *ese*, (B1-B6) *gatac*, (C1-C4) *gatae*, (D1-D6) *gcm*, (E1-E6) *prox*, (F1-F4) *scl*.  
17 Additionally, double WMISH is reported for (G1,G2) *gcm* and *ese*, (H1,H2) *gcm* and  
18 *alx1*, and (I1,I2) *ets1* and *tbrain*.

19

20 These data on spatial dynamics of NSM regulatory factors suggest that there  
21 exist numerous regulatory states in the anterior archenteron. To provide some clarity,  
22 double fluorescent WMISH (dfWMISH) indicated this was indeed the case. Previous  
23 observations suggested that *E. tribuloides* mesodermal domains broadly express *ets1/2*

1 and *tbrain* [20], and dfWMISH confirmed this result (Figure S5I1, S5I2). Within this  
2 broad *ets1/2-tbrain* domain, three regulatory states are identified (Figure S5G-S5I): (1)  
3 ventrally localized *ets1/2*, *tbrain* and *ese*; (2) dorsally localized *ets1/2*, *tbrain*, and *gcm*;  
4 and (3) an anteriorly localized micromere-descendant regulatory state at the tip of the  
5 archenteron of *ets1/2*, *tbrain*, *ese* and *alx1*. These early mesodermal partitions are  
6 superficially consistent with those seen in euechinoids, as *ese* is restricted to ventral  
7 NSM and *gcm* to dorsal NSM [29]. However, the regulatory states expressed in these  
8 mesodermal domains are very different, and in *E. tribuloides* it is clear from the  
9 preceding data that the archenteron harbors multiple NSM regulatory states, the  
10 sequential of which is markedly different from that in euechinoids.

## 11 **Effects of perturbation of D-V axis specification on** 12 **ectodermal regulatory factors in *E. tribuloides***

13 The spatiotemporal data presented thus far are highly suggestive that D-V axis  
14 specification, as well as gastrular CB formation, in *E. tribuloides* is consistent with  
15 similar processes in euechinoids and that NSM specification has ostensibly diverged.  
16 To establish differences in the topology of these developmental GRNs, perturbation  
17 experiments disrupting initial inputs into D-V axis specification were conducted. In  
18 euechinoids, the primary molecular event responsible for animal-vegetal (A-V) axis  
19 polarity is nuclearization of  $\beta$ -catenin in micromere nuclei at the vegetal pole, and,  
20 unexpectedly, these experiments showed that perturbation of A-V axis formation  
21 disrupted D-V axis specification [33, 35]. One mechanism underlying the crosstalk of  
22 these two deuterostome specification events was found to be restriction of *foxq2* to  
23 ANE, as its presence in VE blocked *nodal* transcription [25]. To test for this GRN

1 linkage, I overexpressed dn-Cadherin RNA in *E. tribuloides* to block nuclearization of  $\beta$ -  
2 catenin at the vegetal pole. As in euechinoids, this perturbation led to upregulation of  
3 *foxq2*, whereas *nodal* and its euechinoid downstream components of D-V axis GRN  
4 circuitry—e.g. *bmp2/4*, *not*, and *tbx2/3*—were strongly downregulated (Figure 4A). This  
5 result suggests that the molecular crosstalk between and GRN topology of  $\beta$ -  
6 catenin/TCF, *foxq2* and *nodal* are conserved between euechinoid and cidaroid  
7 echinoids.

8

9 **Fig 4. Perturbation of dorsal-ventral axis formation in *E. tribuloides* reveals**  
10 **conserved and divergent aspects of regulatory factor deployment in echinoids.**

11 Disruption of dorsal-ventral (D-V) specification was achieved by overexpression of  
12 cadherin mRNA (MOE) and culturing embryos in the presence of the alk4/5/7 small  
13 molecule inhibitor SB431542. (A1) Cadherin MOE affects Nodal and its downstream  
14 targets. Change in Ct (ddCt) values relative to internal control is listed on the y-axis.  
15 When cadherin is overexpressed in *E. tribuloides*, *foxq2* is not substantially cleared and  
16 *nodal* and its targets are strongly downregulated. (B1-B3) Effect of SB431542 on  
17 embryonic morphology of *E. tribuloides*. At 120 hpf, *Eucidaris* shows two triradiate  
18 skeletal rods extending anteriorly and ventrally. When cultured in the presence of 15  $\mu$ M  
19 SB431542, *E. tribuloides* embryos show dorsal radialization and exhibit serial loci of  
20 spiculogenesis (black arrows). (C1) Quantitative effect of SB431542 on expression of  
21 30 *E. tribuloides* regulatory factors as revealed by qPCR. Change in Ct (ddCt) is show  
22 on the y-axis. Two timepoints from two independent replicates are shown. Regulatory  
23 factors are listed on the x-axis and font color designates their embryonic domain: black,

1 anterior neural ectoderm; blue, dorsal ectoderm; green, ventral ectoderm; yellow,  
2 endoderm; red, mesoderm.

3

4 Next, I aimed to determine the spatiotemporal effects of perturbation of D-V  
5 specification by culturing *E. tribuloides* embryos in the presence of SB43152, a small  
6 molecule antagonist of the TGF- $\beta$  (Nodal) receptor Alk4/5/7 [78]. At four days post  
7 fertilization, these embryos exhibited strong dorsalization, archenterons that failed to  
8 make contact with VE, and supernumerary skeletal elements (Figure 4B). Quantitative  
9 PCR (qPCR) analysis at four different timepoints in *E. tribuloides* development showed  
10 strong downregulation of VE regulatory factors *chordin*, *gsc*, *lefty*, *nodal* and *not* (Figure  
11 4C). This result was confirmed spatially by WMISH for mRNA transcripts of *chordin*,  
12 *nodal* and *not* (Figure 5A, 5B). Another critical VE regulatory factor is the secreted TGF-  
13  $\beta$  ligand *bmp2/4*. This gene was clearly not affected to the same degree as the  
14 aforementioned cohort of VE factors (Figure 4C). This result is strikingly different from  
15 the strong downregulation of *bmp2/4* observed in the euechinoid *P. lividus* when it was  
16 cultured in the presence of SB431542 or when injected with Nodal morpholino (MASO)  
17 [40, 42]. Lastly for VE, this quantitative assay does not indicate disturbance in the  
18 regulation of *brachyury* (*bra*) and *foxa*, two euechinoid stomodeum (larval mouth)  
19 regulatory factors strongly downregulated upon Nodal perturbation in euechinoids  
20 (Figure 4C) [42, 79]. However, there is a clear heterochrony in the onset of *bra* and *foxa*  
21 in VE of *E. tribuloides* as stomodeum-specific genes such as these are not activated in  
22 VE until, at least for *brachyury*, around 36 hpf in *E. tribuloides* development (Figure S1).

1 Notably, *foxa* expression was never observed in the *E. tribuloides* stomodeum up to 40  
2 hpf.

3

4 **Fig 5. Spatial effect of perturbation of dorsal-ventral axis formation on expression**  
5 **of selected ectodermal, mesodermal and ciliary band regulatory factors.** (A) At 28  
6 hpf expression of *chordin*, *nodal* and *not* are completely extinguished. Whereas *gcm* is  
7 regularly restricted to one side of the archenteron, in the presence of SB431542 it  
8 exhibits expression throughout the archenteron. In the ectoderm, expression *tbx2/3*  
9 expands from dorsal ectoderm (DE) into ventral ectoderm in the presence of the  
10 inhibitor. (B) At 40 hpf, *chordin*, *nodal* and *not* are not detected. *Gcm* fails to be  
11 restricted to one side of the archenteron. *Tbx2/3*, which is normally expressed in DE  
12 and the dorsal side of the archenteron, is now expressed in a concentric band nearer  
13 the blastopore than the equator. (C) The ciliary band marker *onecut* is normally  
14 observed in a band of cells between the boundaries of DE and VE. However, in the  
15 presence of SB431542, *onecut* is expressed in an equatorial band that is 6-10 cell  
16 diameters across.

17

18 On the dorsal side, a striking difference is the effect of this treatment on  
19 regulatory factor *tbx2/3*. In euechinoids, *tbx2/3* is downstream of *bmp2/4* ligand, which  
20 diffuses from VE to DE [60, 61, 80]. Treatment of *P. lividus* embryos with SB431542  
21 inhibitor completely and specifically extinguishes *tbx2/3* in DE while not interfering with  
22 its SM expression [42]. In *E. tribuloides*, qPCR data suggest SB431542 inhibitor has no  
23 effect on *tbx2/3* regulation (Figure 4C). However, when I assayed *tbx2/3* by WMISH, its

1 spatial distribution expanded into VE (Figure 5A, 5B). Similarly, whereas in *E.*  
2 *tribuloides* qPCR data indicate strong downregulation of the DE regulatory factor *irxa*  
3 (Figure 4C), its domain of expression expanded into VE in *P. lividus* embryos upon  
4 SB431542-treatment [42]. These results suggest distinct GRN topologies exist  
5 immediately downstream of the initial *nodal* and *bmp2/4* circuitry in echinoids.

6       The preceding results detailing the effect of SB431542 on specification of VE and  
7 DE in *E. tribuloides* suggest that cidaroids and euechinoids share multiple  
8 transcriptional targets directly downstream of Nodal in VE. However, the notable  
9 exception in the euechinoid VE cohort is *bmp2/4*, the spatial expression of which has  
10 not been detailed in *E. tribuloides* and was not detailed in this study. In DE it would  
11 appear that multiple euechinoid GRN linkages are different in *E. tribuloides*, including  
12 the spatial regulation of *tbx2/3* and *irxa*. Taken together these results suggest that the  
13 initial specification of regulatory factors immediately downstream of Nodal in euechinoid  
14 VE exhibit similar deployment than regulatory interactions that are immediately  
15 downstream of the ventral to dorsal signal.

## 16 **Effects of perturbation of D-V axis specification on** 17 **mesodermal regulatory factors in *E. tribuloides***

18       In euechinoids studied thus far, polarity in NSM (D-V) lineages is also regulated  
19 by regulatory factors downstream of Nodal signaling [29, 73]. In *E. tribuloides*, qPCR  
20 data did not indicate consistent differences in mRNA abundance for NSM regulatory  
21 factors (Figure 4C). However, WMISH assays revealed that embryos treated with  
22 SB431542 failed to restrict *gcm* to the dorsal side (Figure 5A, 5B). This observation is  
23 consistent with the euechinoid GRN linkage of the Nodal-responsive *not* repressing

1 dorsal NSM in the ventral-facing region of the archenteron [29]. Indeed, in *E. tribuloides*,  
2 *not* can be seen observed in the archenteron throughout gastrulation (Figure 1C2-1C4).  
3 However, upon disruption of the Nodal signal, *not* expression is extinguished and *gcm* is  
4 not properly restricted (Figure 5A, 5B). These observations are consistent with a  
5 conserved role for Nodal signaling in NSM segregation in the archenteron of *E.*  
6 *tribuloides*.

7         Lastly, CB formation in euechinoids is dependent on repression of *gsc* in VE and  
8 *irxa* in DE [42, 67]. While little is known about CB formation in *E. tribuloides*, recent work  
9 indicated that *Onecut* is expressed in CB and that disruption of endomesoderm  
10 formation by treatment with zinc resulted in embryos exhibiting a ring of highly  
11 concentrated proneural synaptotagmin-B positive cells at the equator of the embryo  
12 [81]. This result is remarkably similar to that shown in Figure 5C, which shows *onecut*  
13 mRNA transcripts detected by WMISH in an equatorial band in *E. tribuloides* embryos  
14 cultured with SB431542. Thus, by blocking D-V axis specification in *E. tribuloides*,  
15 embryos produce a single proneural CB encircling the embryo at the equator. However,  
16 this perturbation is drastically different in euechinoids, where treatment with SB431542  
17 or injection of Nodal MASO markedly increases *onecut* expression throughout the  
18 ectoderm [80]. However, this is not the case in cidaroids, as perturbation data presented  
19 here and elsewhere [81] suggest that, in the absence of proper D-V patterning, a  
20 proneural CB appears only at the equator in the cidaroid sister-clade. These conflicting  
21 results are consistent with the hypothesis that there are anteriorly positioned regulatory  
22 factors repressing *onecut* in cidaroids.



## 1 **Comparative analysis of global developmental GRN** 2 **dynamics in early echinoid embryos**

3       Next I undertook a statistical comparative analysis between *E. tribuloides* and  
4 two euechinoids that would inform hypotheses on correlation of transcriptional activity of  
5 GRN regulatory factors and global developmental GRN topology. While there are  
6 multiple datasets published with timecourse data of transcript abundance in *S.*  
7 *purpuratus* [82, 83], until recently there were no large datasets for other euechinoids.  
8 However, a high density timecourse dataset of temporal expression dynamics and  
9 initiation times was recently published for early regulatory factors operating in *P. lividus*,  
10 and their inclusion with *S. purpuratus* data provided the foundation for a comparative  
11 analysis between three species [84]. To conduct this analysis, distinct ontogenetic rates  
12 between the species were corrected for by comparing the timing of major  
13 developmental events, e.g. gastrulation, between the species, and relative transcript  
14 abundance in each species combined with Spearman's rank correlation coefficients ( $\rho$ )  
15 were compiled for orthologues. Previous analyses had already posited the absence of a  
16 double-negative gate in cidaroids [19, 20], an observation that even without additional  
17 data supports the notion of large scale rewiring at the top of the SM GRN hierarchy. To  
18 determine if altered deployment of early GRN topologies is the rule and not the  
19 exception for early patterning of embryonic territories in echinoids, an analysis of 18  
20 regulatory factors in *E. tribuloides*, *P. lividus* and *S. purpuratus* was conducted. Plotting  
21 relative mRNA transcriptional dynamics for the three species were indicative of  
22 compelling correlation for ectodermal and endodermal regulatory factors and supported

1 the notion of poor correlation for regulatory factors driving mesoderm specification  
2 (Figure 6).

3

4 **Fig 6. Comparative gene expression analysis suggests conserved deployment of**  
5 **ectodermal and endodermal regulatory factors and divergent deployment of**

6 **mesodermal regulatory factors in echinoids.** *Strongylocentrotus purpuratus*, purple  
7 line; *Paracentrotus lividus*, green dashed line; *Eucidaris tribuloides*, black dashed line.

8 Transcripts per embryo for each gene were normalized to their maximal expression over  
9 the first 30 hours of development and are plotted against *E. tribuloides* development on  
10 the x-ordinate. Comparative developmental staging for each species is listed in Table  
11 S4. Each analysis is accompanied by a matrix of Spearman correlation coefficients  
12 (marked as greek rho).

13

14 To provide further support for the hypothesis of domain-specific change to GRN  
15 topology, a two-species comparison between *E. tribuloides* and *S. purpuratus* was  
16 conducted to analyze an increased sample size of 34 regulatory genes, the spatial  
17 distributions of which are all known in *S. purpuratus* and *E. tribuloides*. Spearman's rank  
18 correlation coefficients ( $\rho$ ) were calculated pairwise for each orthologue. Values for  $\rho$   
19 were then binned by their embryonic domain of expression in *S. purpuratus*.  
20 Comparison of the domain-specific  $\rho$  of regulatory factors expressed in each of the  
21 three canonical bilaterian embryonic domains (germ layers) against the mean of all  $\rho$   
22 values, regulatory factors expressed in both *S. purpuratus* and *E. tribuloides* endoderm  
23 and ectoderm exhibited significantly higher  $\rho$  relative to the mean of all  $\rho$  values,

1 suggesting strong conservation of transcriptional dynamics of these factors in echinoids  
2 (Figure 7A). However, regulatory factors expressed in *S. purpuratus* and *E. tribuloides*  
3 mesodermal germ layers did not depart significantly from the mean  $\rho$ , suggesting  
4 transcriptional dynamics of mesodermal regulatory factors have changed markedly  
5 since the cidaroid-euechinoid divergence (Figure 7A). To determine whether  
6 mesodermal subdomains had undergone changes to GRN deployment, regulatory  
7 factors were further binned into embryonic subdomains. This finer-scale analysis  
8 revealed that whereas both SM and NSM regulatory factors showed significant variation  
9 in their transcriptional dynamics relative to the mean of all  $\rho$  values, the SM showed  
10 significantly more variation than the NSM (Figure 7B). In contrast to this, deployment of  
11 subdomains of ectodermal and endodermal regulatory factors exhibit statistically  
12 significant departures from the mean of all  $\rho$  values (Figure 7B).

13

14 **Fig 7. Distribution plots of Spearman's rank correlation coefficients ( $\rho$ ) for**  
15 **temporal dynamics in *E. tribuloides* and *S. purpuratus* reveals domain-specific**  
16 **alterations to deployment of regulatory factors.** Genes were binned by embryonic  
17 domain of *S. purpuratus* expression. Boxplot boundaries show interquartile range,  
18 means and standard deviation. Asterisks mark statistical significance as determined by  
19 a two-tailed t-test. (A) Boxplots for statistical distribution of endodermal, ectodermal and  
20 mesodermal regulatory factors in *E. tribuloides* and *S. purpuratus*. Mean  $\rho$  for  
21 endodermal and ectodermal regulatory factors were significantly higher than the mean  
22  $\rho$ . Mesodermal regulatory factors did not significantly vary from the mean. (B) Boxplots  
23 for statistical distribution of subdomains of endodermal, ectodermal and mesodermal

1 regulatory factors in *E. tribuloides* and *S. purpuratus*. Whereas veg2 endoderm and  
2 dorsal and ventral ectodermal domains showed statistically significant differences from  
3 the mean, both skeletogenic and non-skeletogenic regulatory factors did not differ  
4 significantly from the mean  $\rho$ .

5

## 6 **Discussion**

### 7 **Divergence of embryonic domain specification in early** 8 **development of echinoids**

9         Since the divergence of cidaroids and euechinoids at least 268.8 mya, echinoid  
10 developmental GRNs have significantly diverged, as shown above by the large-scale  
11 survey of regulatory factors establishing D-V polarity in mesoderm and ectoderm of *E.*  
12 *tribuloides*. Importantly, these networks are not so dissimilar as to be unrecognizable.  
13 Indeed, at all levels of GRN deployment there exist commonalities. By contrasting these  
14 observations with those in other echinoderms, we can begin to appreciate the degree to  
15 which embryonic developmental GRNs are constrained or malleable over vast  
16 evolutionary distances and can reconstruct the ancestral regulatory states that must  
17 have existed in the embryos of echinoderm ancestors [49].

### 18 **Regulatory states and polarity of NSM in *E. tribuloides***

19         The most conspicuous morphological differences during embryogenesis of  
20 cidaroids and euechinoids are the asymmetric cleavage of micromeres and the  
21 heterochrony of primary mesenchymal ingression. Euechinoids exhibit asymmetric  
22 cleavage of vegetal blastomeres at 4<sup>th</sup> and 5<sup>th</sup> cleavage to yield large micromeres and

1 small micromeres. Large micromeres present the Delta ligand to immediately adjacent  
2 cell layers, which give rise to mesodermal NSM anteriorly and the small micromere  
3 quartet (SMQ) posteriorly. In mesodermal NSM, *gcm* is directly downstream of Notch  
4 signaling and is restricted to dorsal NSM by the time that SM ingresses into the  
5 blastocoel prior to gastrulation [39, 73, 75, 85]. In cidaroids, mesodermal polarity of *gcm*  
6 occurs 4-6 hours prior to SM ingression and does not occur until after gastrulation has  
7 begun. Thus, if *gcm* is near the top of the NSM GRN in cidaroids [19] as is the case in  
8 euechinoids [85], then this pregastrular NSM polarization can be viewed as a  
9 euechinoid synapomorphy. This hypothesis is supported by the observation that no  
10 significant polarity occurs in mesodermal specification in holothuroids [86]. Two  
11 observations make it likely that euechinoid regulatory linkages mediating *gcm*  
12 polarization via the transcription factor *not* [29] are likely to exist in *E. tribuloides* as well:  
13 (1) *not* expression is observed at on the ventral side of the archenteron by early gastrula  
14 stage when *gcm* is spatially restricted (Figure 1C1, Figure 3D1-3D4) and (2) dorsal  
15 localization of *gcm* does not obtain when D-V axis patterning is perturbed (Figure 5A).  
16 Together these observations suggest a conserved role for VE regulatory factors in  
17 patterning the NSM of echinoids and that, in the lineage leading to modern euechinoids,  
18 deployment of GRN circuitry polarizing NSM underwent a heterochronic shift in the  
19 lineage leading to euechinoids.

20 Intriguingly, *gcm* expression is observed in the ectoderm prior to SM ingression.  
21 One hypothesis that would explain this observation in *E. tribuloides* is that NSM  
22 ingresses prior to SM ingression. However, as *gcm*-expressing cells have never been  
23 observed in the blastocoel prior to 30 hpf, these cells would not express *gcm* until they

1 intercalate into ectoderm. This scenario is very unlikely, though, given that numerous  
2 independent observations show that the primary mesenchymal ingression event in *E.*  
3 *tribuloides* is executed by SM and occurs only after the archenteron has extended  
4 considerably into the blastocoel [14-17, 20, 87]. A competing hypothesis is that  
5 ectodermal *gcm* expression in *E. tribuloides* is evolutionarily related to *gcm* expression  
6 seen in late blastula stages of asteroids [76]. Indeed, follow up experiments indicated  
7 that perturbation of Notch signaling increased the spatial domain of ectodermal *gcm* and  
8 resulted in supernumerary pigment cell formation (Figure S6). These observations  
9 support the hypothesis that *gcm* in *E. tribuloides* has roles both in mesodermal NSM  
10 and ectoderm. If this is the case, two more things are clear evolutionarily: (1) *gcm* was  
11 likely expressed in the ectoderm in the echinozoan ancestor at least 481 mya; and (2)  
12 the lineage leading to camaradont euechinoids lost ectodermally-derived *gcm* activity,  
13 which may have been a consequence of the endomesodermal Notch-dependent *gcm*  
14 linkage now observed. Further investigation disentangling the roles of *gcm* in cidaroids  
15 will provide insight into how the regulation and function of this gene has evolved in  
16 echinoderms.

17

18 **Fig S6. Ectodermal *gcm* expression and pigment cell abundance are altered in a**  
19 **Delta-Notch perturbation background.** (A-D) Morpholino antisense oligonucleotide  
20 targeting the Delta-Notch mediator *hesC* induces supernumerary pigment cells in the  
21 ectoderm of *E. tribuloides*. (A) Pigment cell counts for individual larvae (5 days post  
22 fertilization) either injected with *hesC* MASO or uninjected. (B) Bar graph showing mean  
23 number of pigment cells per larva in either uninjected control or injected with *hesC*

1 MASO. Larvae injected with MASO targeting *hesc* exhibited significantly more pigment  
2 cells.  $p$  value  $\leq 0.005$ , Mann-Whitney rank-sum test. (C, D) Example larvae from both  
3 uninjected control and larvae injected with *hesc* MASO at 36 hpf. (E, F) *Gcm* expression  
4 is elevated in the ectoderm of embryos injected with *hesc* MASO. (G, H) Embryos  
5 treated with the Notch-inhibitor DAPT exhibit increased numbers of *gcm*-positive cells in  
6 the ectoderm at 26 and 40 hpf.

7  
8 The data presented on D-V polarity in the NSM of *E. tribuloides* suggest that  
9 multiple regulatory domains unfold at and around the tip of the archenteron as  
10 gastrulation proceeds. Similar to euechinoids, this study determined that *ese* operates  
11 in the ventral NSM exclusive of *gcm* in the dorsal NSM. While the regulatory states in *E.*  
12 *tribuloides* NSM need further refinement by two-color WMISH, for our purposes the  
13 overt disorder in its formation relative to the overt order of *S. purpuratus* NSM makes  
14 two salient points. First, early pregastrular or early gastrular polarity of NSM regulatory  
15 states represents an echinoid novelty, as no evidence for early mesodermal polarity  
16 exists in outgroup echinoderms [86, 88]. Second, if we take *E. tribuloides* as a proxy to  
17 the ancestral state for this character/regulatory state, then it is clear that the D-V polarity  
18 observed in the euechinoid NSM was shifted to occur prior to gastrulation in the lineage  
19 leading to modern euechinoids. On the other hand, an alternate evolutionary scenario is  
20 that NSM polarity manifested in these two modern echinoids is the result of two  
21 independent evolutionary trajectories with heterochronic and spatial differences, but  
22 both meeting a similar end in the diversification of NSM cell types in early development.  
23 That at least two D-V regulatory states are common to these embryos and that *gcm* is

1 downstream of Nodal and Notch signaling provide support for the first scenario. Further  
2 investigation into the developmental timing and regulatory states of cidaroid NSM will be  
3 required to parse out the most likely evolutionary scenario.

#### 4 **Ectodermal regulatory states in *E. tribuloides***

5 Correspondence between *E. tribuloides* and euechinoids in deployment of  
6 ectodermal regulatory factors provides support to the idea that ectodermal specification  
7 is constrained and that alteration to the circuitry is nontrivial in early development.  
8 However, major alterations have occurred to ectodermal patterning pathways in regards  
9 to deployment and rewiring of circuitry during the evolution of euechinoid lineages that  
10 possess direct-developing, non-feeding larvae [54, 89-91]. These observations support  
11 the idea that the pressures of selection can overwhelm strong evolutionary constraint in  
12 early development. Of course there are very interesting differences in *E. tribuloides*  
13 ectodermal spatiotemporal dynamics and regulatory states relative to euechinoids. For  
14 instance, perturbation of Nodal signaling reveals that, while initial specification events  
15 are highly similar, alterations likely have occurred to the regulation of *bmp2/4* and  
16 *tbx2/3*. In *E. tribuloides* *tbx2/3* is expressed in DE and dorsal NSM by mid-gastrula. By  
17 late gastrula, it is expressed in the lateral clusters of skeletogenic synthesis, at the tip of  
18 the gut, in the gut endoderm, and residually in the ectoderm. This unfolding pattern of  
19 *tbx2/3* expression in *E. tribuloides* has essentially been compressed into the early  
20 stages of euechinoid development [62]. In euechinoids, perturbation of Nodal signaling  
21 with SB431542 extinguishes dorsal ectodermal *tbx2/3* specifically in *P. lividus*, while not  
22 affecting its expression in SM [42]. In *E. tribuloides* I observed the expression domain of  
23 *tbx2/3* expand into VE upon perturbation with this inhibitor (Figure 5A, 5B). This



1 observation combined with the result that *bmp2/4* responds differently to Nodal  
2 perturbation suggests altered GRN circuitry downstream of Nodal. However, the vast  
3 evolutionary distances between cidaroids and euechinoids and the conserved  
4 spatiotemporal deployment of regulatory factors strongly argue for developmental  
5 constraint of ectodermal patterning mechanisms.

6 Ciliary band formation and ANE patterning in *E. tribuloides* are evolutionarily  
7 interesting evolutionarily given the fact that cidaroids lack the pan-deuterostome apical  
8 sensory organ [15, 16, 92, 93]. Understanding the alterations in GRN circuitry that  
9 accompanied the loss of this embryonic structure and its downstream consequences  
10 would provide insight into the evolution of embryonic morphology and GRN architecture.  
11 Previous studies indicated that ANE patterning in *E. tribuloides* is more similar to  
12 outgroup echinoderms than it is in euechinoids; though expression of CB and anterior  
13 regulatory factors, e.g. *onecut* and *nk2.1*, exhibited spatial distributions similar to those  
14 seen in euechinoids [81]. Here, I observed patterning and regulation of CB that are  
15 consistent with the hypothesis that this process is conserved in echinoids. Additionally, I  
16 observed the sequential spatial restriction of *foxq2* to ANE, a pan-bilaterian observation  
17 driven by endomesodermal *wnt* factors [25, 94-97]. These data suggest that  
18 specification of the apical sensory organ in *E. tribuloides* is developmentally  
19 downstream of these events and that the loss of this embryonic structure had little effect  
20 on conserved patterning of CB and anterior localization of *foxq2*.

21 Lastly, perturbation of D-V patterning drastically altered the spatial distribution of  
22 CB regulatory factor *onecut* and resulted in a belt of 6-10 cells encircling the *E.*  
23 *tribuloides* embryo as a single dense ciliary band. A similar result was also obtained for

1 Synaptotagmin in *E. tribuloides* by disruption of endomesodermal specification via zinc  
2 perturbation [81]. These results are consistent with the hypothesis that anteriorly  
3 positioned ANE repressors restrict CB fate to the equator when D-V patterning is  
4 disrupted. Indeed, in *S. purpuratus*, *foxq2* restricts CB positioning anteriorly in ANE [30].  
5 Although it is clear from work in euechinoids that ANE regulatory factors do not expand  
6 when D-V patterning is disrupted [42], this is likely not the case in *E. tribuloides*. While  
7 ANE is greatly expanded in *E. tribuloides* relative to other echinoderms [94, 98], there is  
8 no evidence to indicate that it extends to the embryonic equator. The most likely  
9 scenario is that disruption of D-V patterning expands anteriorly positioned ANE  
10 repressors of CB, e.g. candidate regulatory factors being *foxq2* and *nk2.1*, and CB  
11 positioning occurs at the equator where a pan-ectodermal driver, e.g. SoxB1 [30, 42,  
12 61], is able to drive *onecut* expression. Elevated mRNA levels of *foxq2* in *E. tribuloides*  
13 upon disruption of D-V patterning support this hypothesis (Figure 4A,4C). Further, the  
14 sequential vegetal-to-animal zygotic activation of *onecut* seen during *E. tribuloides* early  
15 development is consistent with the hypothesis of anteriorly positioned ANE repressors  
16 that must be cleared for proper *onecut* expression.

## 17 **Evolution of global embryonic domains in early development**

### 18 **of echinoids**

19 Previous analyses of embryonic domain regulatory states in *E. tribuloides*  
20 surveyed SM regulatory factors [20] and anterior neural ectoderm specification [81].  
21 Additionally, two previous studies investigated SM and early endomesodermal  
22 micromere regulatory factors in the Pacific-dwelling cidaroid *Prionocidaris baculosa* [19,  
23 99]. Integrating these data into this study affords an analysis of global embryonic

1 regulatory states and GRN linkages over 268.8 mya of evolution in indirect-developing  
2 sea urchins. From these studies, numerous alterations to deployment and GRN circuitry  
3 at all levels of GRN topology can be enumerated. Here, I enumerate 19 changes in  
4 spatiotemporal deployment or regulation of ectodermal and mesodermal embryonic  
5 regulatory factors since the cidaroid-euechinoid divergence (Table 2). Prominent among  
6 rewiring events are those that have occurred in establishing polarity in mesodermal  
7 embryonic domains. Endodermal and ectodermal specification and regulatory states  
8 also have undergone change, but to a lesser degree. One hypothesis that can  
9 accommodate these observations is that endodermal and ectodermal developmental  
10 programs may be more recalcitrant to change than mesodermal programs due to their  
11 more ancient evolutionary origin, suggesting that accretion of process over evolutionary  
12 time is a mechanism of constraint in developmental programs [5]. Indeed, in  
13 euechinoids there have been additional layers of GRN topology accrued in mesodermal  
14 specification, e.g. the *pmar1-hesc* double-negative gate novelty [19, 20, 24], delta-  
15 dependent NSM specification [20, 36], etc., which cidaroids do not exhibit, and which  
16 may explain the observation that little to no appreciable change has been observed in  
17 the mesodermal developmental programs of *L. variegatus*, *P. lividus* and *S. purpuratus*,  
18 representatives of modern euechinoid lineages that diverged approximately 90 mya.

19

20 **Table 2. Enumeration of evolutionary changes to GRN deployment since the**  
21 **cidaroid-euechinoid divergence.**

No.	Regulatory factor	Change in spatiotemporal dynamics	Description of change	Euechinoid citations
1	<i>bmp2/4</i>	heterotopy	Altered regulation in D-V perturbation background	42

2	<i>brachyury</i>	heterochrony	Heterochronic shift in VE	41
3	<i>ese</i>	heterochrony	Heterochronic shift in NSM, <i>E. tribuloides</i> polarity prior to SM ingression	73, 74
4	<i>ese</i>	heterotopy	Altered spatial distribution, first broadly mesodermal in <i>E. tribuloides</i> then polarized	29
5	<i>foxa</i>	heterochrony	Heterochronic shift in VE	42,79
6	<i>foxq2</i>	heterotopy	Altered spatial distribution in ectoderm	94
7	<i>gatac</i>	heterochrony	Heterochronic shift in NSM, <i>E. tribuloides</i> polarity after SM ingression	29, 73
8	<i>gatac</i>	heterotopy	Altered spatial distribution, first broadly mesodermal then polarized	29
9	<i>gatae</i>	heterochrony	Heterochronic shift in NSM, <i>E. tribuloides</i> polarity after SM ingression	29
10	<i>gcm</i>	heterotopy	Altered spatial distribution in ectoderm	85
11	<i>gcm</i>	heterochrony	Heterochronic shift in NSM, <i>E. tribuloides</i> polarity prior to SM ingression	29, 73, 85
12	<i>onecut</i>	heterotopy	Altered spatial distribution in D-V perturbation background	42
13	<i>onecut</i>	heterochrony	Heterochronic shift in CB restriction/activation	30, 69
14	<i>prox</i>	heterotopy	Altered maternal distribution, maternal in <i>S. purpuratus</i>	29
15	<i>prox</i>	heterotopy	Altered spatial distribution in NSM, no observed polarity in <i>E. tribuloides</i>	29,68
16	<i>scl</i>	heterotopy	Altered spatial distribution, in <i>E. tribuloides</i> broadly mesodermal then polarized	29
17	<i>tbx2/3</i>	heterochrony	Heterochronic shift in SM	62, 63
18	<i>tbx2/3</i>	heterotopy	Altered spatial distribution in D-V perturbation background	42
19	<i>tbx2/3</i>	heterotopy	Altered spatial distribution in DE	62, 63

1

## 2 **Biased rates of change to GRN topology in early** 3 **development**

4       Davidson and Erwin [7] first proposed the hypothesis that the hierarchical nature  
5 of GRN structure would manifest unequal rates of change during developmental  
6 evolution. This hypothesis was formulated from experimental observations in multiple  
7 bilaterian lineages [3, 100], and its underlying principle is to couch the systematic

1 structure of Linnean phylogeny in terms of molecular mechanistic explanation [6, 101].  
2 Here evidence was presented that affords a first approximation of the lability of GRN  
3 deployment and circuitry underlying GRN topology in early echinoid development. I  
4 have presented a comparative analysis of developmental programs that diverged in the  
5 middle Permian and that argues for domain-specific, biased rates of change in  
6 deployment of GRN regulatory factors. While the genomic hardwired changes  
7 underlying this bias were not revealed here, the confluence of spatial, temporal and  
8 experimental evidence strongly suggests that regulatory circuitry specifying mesodermal  
9 domains in early echinoid embryonic development has undergone substantially more  
10 alteration at all levels of GRN topology than endodermal and ectodermal domains. For  
11 the early embryo it is imperative to establish canonical domains that are tasked with  
12 highly conserved processes, e.g. boundary formation and gastrulation. Thus, rates of  
13 change to GRN topology will vary during embryonic development depending on the  
14 capacity of the domain to buffer the effect of any mutation. The prediction that  
15 recursively wired, hierarchical developmental GRNs constrain the possible trajectories  
16 of change in future lineages was a prescient observation that we are only now  
17 beginning to fully appreciate.

## 18 **Materials and Methods**

### 19 **Animals and embryo culture**

20 Adult *E. tribuloides* were obtained from KP Aquatics (Tavernier, Florida). Eggs  
21 were collected by gravity and washed four times in Millipore filtered sea water (MFSW).  
22 Eggs were fertilized with a dilute sperm solution, and embryo cultures with less than

1 95% fertilization were discarded. Embryos were developed in glass pyrex dishes in a  
2 temperature-controlled setting of 22°C, and MFSW was refreshed daily.

### 3 **Cloning and gene isolation**

4 RNAseq and genomic databases of *E. tribuloides* reads were utilized for primer  
5 design using euechinoid sequences as seeds for BLAST searches and subsequent  
6 verification of orthology. PCR products were cloned into PGEM-T vector (Promega) and  
7 sequence verified in house using an ABI 3730xl sequencer. WMISH antisense RNA  
8 probes were synthesized from restricted plasmid vectors using T7 or SP6 RNA  
9 polymerase with digoxigenin or fluorescein dUTP incorporation (Roche). Primers for  
10 WMISH and qPCR are listed in Table S1.

11

12 **Table S1. WMISH and qPCR primer sequences. To be placed in Supporting**  
13 **Information or uploaded as Excel spreadsheet.**

14

### 15 **Whole-mount *in situ* hybridization and mRNA transcript** 16 **abundance**

17 Transcript abundance of mRNA was estimated as described [49]. Briefly,  
18 transcripts were estimated by counting the number of embryos and spiking in an  
19 external standard of quantified synthetic XenoRNA (Power SYBR Green Cells-to-Ct Kit,  
20 Thermo-Fisher Scientific) prior to RNA isolation (RNeasy, Qiagen). Thus, to each qPCR  
21 reaction a known amount of embryos and RNA were added and the transcript number is

1 deduced by ddCt method. Additionally, some estimates were made with an internal  
2 standard that had been previously quantified.

3 Whole-mount *in situ* hybridization (WMISH) was conducted as previously  
4 described [20]. The WMISH protocol slightly modified for double fluorescent WMISH  
5 (dfWMISH) with different antibodies and probe detection. Antibodies for dfWMISH were  
6 either Anti-DIG or Anti-FLU conjugated to horseradish peroxidase (Roche) at a  
7 concentration of 0.25  $\mu\text{g}/\text{mL}$ . Probes were detected with the Tyramide Signal  
8 Amplification Plus kit (Perkin Elmer) by using cyanine 5 or fluorescein conjugates at a  
9 dilution of 1:4000 in TBST. The amplification reaction was quenched by addition of 1%  
10 hydrogen peroxide. The protocol then cycled back to the blocking step and proceeded  
11 as described to detect the second probe.

## 12 **Perturbations**

### 13 **Microinjections**

14 Dominant-negative cadherin RNA overexpression (dnCad or  $\Delta$ -cadherin) was  
15 microinjected at a concentration of 1,000 ng/ $\mu\text{L}$  as previously described [20]. Translation  
16 blocking morpholino (MASO) targeting *hesc* mRNA transcript  
17 (AATCACAAGGTAAGACGAGGATGGT) was purchased from Gene Tools (Philomath,  
18 OR, USA) and microinjected at a concentration of 1 mM as described [20]. BACs were  
19 microinjected at a concentration of 60 ng per mL nuclease-free water in the presence of  
20 10 ng HindIII-digested genomic carrier DNA.

### 21 **Small molecule inhibitors**

22 For perturbation of D-V patterning, both timing and concentration of treatment  
23 with the Alk4/5/7-antagonist SB431542 (Cat no. 1614, Tocris Bioscience) were

1 determined. MFSW containing 2x concentration of the inhibitor was added to an equal  
2 volume of embryo culture in a 6-well tissue culture plate. To determine the optimum  
3 concentration, embryo cultures were reared in 5, 15 and 30  $\mu\text{M}$  SB431542. Embryos  
4 reared at 5  $\mu\text{M}$  showed no gross morphological deformities, whereas embryos reared at  
5 30  $\mu\text{M}$  exhibited significant developmental delays and gross deformities. To determine  
6 the sensitive period of inhibitor exposure, embryo cultures were exposed to the inhibitor  
7 at 1, 12 and 24 hpf. Embryos cultured in the inhibitor from 1 hpf or 24 hpf onwards  
8 showed significant developmental delays or no significant morphological differences,  
9 respectively. Results of these manipulations showed that treatment with 15  $\mu\text{M}$   
10 SB431542 at 12 hpf was the concentration and sensitive period at which a majority of  
11 larvae in the culture showed the characteristic phenotypes of dorsalization: multiple  
12 centers of skeletal synthesis and an hourglass phenotype. For Notch perturbation,  
13 embryos were cultured in the Notch-antagonist DAPT (Cat No. S2215, Selleck  
14 Chemicals) at a concentration of 12  $\mu\text{M}$  from 1 hpf onwards.

## 15 **Comparative RNA timecourse analysis and statistics**

16 Absolute mRNA transcript number was estimated as described above for  
17 regulatory genes in early development of *E. tribuloides* (Table S2). Comparative  
18 analyses of this dataset were based on published data from two euechinoids, *S.*  
19 *purpuratus* [82] and *P. lividus* [84]. As developmental timing differs between the three  
20 species, a one-to-one comparison of timecourse datapoints could not be obtained. This  
21 issue was resolved by utilizing the adjustments for *S. purpuratus* and *P. lividus*  
22 described in Gildor and Ben-Tabou de Leon [84]. The comparative timepoints used in  
23 this study are presented in Table S4. Absolute transcript number for each timepoint was



1 then ranked highest to lowest for each gene relative to itself. Spearman's rank  
2 correlation coefficient ( $\rho$ ) was chosen over Pearson's correlation in order to reduce the  
3 influence of large differences sometimes observed in estimates of absolute mRNA  
4 transcript numbers. For each pair of orthologous genes for which data were available in  
5 two species  $\rho$  was calculated; these data are presented for three species in Figure 6  
6 and are found in Table S3. For comparative analysis of global embryonic regulatory  
7 factors shown in Figure 7, values for  $\rho$  were calculated for 34 regulatory genes in *E.*  
8 *tribuloides* and *S. purpuratus* and were compared. Only regulatory factors for which the  
9 embryonic domain of expression is known in *E. tribuloides* were used in the analysis,  
10 though data for 55 regulatory genes are presented in Table S3. Values for  $\rho$  were  
11 binned by their expression in embryonic regulatory domains in the *S. purpuratus* global  
12 developmental GRN (available at <http://sugp.caltech.edu/endomes/>). The standard  
13 statistical distribution is represented in Figure 7. Statistical significance was calculated  
14 for each embryonic domain using the average of all  $\rho$  values (55 regulatory genes) as  
15 the expected mean. Conservation of regulatory gene deployment is then interpreted as  
16  $\rho$  values near 1, i.e. high correlation of temporal deployment between two species.

17

18 **Table S2. Spreadsheet of mRNA transcript abundance estimates in *E. tribuloides*.**  
19 **To be placed in Supporting Information or uploaded as Excel spreadsheet.**

20

21 **Table S3. Spreadsheet of Spearman's rank correlation coefficients between *E.***  
22 ***tribuloides*, *P. lividus* and *S. purpuratus*. To be placed in Supporting Information**  
23 **or uploaded as Excel spreadsheet.**

1 **Table S4. Comparative developmental timepoints for *E. tribuloides*, *P. lividus* and**  
2 ***S. purpuratus*.**

	Species	Species	Species
Timepoint	<i>E. tribuloides</i>	<i>P. lividus</i>	<i>S. purpuratus</i>
1	0	0	0
2	3	2	3
3	6	5	7
4	8	6	8
5	10	8	10
6	12	10	13
7	13	11	14
8	14	12	16
9	16	14	18
10	18	15	20
11	20	18	24
12	22	20	26
13	24	22	29
14	26	24	31

3

4

5

6

7

## 1 References

- 2 1. Davidson EH. Gene activity in early development. 3rd ed. New York: Academic  
3 Press; 1986.
- 4 2. Wikramanayake AH, Hong M, Lee PN, Pang K, Byrum CA, Bince JM, et al. An  
5 ancient role for nuclear beta-catenin in the evolution of axial polarity and germ layer  
6 segregation. *Nature*. 2003;426(6965):446-50.
- 7 3. Davidson EH. The regulatory genome: gene regulatory networks in development  
8 and evolution. Oxford: Academic; 2006.
- 9 4. Peter IS, Davidson EH. Genomic Control Process, Development and Evolution.  
10 Oxford: Academic Press; 2015.
- 11 5. Hashimshony T, Feder M, Levin M, Hall BK, Yanai I. Spatiotemporal  
12 transcriptomics reveals the evolutionary history of the endoderm germ layer. *Nature*.  
13 2015;519(7542):219-22.
- 14 6. Peter IS, Davidson EH. Evolution of gene regulatory networks controlling body  
15 plan development. *Cell*. 2011;144(6):970-85.
- 16 7. Davidson EH, Erwin DH. Gene regulatory networks and the evolution of animal  
17 body plans. *Science*. 2006;311(5762):796-800.
- 18 8. Davidson EH. Spatial mechanisms of gene regulation in metazoan embryos.  
19 *Development*. 1991;113(1):1-26.
- 20 9. Davidson EH, Cameron RA, Ransick A. Specification of cell fate in the sea urchin  
21 embryo: summary and some proposed mechanisms. *Development*. 1998;125(17):3269-  
22 90.
- 23 10. Kroh A, Smith AB. The phylogeny and classification of post-Palaeozoic  
24 echinoids. *J Syst Palaeontol*. 2010;8(2):147-212.
- 25 11. Thompson JR, Petsios E, Davidson EH, Erkenbrack EM, Gao F, Bottjer DJ.  
26 Reorganization of sea urchin gene regulatory networks at least 268 million years ago as  
27 revealed by oldest fossil cidaroid echinoid. *Sci Rep-Uk*. 2015;5.
- 28 12. Gao F, Thompson JR, Petsios E, Erkenbrack E, Moats RA, Bottjer DJ, et al.  
29 Juvenile skeletogenesis in anciently diverged sea urchin clades. *Dev Biol*.  
30 2015;400(1):148-58.
- 31 13. Wray GA, Bely AE. The evolution of echinoderm development is driven by  
32 several distinct factors. *Development*. 1994;1994(Supplement):97-106.
- 33 14. Tennent D. The early influence of the spermatzoan upon the characters of  
34 echinoid larvae. *Carn Inst Wash Publ*. 1914;182:129-38.
- 35 15. Mortensen T. Contributions to the study of the development and larval forms of  
36 echinoderms. IV. *Danske Vid Selsk Ser*. 1938;9(7(3)):1-59.
- 37 16. Schroeder TE. Development of a 'primitive' sea urchin (*Eucidaris tribuloides*):  
38 irregularities in the hyaline layer, micromeres, and primary mesenchyme. *Biological*  
39 *Bulletin*. 1981;161(1):141-51.
- 40 17. Wray GA, McClay DR. The origin of spicule-forming cells in a 'primitive' sea  
41 urchin (*Eucidaris tribuloides*) which appears to lack primary mesenchyme cells.  
42 *Development*. 1988;103(2):305-15.
- 43 18. Wray GA, McClay DR. Molecular heterochronies and heterotopies in early  
44 echinoid development. *Evolution*. 1989:803-13.

- 1 19. Yamazaki A, Kidachi Y, Yamaguchi M, Minokawa T. Larval mesenchyme cell  
2 specification in the primitive echinoid occurs independently of the double-negative gate.  
3 *Development*. 2014;141(13):2669-79.
- 4 20. Erkenbrack EM, Davidson EH. Evolutionary Rewiring of Gene Regulatory  
5 Network Linkages at Divergence of the Echinoid Subclasses. *PNAS*. 2015.
- 6 21. Angerer LM, Oleksyn DW, Logan CY, McClay DR, Dale L, Angerer RC. A BMP  
7 pathway regulates cell fate allocation along the sea urchin animal-vegetal embryonic  
8 axis. *Development*. 2000;127(5):1105-14.
- 9 22. Davidson EH, Rast JP, Oliveri P, Ransick A, Caletani C, Yuh CH, et al. A  
10 genomic regulatory network for development. *Science*. 2002;295(5560):1669-78.
- 11 23. Revilla-i-Domingo R, Oliveri P, Davidson EH. A missing link in the sea urchin  
12 embryo gene regulatory network: *hesC* and the double-negative specification of  
13 micromeres. *Proc Natl Acad Sci U S A*. 2007;104(30):12383-8.
- 14 24. Oliveri P, Tu Q, Davidson EH. Global regulatory logic for specification of an  
15 embryonic cell lineage. *Proc Natl Acad Sci U S A*. 2008;105(16):5955-62.
- 16 25. Yaguchi S, Yaguchi J, Angerer RC, Angerer LM. A Wnt-FoxQ2-nodal pathway  
17 links primary and secondary axis specification in sea urchin embryos. *Developmental*  
18 *cell*. 2008;14(1):97-107.
- 19 26. Su Y-H, Li E, Geiss GK, Longabaugh WJ, Krämer A, Davidson EH. A  
20 perturbation model of the gene regulatory network for oral and aboral ectoderm  
21 specification in the sea urchin embryo. *Developmental biology*. 2009;329(2):410-21.
- 22 27. Peter IS, Davidson EH. The endoderm gene regulatory network in sea urchin  
23 embryos up to mid-blastula stage. *Dev Biol*. 2010;340(2):188-99.
- 24 28. Peter IS, Davidson EH. A gene regulatory network controlling the embryonic  
25 specification of endoderm. *Nature*. 2011;474(7353):635-9.
- 26 29. Materna SC, Ransick A, Li E, Davidson EH. Diversification of oral and aboral  
27 mesodermal regulatory states in pregastrular sea urchin embryos. *Dev Biol*.  
28 2013;375(1):92-104.
- 29 30. Barsi JC, Li EH, Davidson EH. Geometric control of ciliated band regulatory  
30 states in the sea urchin embryo. *Development*. 2015;142(5):953-61.
- 31 31. Nam JM, Su YH, Lee PY, Robertson A, Coffman J, Davidson E. Cis-regulatory  
32 control of the nodal gene, initiator of the sea urchin oral ectoderm gene network. *Faseb*  
33 *J*. 2008;22.
- 34 32. Cui M, Siriwon N, Li E, Davidson EH, Peter IS. Specific functions of the Wnt  
35 signaling system in gene regulatory networks throughout the early sea urchin embryo.  
36 *Proceedings of the National Academy of Sciences*. 2014;111(47):E5029-E38.
- 37 33. Wikramanayake AH, Huang L, Klein WH. beta-Catenin is essential for patterning  
38 the maternally specified animal-vegetal axis in the sea urchin embryo. *P Natl Acad Sci*  
39 *USA*. 1998;95(16):9343-8.
- 40 34. Sherwood DR, McClay DR. LvNotch signaling mediates secondary mesenchyme  
41 specification in the sea urchin embryo. *Development*. 1999;126(8):1703-13.
- 42 35. Logan CY, Miller JR, Ferkowicz MJ, McClay DR. Nuclear beta-catenin is required  
43 to specify vegetal cell fates in the sea urchin embryo. *Development*. 1999;126(2):345-  
44 57.

- 1 36. Sweet HC, Gehring M, Etensohn CA. LvDelta is a mesoderm-inducing signal in  
2 the sea urchin embryo and can endow blastomeres with organizer-like properties.  
3 *Development*. 2002;129(8):1945-55.
- 4 37. Flowers VL, Courteau GR, Poustka AJ, Weng W, Venuti JM. Nodal/activin  
5 signaling establishes oral–aboral polarity in the early sea urchin embryo. *Developmental*  
6 *dynamics*. 2004;231(4):727-40.
- 7 38. Etensohn CA, Kitazawa C, Cheers MS, Leonard JD, Sharma T. Gene regulatory  
8 networks and developmental plasticity in the early sea urchin embryo: alternative  
9 deployment of the skeletogenic gene regulatory network. *Development*.  
10 2007;134(17):3077-87.
- 11 39. Croce JC, McClay DR. Dynamics of Delta/Notch signaling on endomesoderm  
12 segregation in the sea urchin embryo. *Development*. 2010;137(1):83-91.
- 13 40. Duboc V, Rottinger E, Besnardeau L, Lepage T. Nodal and BMP2/4 signaling  
14 organizes the oral-aboral axis of the sea urchin embryo. *Developmental Cell*.  
15 2004;6(3):397-410.
- 16 41. Duboc V, Lapraz F, Besnardeau L, Lepage T. Lefty acts as an essential  
17 modulator of Nodal activity during sea urchin oral-aboral axis formation. *Developmental*  
18 *Biology*. 2008;320(1):49-59.
- 19 42. Saudemont A, Haillet E, Mekpoh F, Bessodes N, Quirin M, Lapraz F, et al.  
20 Ancestral Regulatory Circuits Governing Ectoderm Patterning Downstream of Nodal  
21 and BMP2/4 Revealed by Gene Regulatory Network Analysis in an Echinoderm. *Plos*  
22 *Genet*. 2010;6(12).
- 23 43. Lhomond G, McClay DR, Gache C, Croce JC. Frizzled1/2/7 signaling directs  
24 beta-catenin nuclearisation and initiates endoderm specification in macromeres during  
25 sea urchin embryogenesis. *Development*. 2012;139(4):816-25.
- 26 44. Cavalieri V, Spinelli G. Early asymmetric cues triggering the dorsal/ventral gene  
27 regulatory network of the sea urchin embryo. *Elife*. 2014;3:e04664.
- 28 45. Smith AB, Pisani D, Mackenzie-Dodds JA, Stockley B, Webster BL, Littlewood  
29 DT. Testing the molecular clock: molecular and paleontological estimates of divergence  
30 times in the Echinoidea (Echinodermata). *Mol Biol Evol*. 2006;23(10):1832-51.
- 31 46. Croce J, Range R, Wu SY, Miranda E, Lhomond G, Peng JC, et al. Wnt6  
32 activates endoderm in the sea urchin gene regulatory network. *Development*.  
33 2011;138(15):3297-306.
- 34 47. Etensohn CA. Lessons from a gene regulatory network: echinoderm  
35 skeletogenesis provides insights into evolution, plasticity and morphogenesis.  
36 *Development*. 2009;136(1):11-21.
- 37 48. Molina MD, de Croze N, Haillet E, Lepage T. Nodal: master and commander of  
38 the dorsal-ventral and left-right axes in the sea urchin embryo. *Current Opinion in*  
39 *Genetics & Development*. 2013;23(4):445-53.
- 40 49. Erkenbrack EM, Ako-Asare K, Miller E, Tekelenburg S, Thompson JR, Romano  
41 L. Ancestral state reconstruction by comparative analysis of a GRN kernel operating in  
42 echinoderms. *Dev Genes Evol*. 2016;226(1):37-45.
- 43 50. Lapraz F, Haillet E, Lepage T. A deuterostome origin of the Spemann organiser  
44 suggested by Nodal and ADMPs functions in Echinoderms. *Nat Commun*. 2015;6:8927.

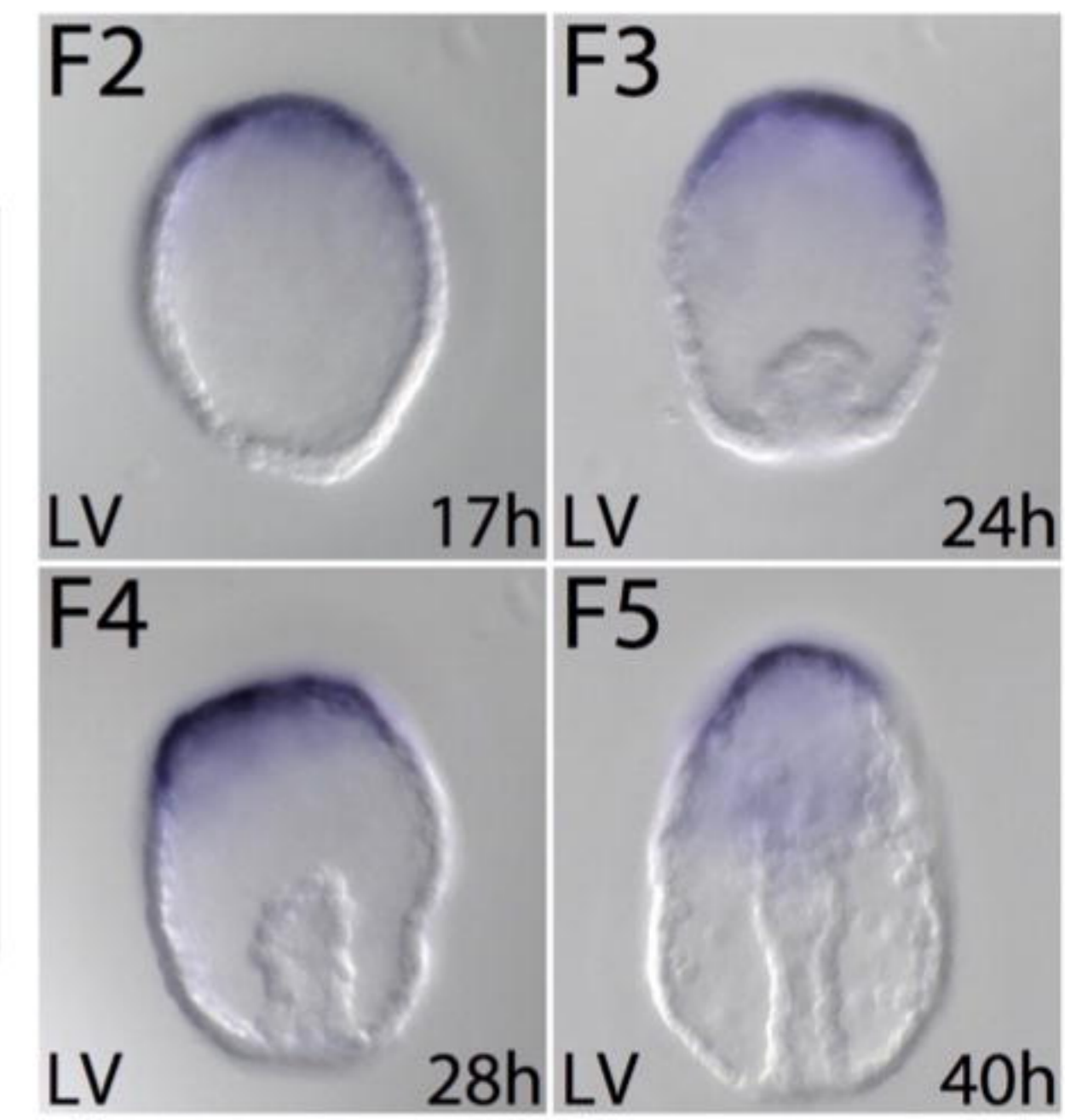
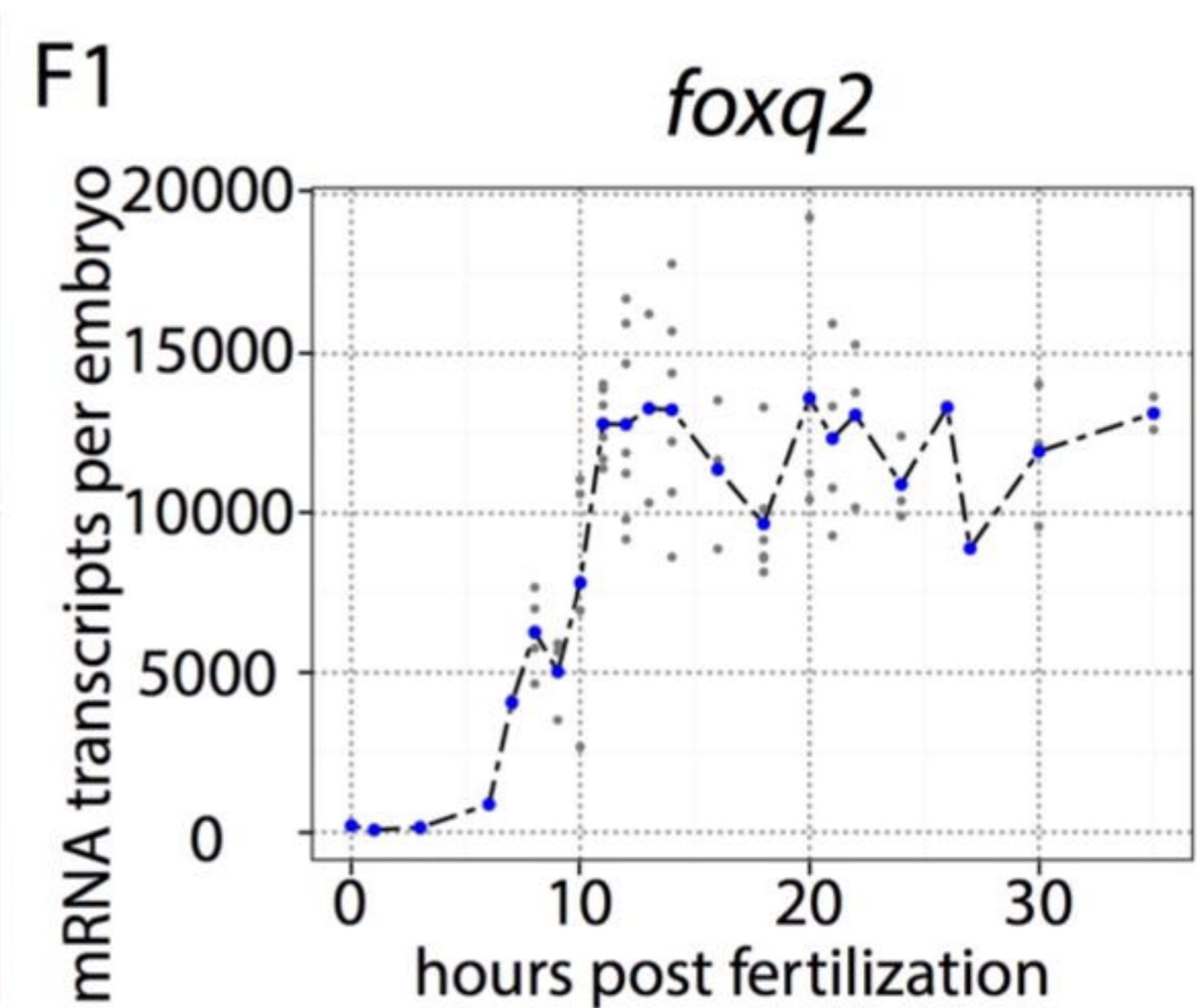
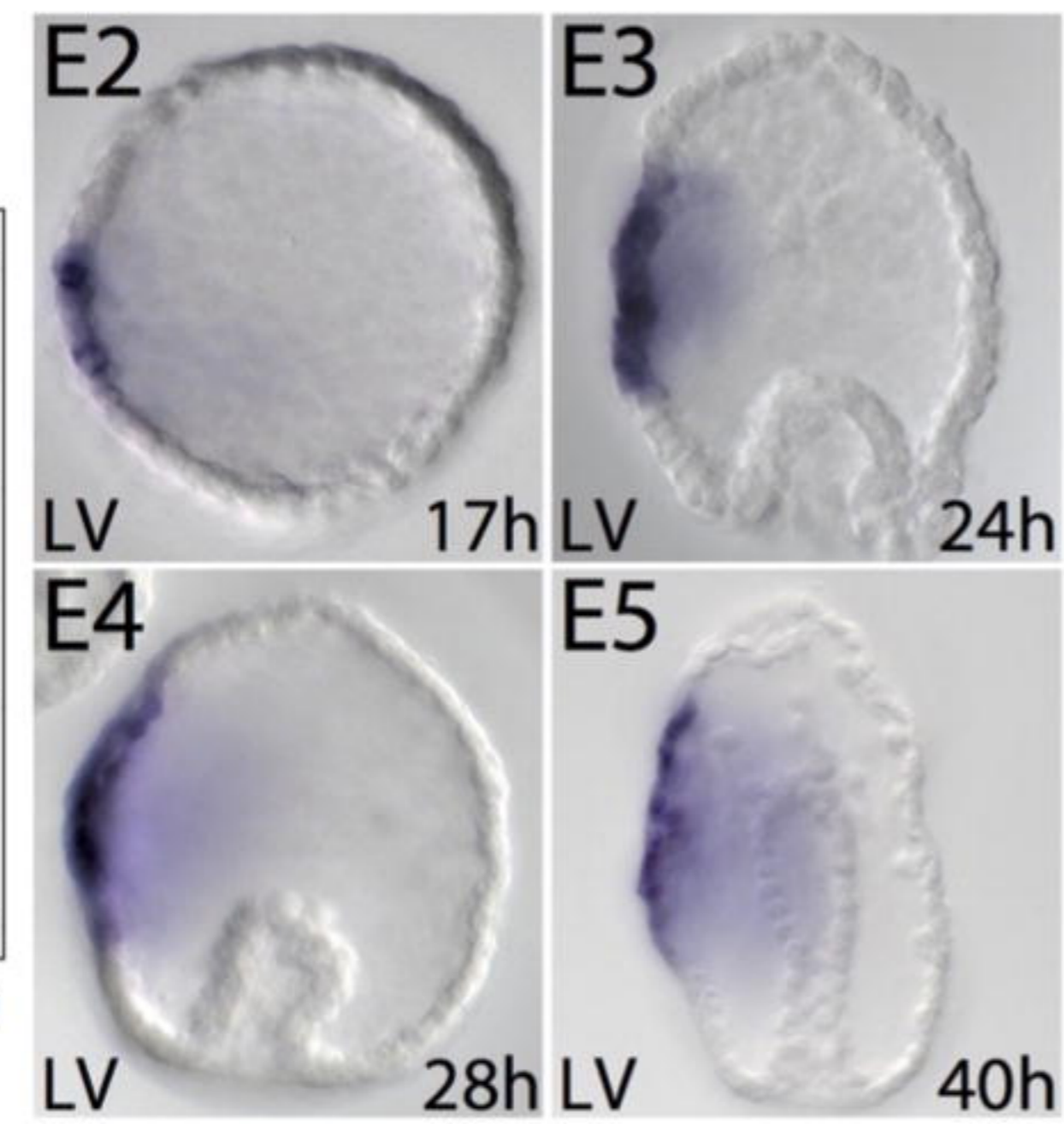
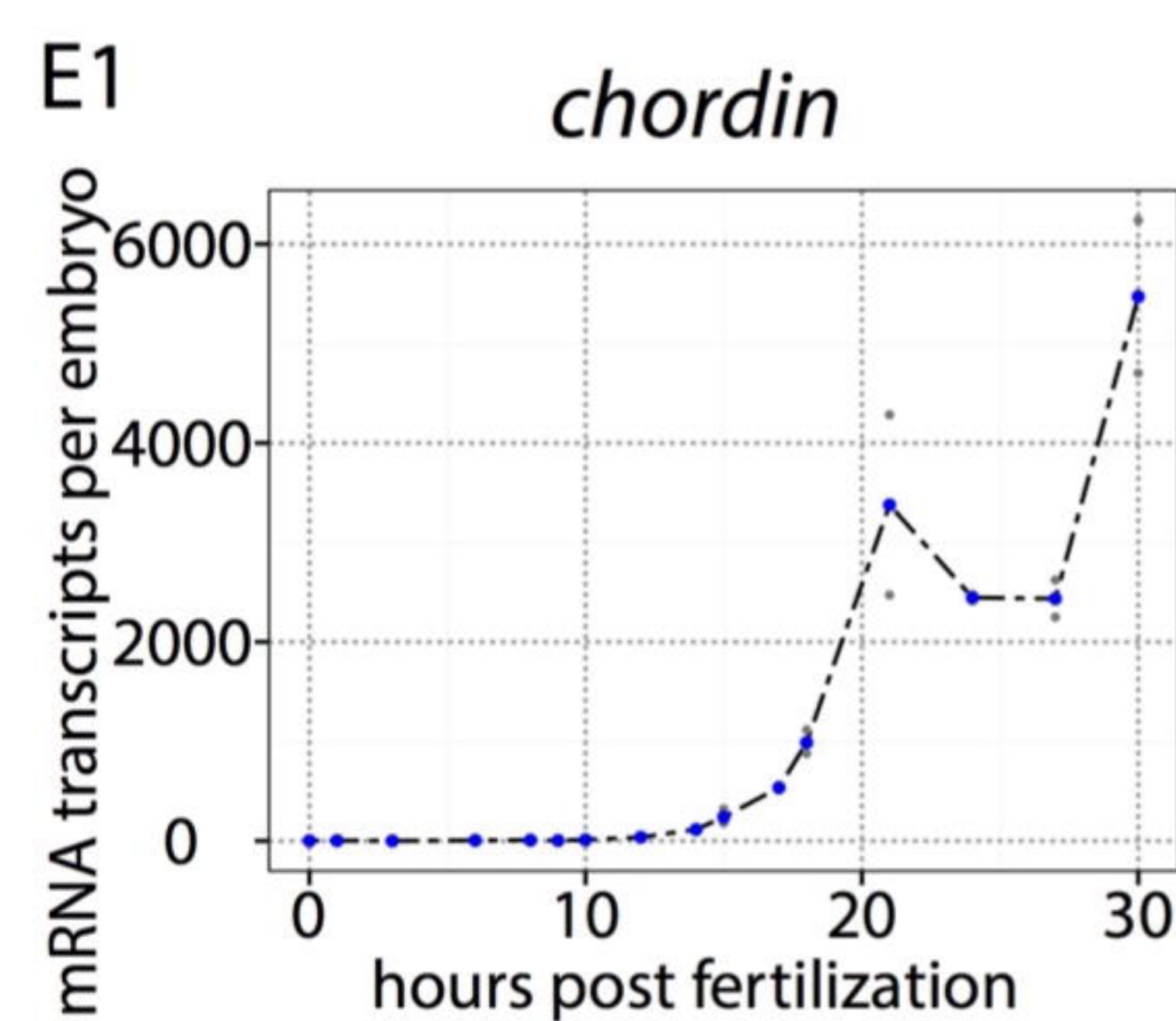
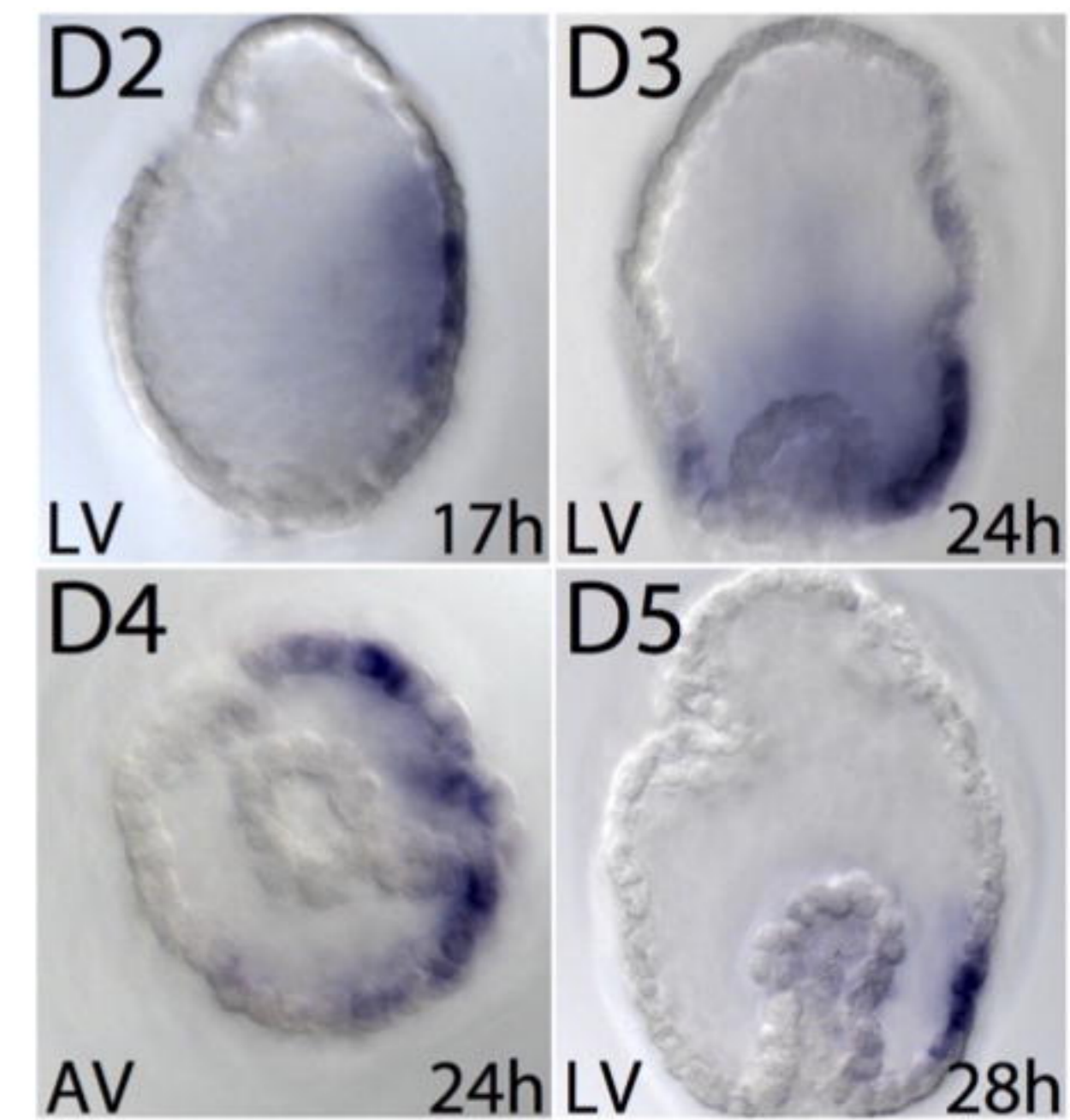
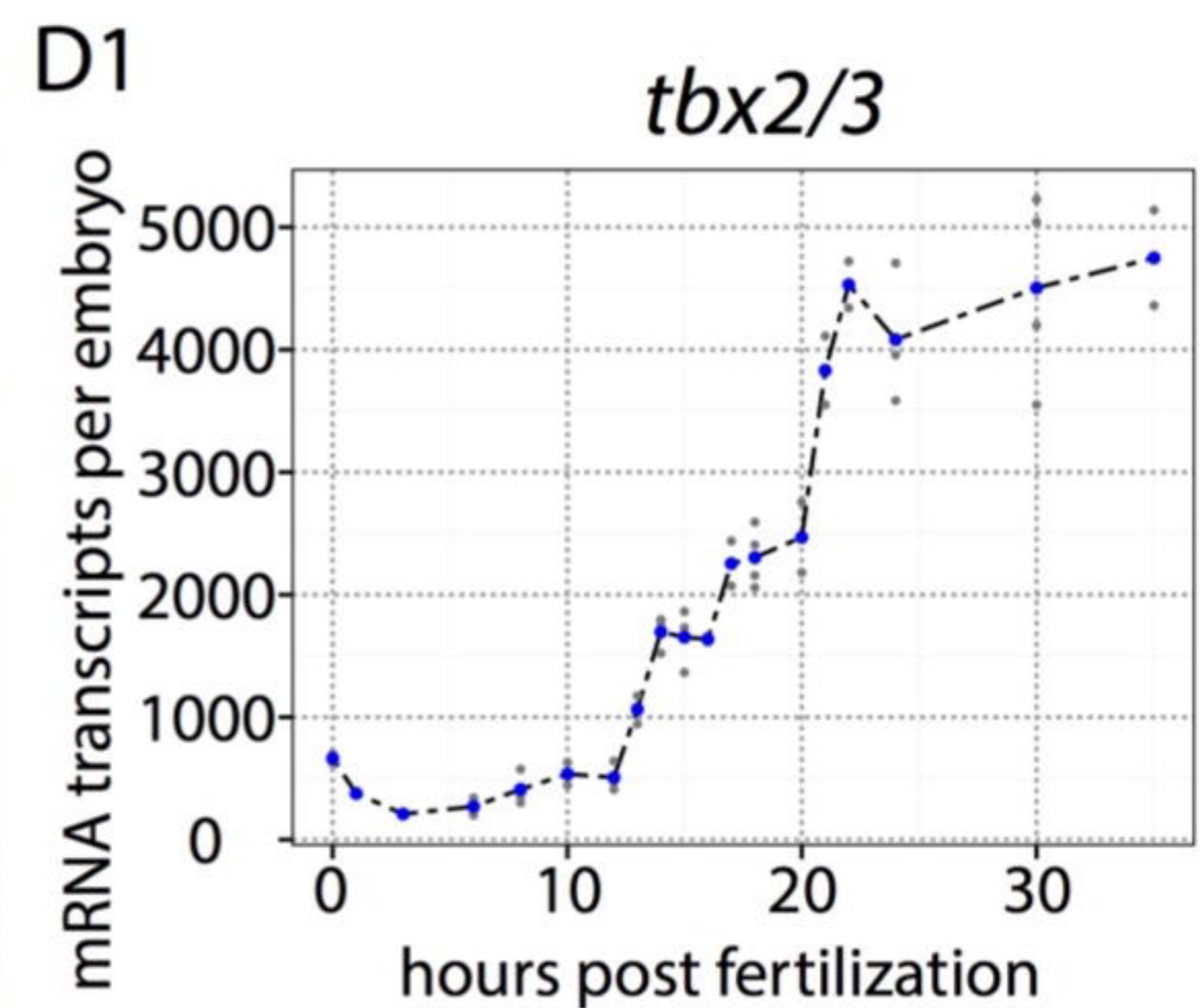
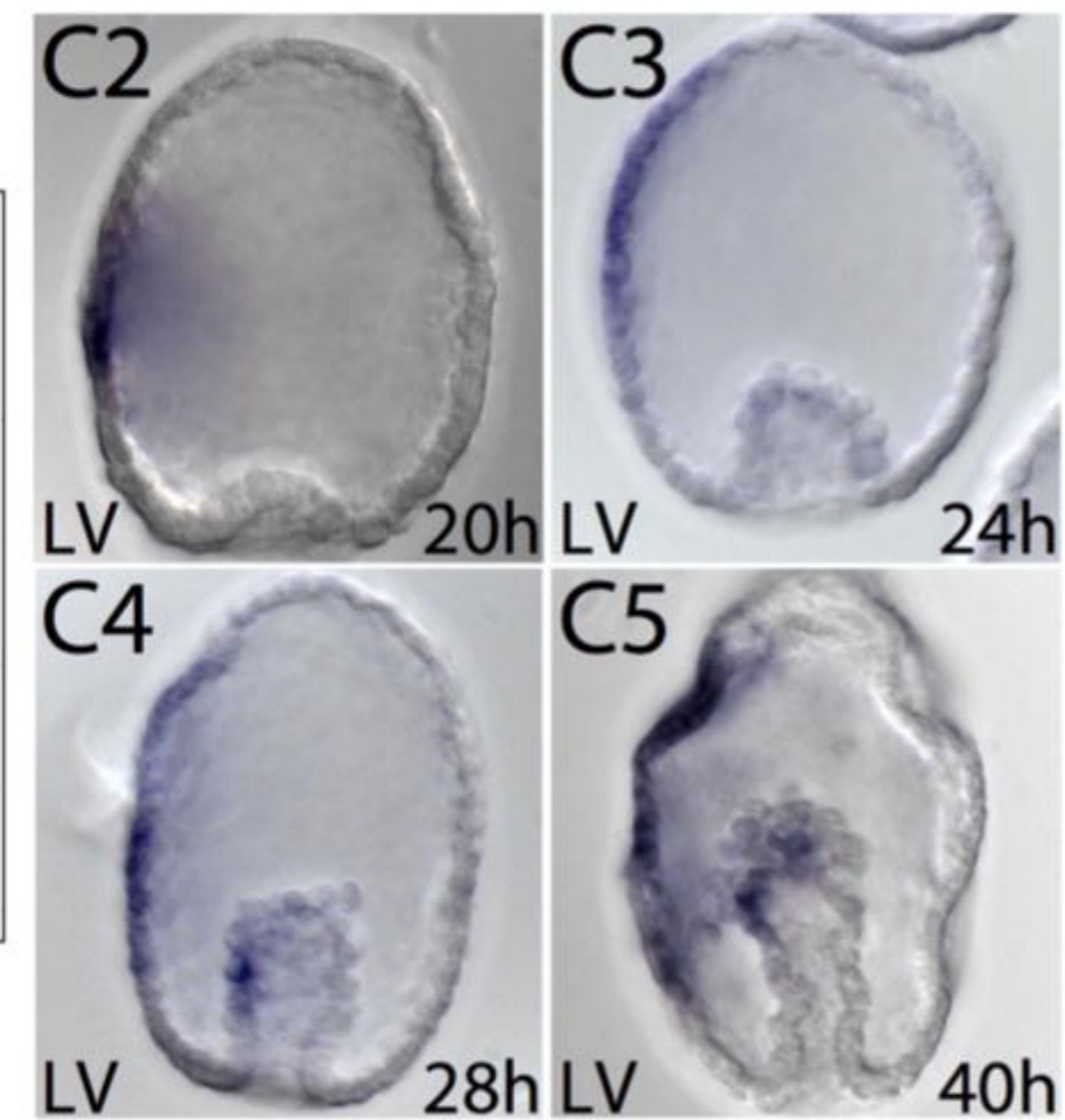
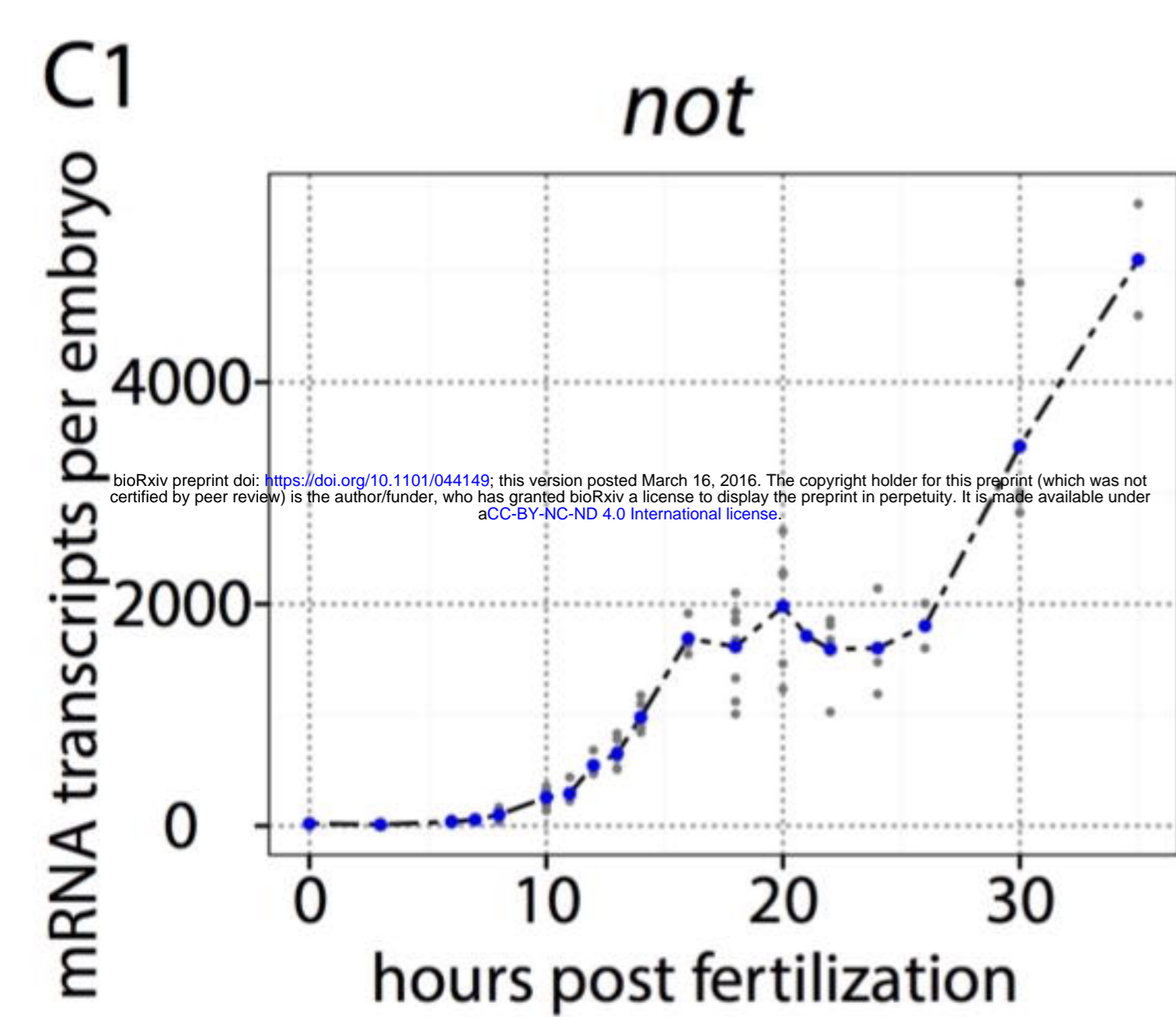
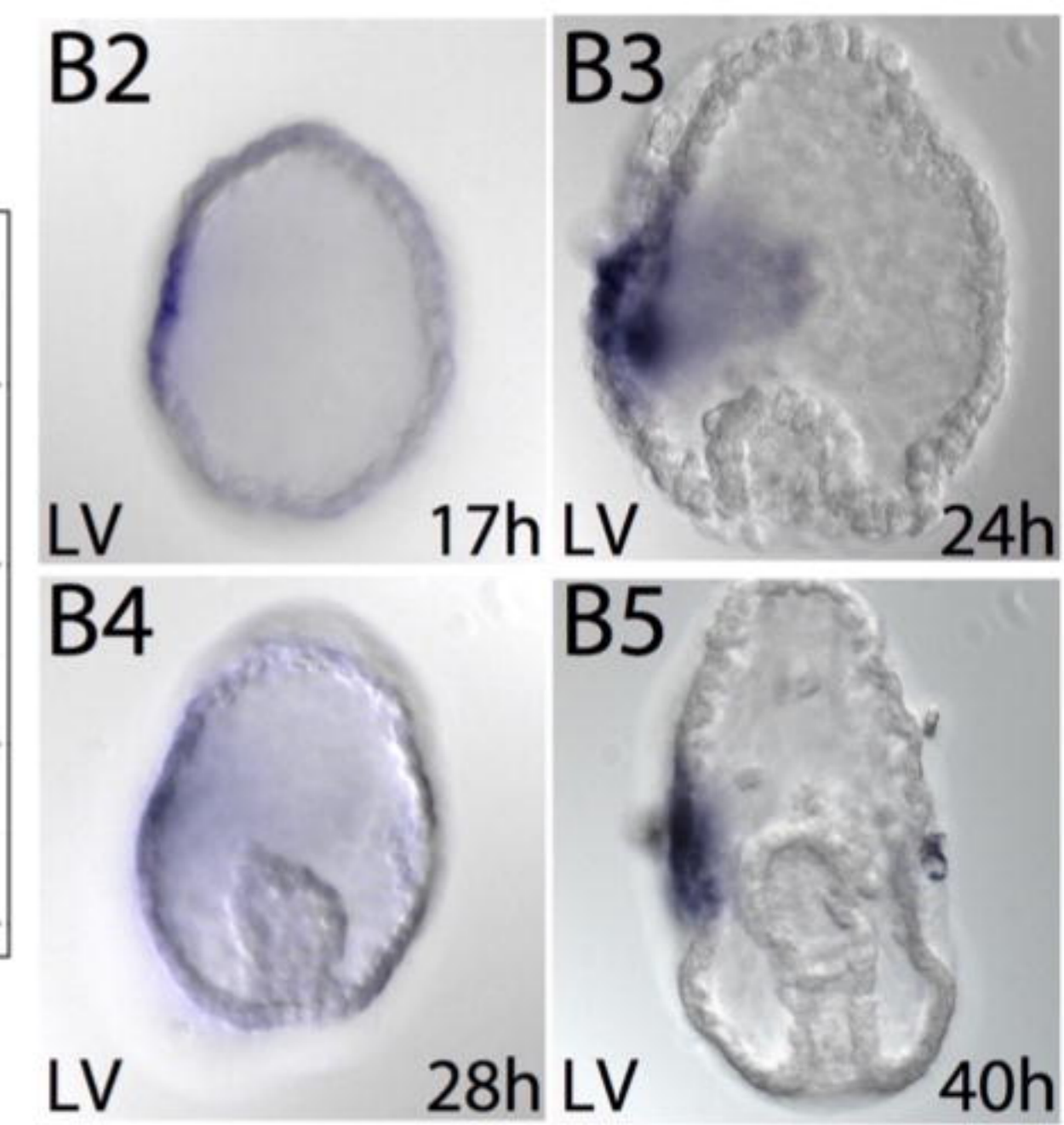
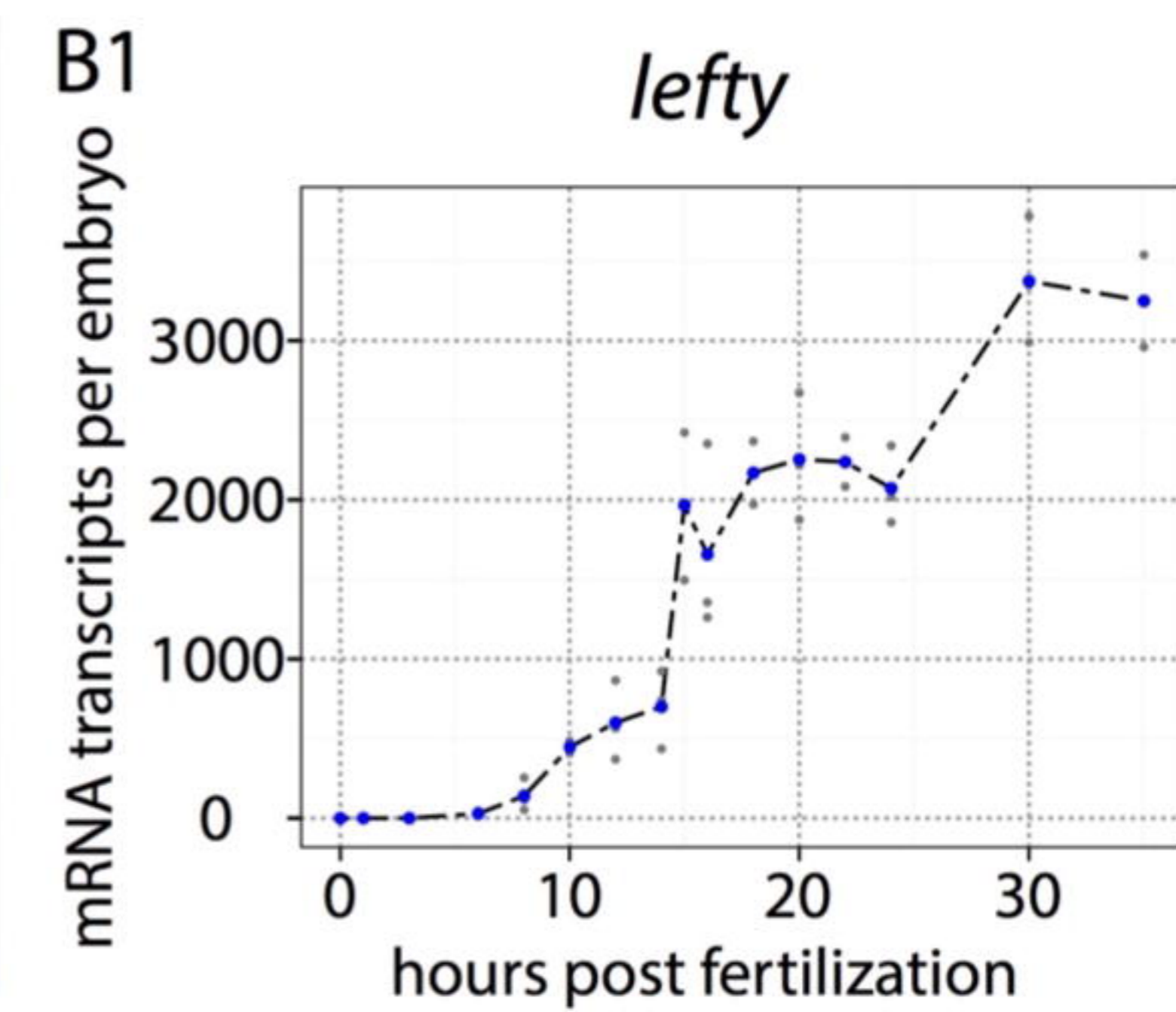
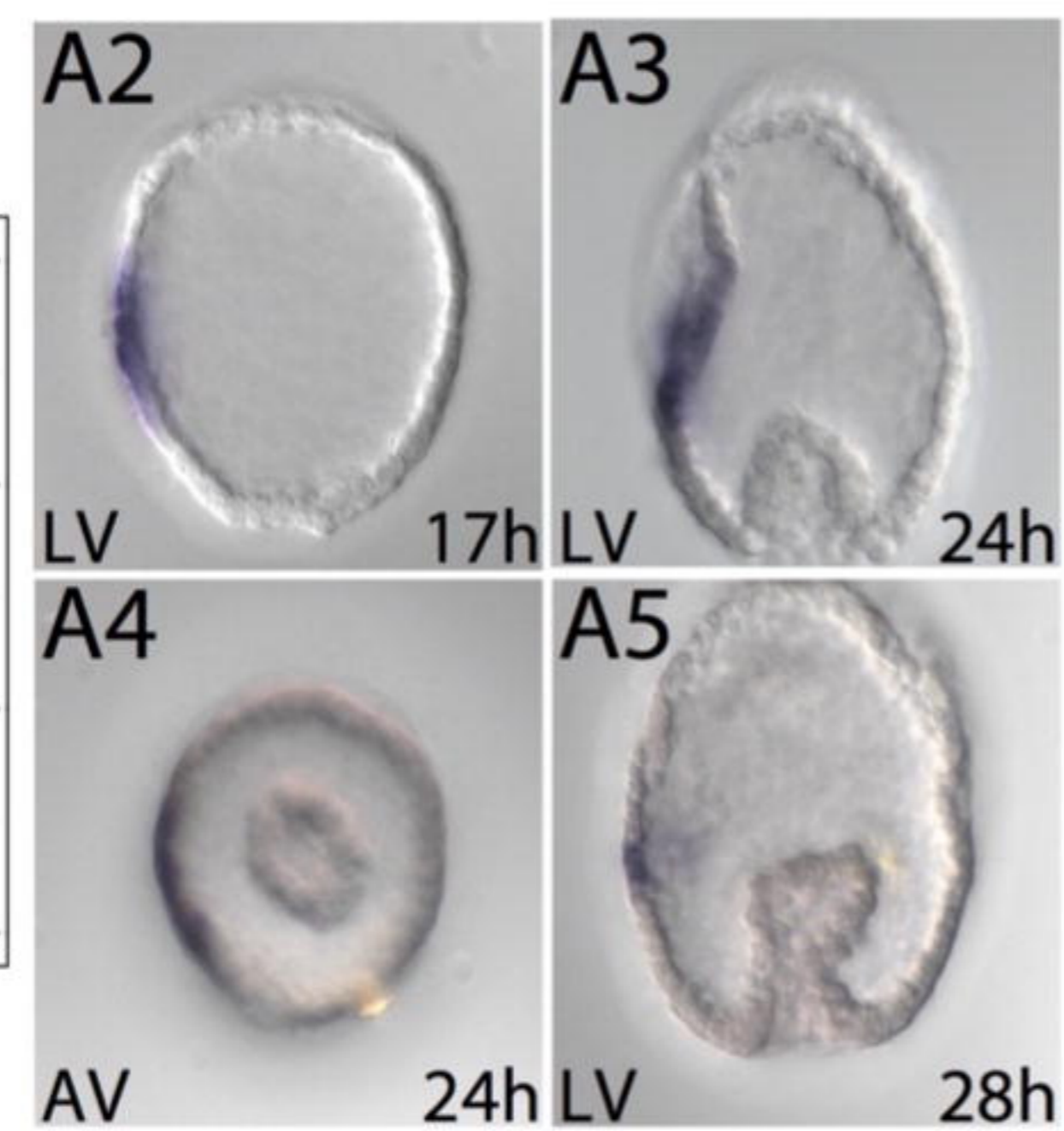
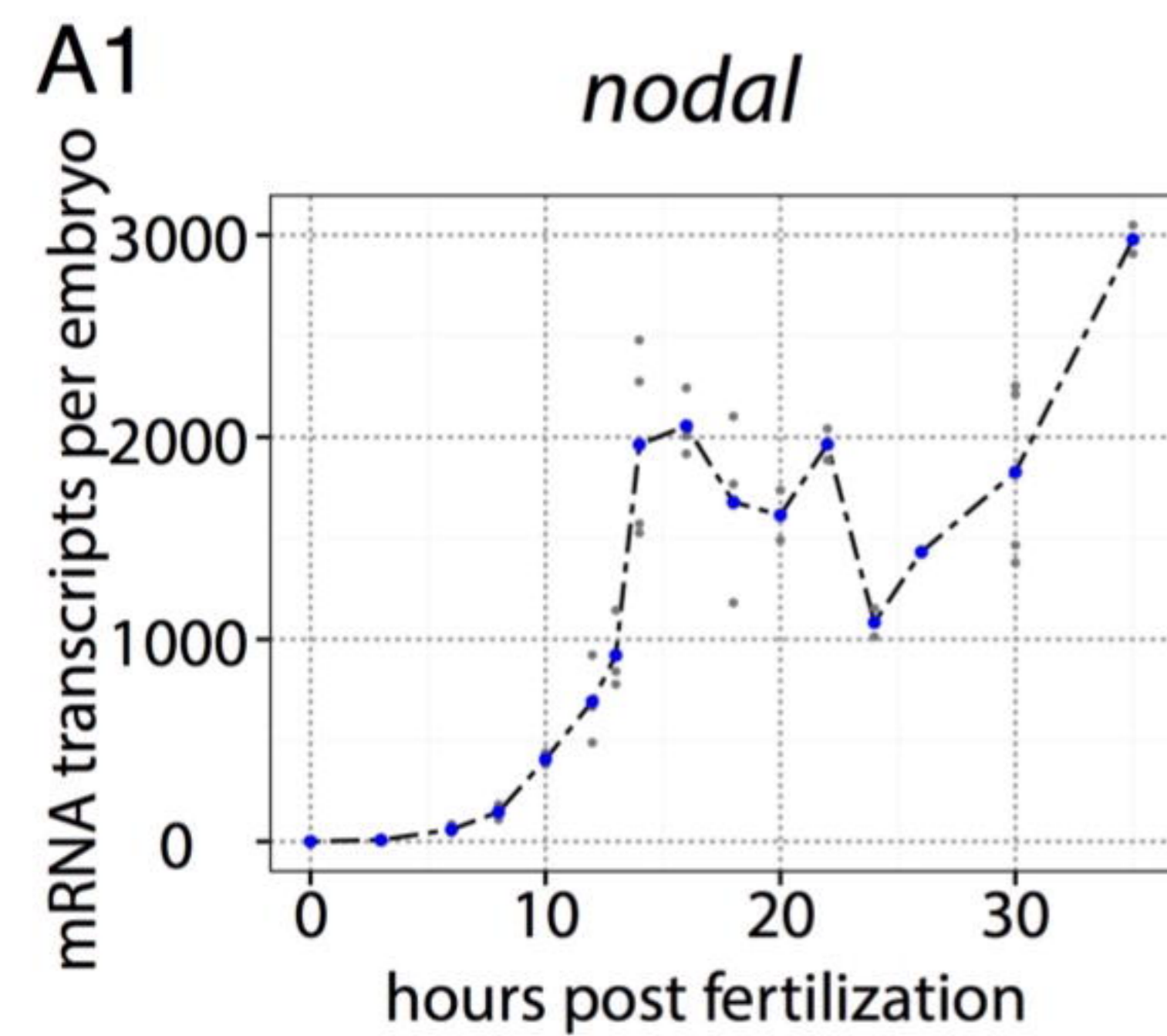
- 1 51. Duboc V, Lepage T. A conserved role for the nodal signaling pathway in the  
2 establishment of dorso-ventral and left-right axes in deuterostomes. *J Exp Zool Part B*.  
3 2008;310b(1):41-53.
- 4 52. Wray GA, Raff RA. The evolution of developmental strategy in marine  
5 invertebrates. *Trends Ecol Evol*. 1991;6(2):45-50.
- 6 53. Smith MS, Collins S, Raff RA. Morphogenetic mechanisms of coelom formation  
7 in the direct-developing sea urchin *Heliocidaris erythrogramma*. *Dev Genes Evol*.  
8 2009;219(1):21-9.
- 9 54. Smith MS, Turner FR, Raff RA. Nodal Expression and Heterochrony in the  
10 Evolution of Dorsal-Ventral and Left-Right Axes Formation in the Direct-Developing Sea  
11 Urchin *Heliocidaris erythrogramma*. *J Exp Zool Part B*. 2008;310b(8):609-22.
- 12 55. Raff RA. Origins of the other metazoan body plans: the evolution of larval forms.  
13 *Philos T R Soc B*. 2008;363(1496):1473-9.
- 14 56. Su Y-H. Gene regulatory networks for ectoderm specification in sea urchin  
15 embryos. *Biochimica et Biophysica Acta (BBA)-Gene Regulatory Mechanisms*.  
16 2009;1789(4):261-7.
- 17 57. Li E, Cui M, Peter IS, Davidson EH. Encoding regulatory state boundaries in the  
18 pregastrular oral ectoderm of the sea urchin embryo. *Proceedings of the National*  
19 *Academy of Sciences*. 2014;111(10):E906-E13.
- 20 58. Li E, Materna SC, Davidson EH. Direct and indirect control of oral ectoderm  
21 regulatory gene expression by Nodal signaling in the sea urchin embryo. *Dev Biol*.  
22 2012;369(2):377-85.
- 23 59. Li E, Materna SC, Davidson EH. New regulatory circuit controlling spatial and  
24 temporal gene expression in the sea urchin embryo oral ectoderm GRN. *Dev Biol*.  
25 2013;382(1):268-79.
- 26 60. Lapraz F, Besnardeau L, Lepage T. Patterning of the Dorsal-Ventral Axis in  
27 Echinoderms: Insights into the Evolution of the BMP-Chordin Signaling Network. *Plos*  
28 *Biology*. 2009;7(11).
- 29 61. de-Leon SB-T, Su Y-H, Lin K-T, Li E, Davidson EH. Gene regulatory control in  
30 the sea urchin aboral ectoderm: spatial initiation, signaling inputs, and cell fate  
31 lockdown. *Developmental biology*. 2013;374(1):245-54.
- 32 62. Croce J, Lhomond G, Gache C. Coquillet, a sea urchin T-box gene of the Tbx2  
33 subfamily, is expressed asymmetrically along the oral-aboral axis of the embryo and is  
34 involved in skeletogenesis. *Mech Dev*. 2003;120(5):561-72.
- 35 63. Gross JM, Peterson RE, Wu SY, McClay DR. LvTbx2/3: a T-box family  
36 transcription factor involved in formation of the oral/aboral axis of the sea urchin  
37 embryo. *Development*. 2003;130(9):1989-99.
- 38 64. Range R. Specification and positioning of the anterior neuroectoderm in  
39 deuterostome embryos. *genesis*. 2014;52(3):222-34.
- 40 65. Strathmann RR. The feeding behavior of planktotrophic echinoderm larvae:  
41 mechanisms, regulation, and rates of suspensionfeeding. *Journal of Experimental*  
42 *Marine Biology and Ecology*. 1971;6(2):109-60.
- 43 66. Wray GA. The Evolution of Larval Morphology during the Postpaleozoic  
44 Radiation of Echinoids. *Paleobiology*. 1992;18(3):258-87.

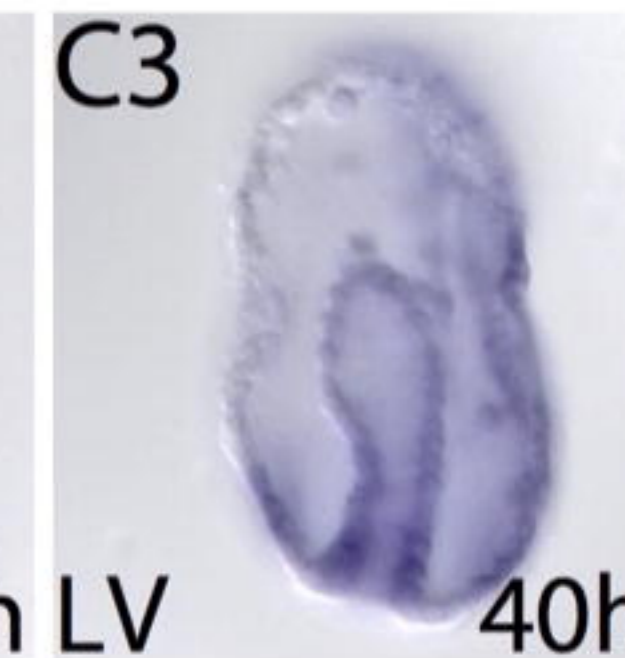
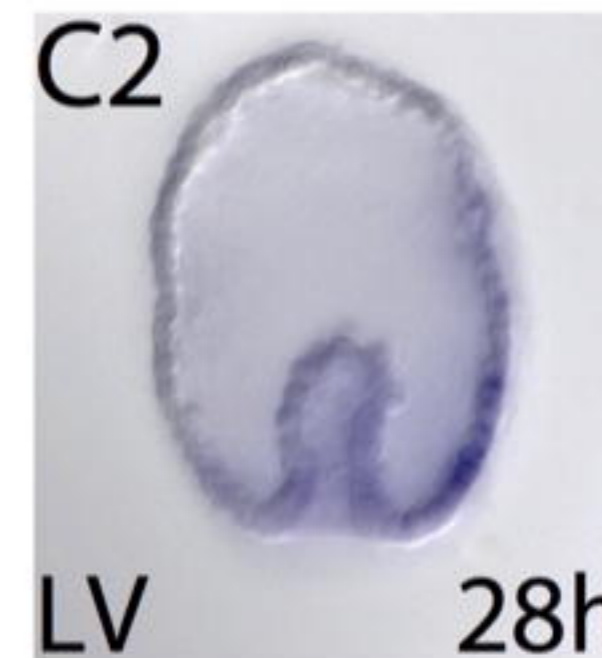
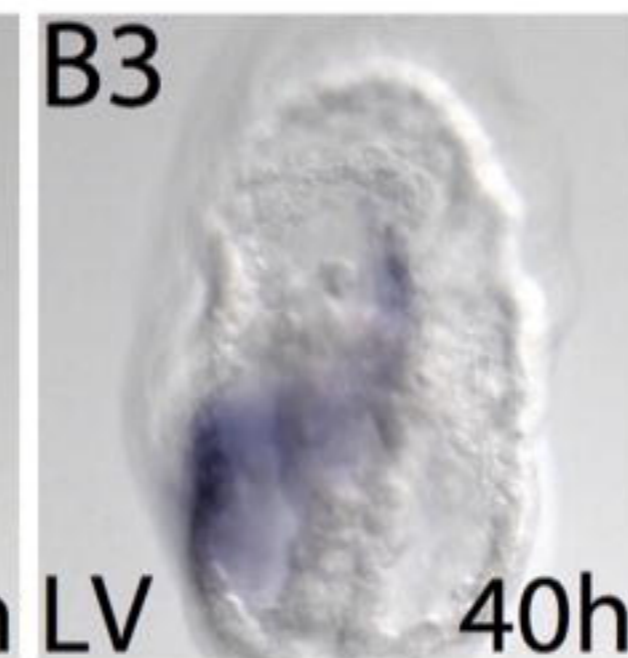
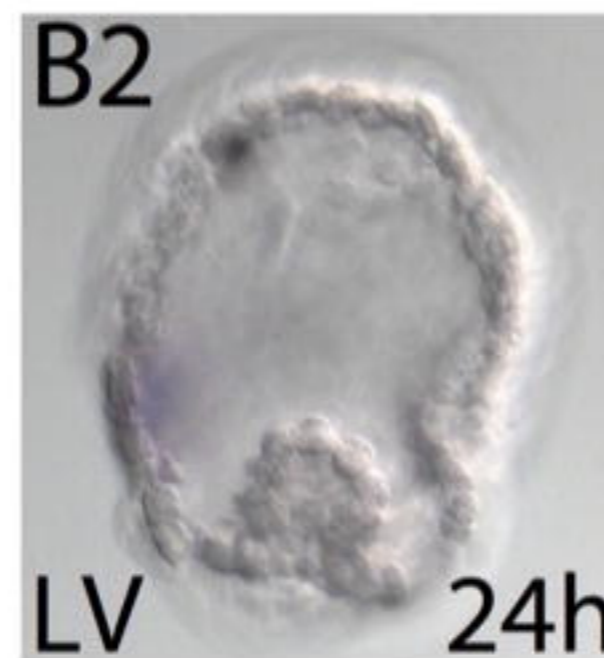
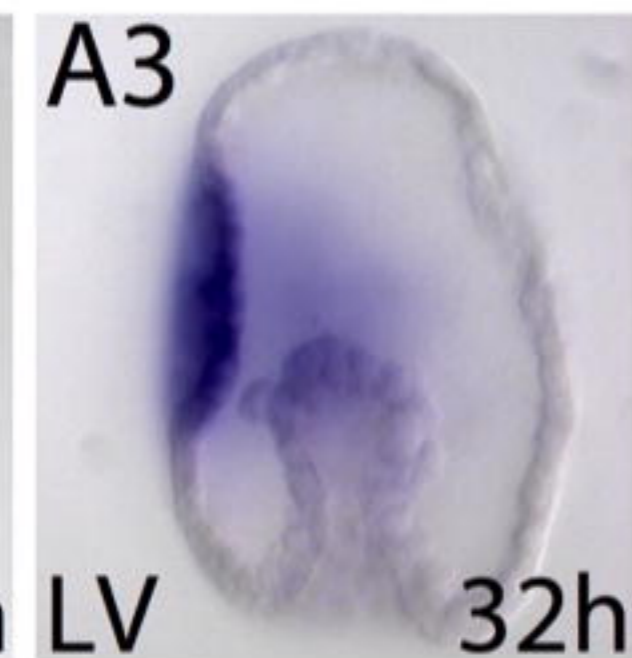
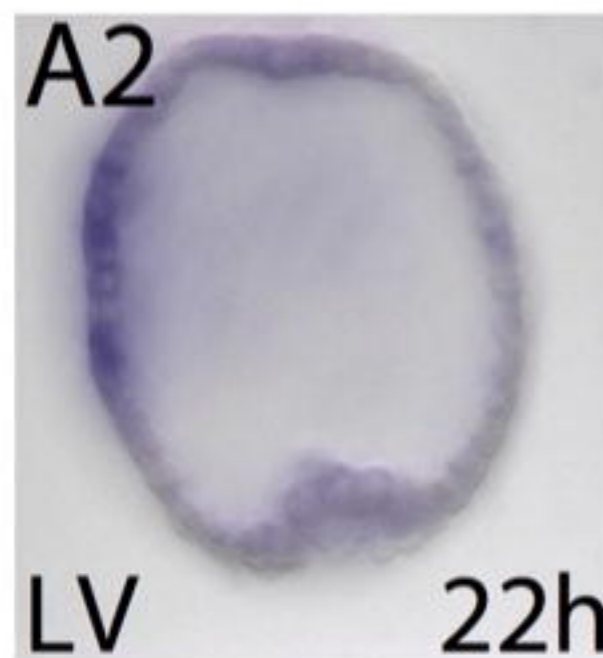
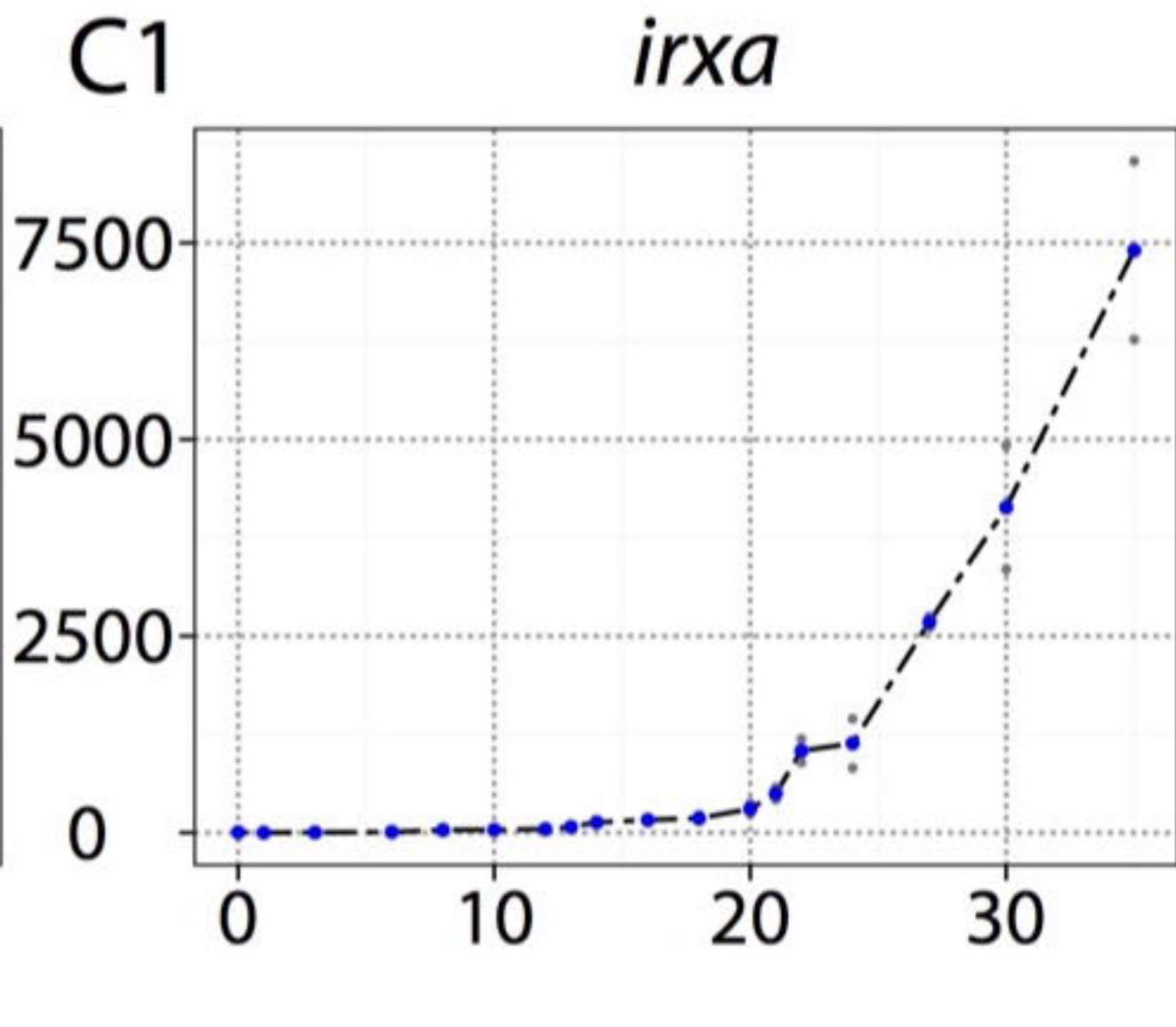
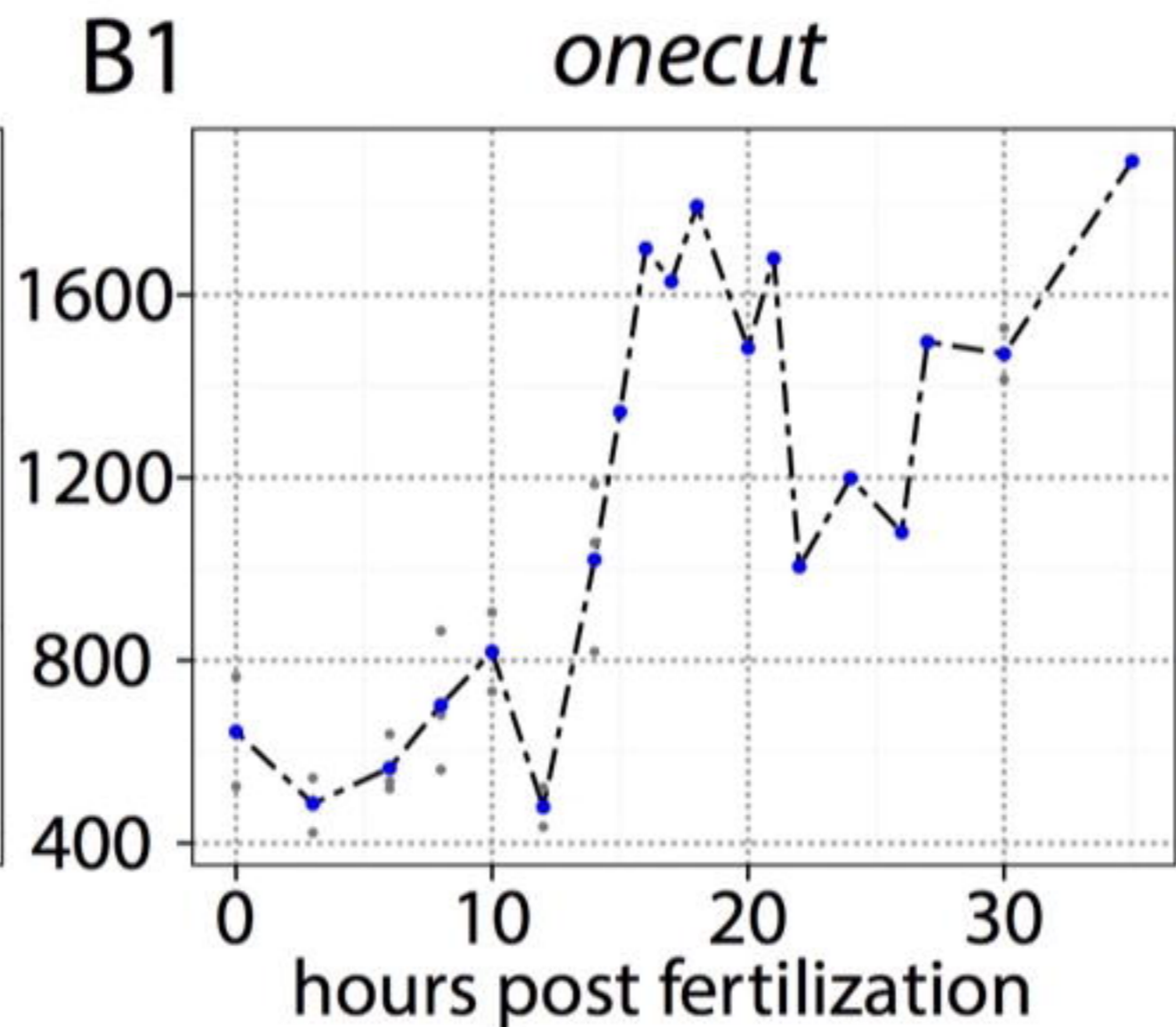
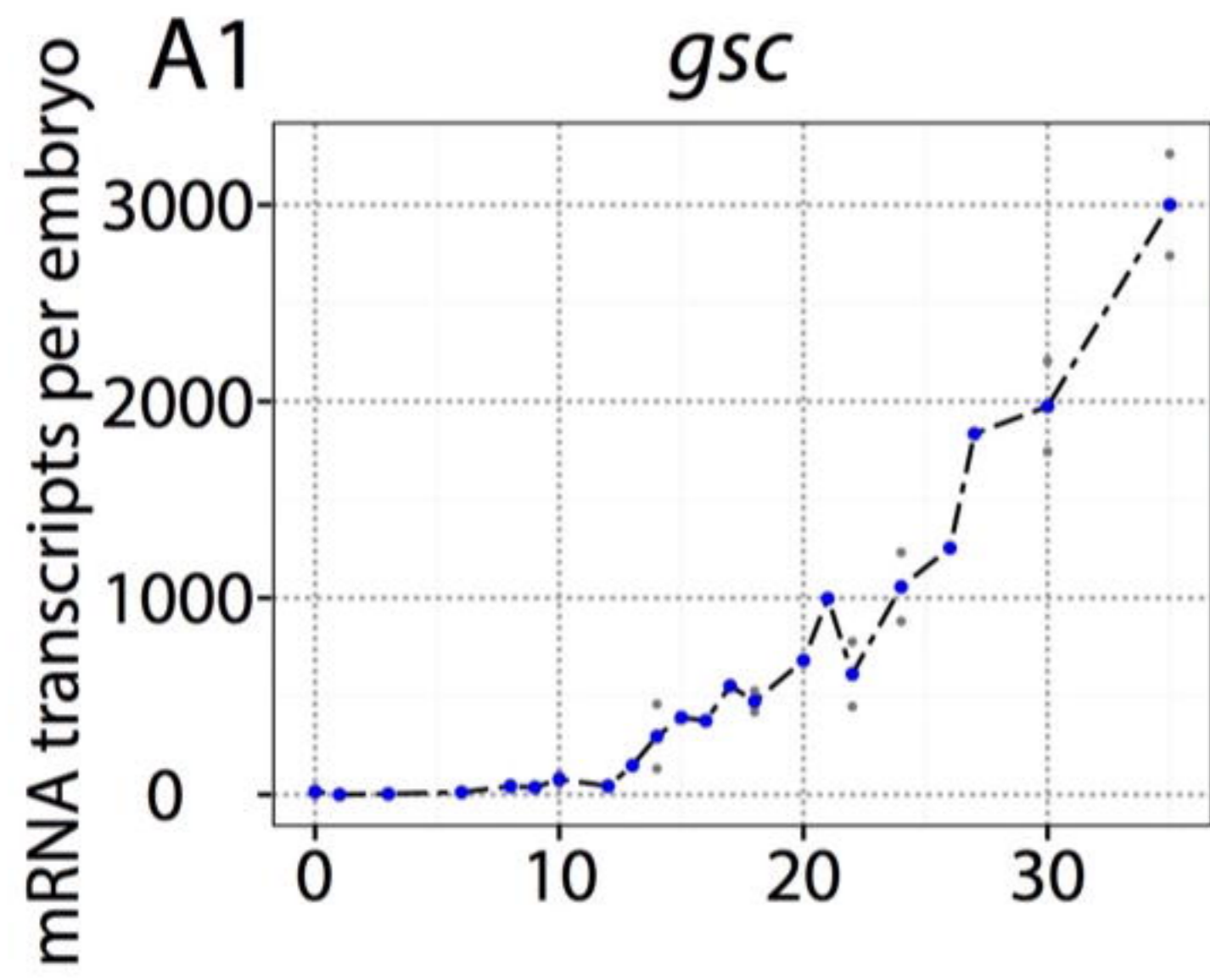
- 1 67. Barsi JC, Davidson EH. cis-Regulatory control of the initial neurogenic pattern of  
2 onecut gene expression in the sea urchin embryo. *Developmental Biology*.  
3 2016;409(1):310-8.
- 4 68. Poustka AJ, Kuhn A, Groth D, Weise V, Yaguchi S, Burke RD, et al. A global  
5 view of gene expression in lithium and zinc treated sea urchin embryos: new  
6 components of gene regulatory networks. *Genome Biol*. 2007;8(5):R85.
- 7 69. Otim O, Amore G, Minokawa T, McClay DR, Davidson EH. SpHnf6, a  
8 transcription factor that executes multiple functions in sea urchin embryogenesis. *Dev*  
9 *Biol*. 2004;273(2):226-43.
- 10 70. Cameron RA, Davidson EH. Cell type specification during sea urchin  
11 development. *Trends Genet*. 1991;7(7):212-8.
- 12 71. Sweet HC, Hodor PG, Etensohn CA. The role of micromere signaling in Notch  
13 activation and mesoderm specification during sea urchin embryogenesis. *Development*.  
14 1999;126(23):5255-65.
- 15 72. Materna SC, Davidson EH. A comprehensive analysis of Delta signaling in pre-  
16 gastrular sea urchin embryos. *Dev Biol*. 2012;364(1):77-87.
- 17 73. Duboc V, Lapraz F, Saudemont A, Bessodes N, Mekpoh F, Haillet E, et al. Nodal  
18 and BMP2/4 pattern the mesoderm and endoderm during development of the sea  
19 urchin embryo. *Development*. 2010;137(2):223-35.
- 20 74. Rizzo F, Fernandez-Serra M, Squarzone P, Archimandritis A, Arnone MI.  
21 Identification and developmental expression of the ets gene family in the sea urchin  
22 (*Strongylocentrotus purpuratus*). *Dev Biol*. 2006;300(1):35-48.
- 23 75. Ransick A, Rast JP, Minokawa T, Calestani C, Davidson EH. New early zygotic  
24 regulators expressed in endomesoderm of sea urchin embryos discovered by  
25 differential array hybridization. *Dev Biol*. 2002;246(1):132-47.
- 26 76. Hinman VF, Davidson EH. Evolutionary plasticity of developmental gene  
27 regulatory network architecture. *Proc Natl Acad Sci U S A*. 2007;104(49):19404-9.
- 28 77. Lee PY, Davidson EH. Expression of Spgatae, the *Strongylocentrotus purpuratus*  
29 ortholog of vertebrate GATA4/5/6 factors. *Gene Expression Patterns*. 2004;5(2):161-5.
- 30 78. Duboc V, Rottinger E, Lapraz F, Besnardeau L, Lepage T. Left-right asymmetry  
31 in the sea urchin embryo is regulated by nodal signaling on the right side.  
32 *Developmental Cell*. 2005;9(1):147-58.
- 33 79. Oliveri P, Walton KD, Davidson EH, McClay DR. Repression of mesodermal fate  
34 by foxa, a key endoderm regulator of the sea urchin embryo. *Development*.  
35 2006;133(21):4173-81.
- 36 80. Bradham CA, Oikonomou C, Kuhn A, Core AB, Modell JW, McClay DR, et al.  
37 Chordin is required for neural but not axial development in sea urchin embryos. *Dev*  
38 *Biol*. 2009;328(2):221-33.
- 39 81. Bishop CD, MacNeil KE, Patel D, Taylor VJ, Burke RD. Neural development in  
40 *Eucidaris tribuloides* and the evolutionary history of the echinoid larval nervous system.  
41 *Dev Biol*. 2013;377(1):236-44.
- 42 82. Materna SC, Nam J, Davidson EH. High accuracy, high-resolution prevalence  
43 measurement for the majority of locally expressed regulatory genes in early sea urchin  
44 development. *Gene Expr Patterns*. 2010;10(4-5):177-84.
- 45 83. Tu Q, Cameron RA, Davidson EH. Quantitative developmental transcriptomes of  
46 the sea urchin *Strongylocentrotus purpuratus*. *Dev Biol*. 2014;385(2):160-7.

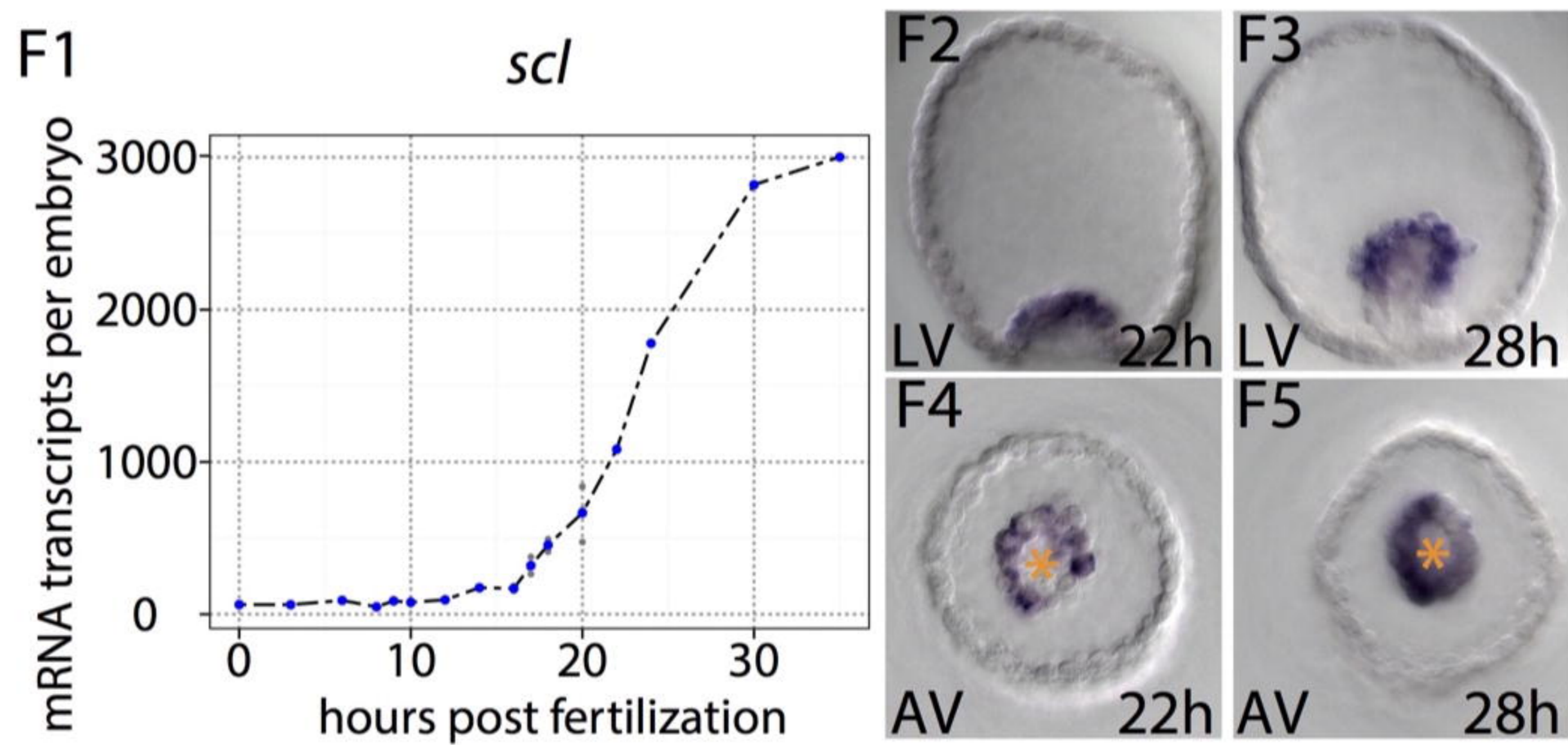
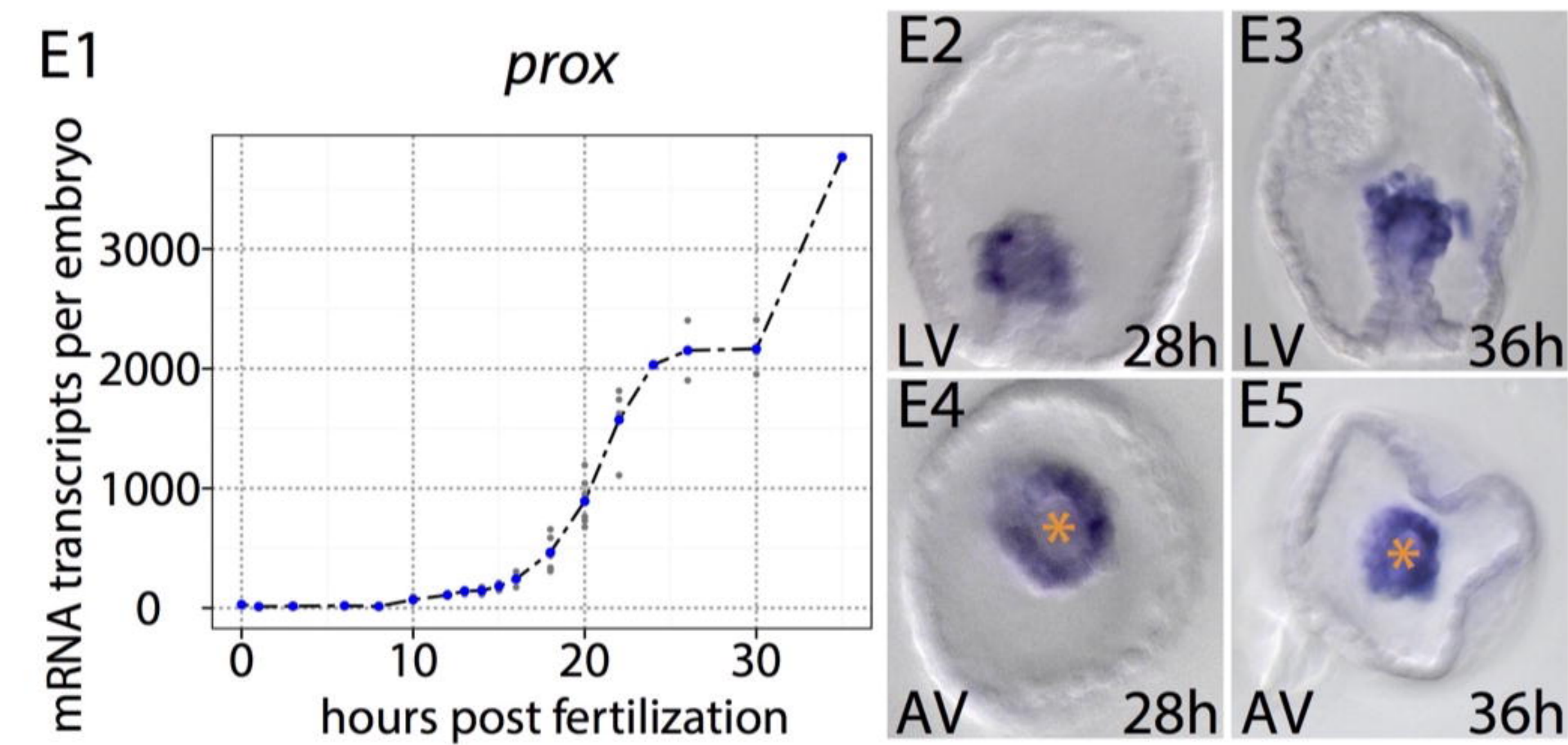
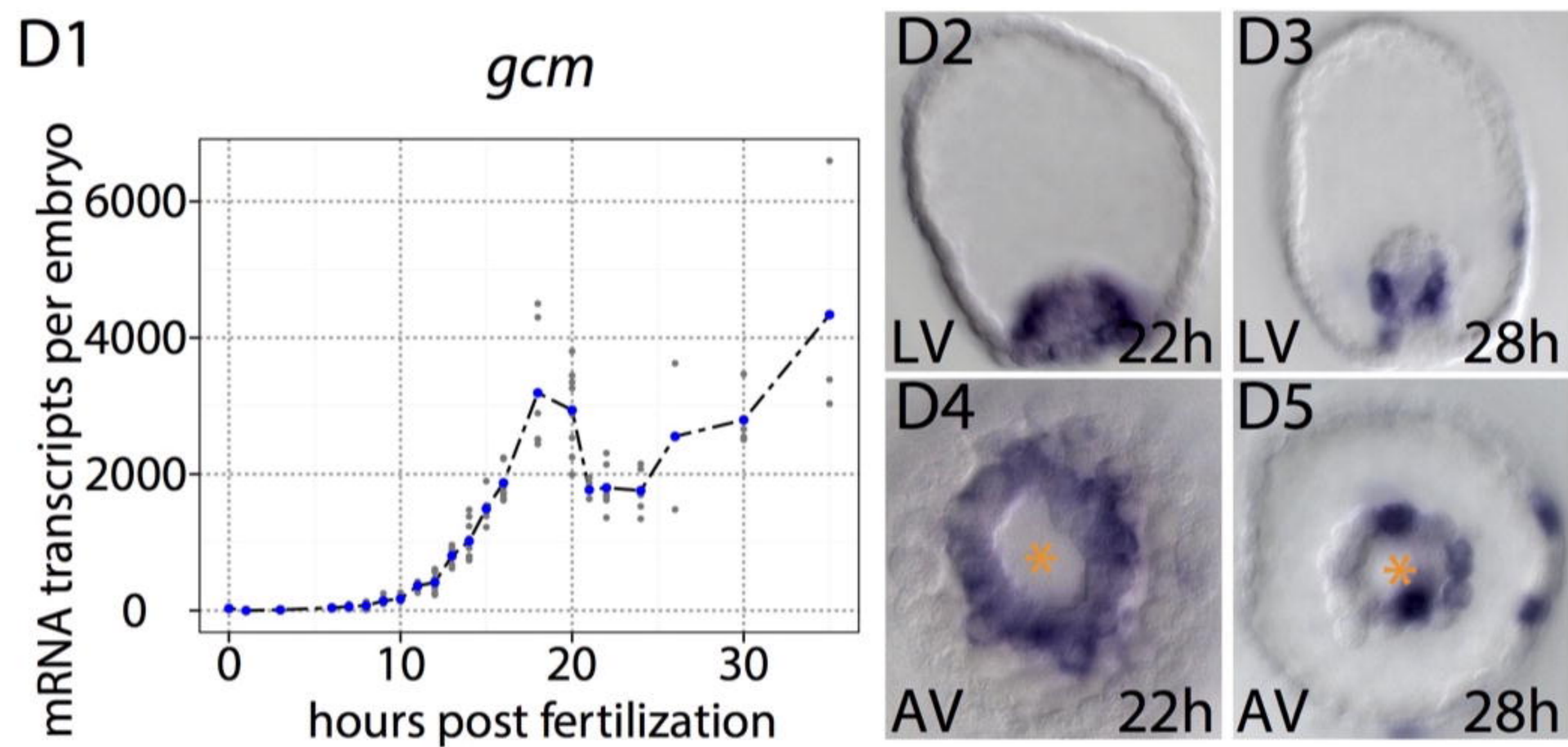
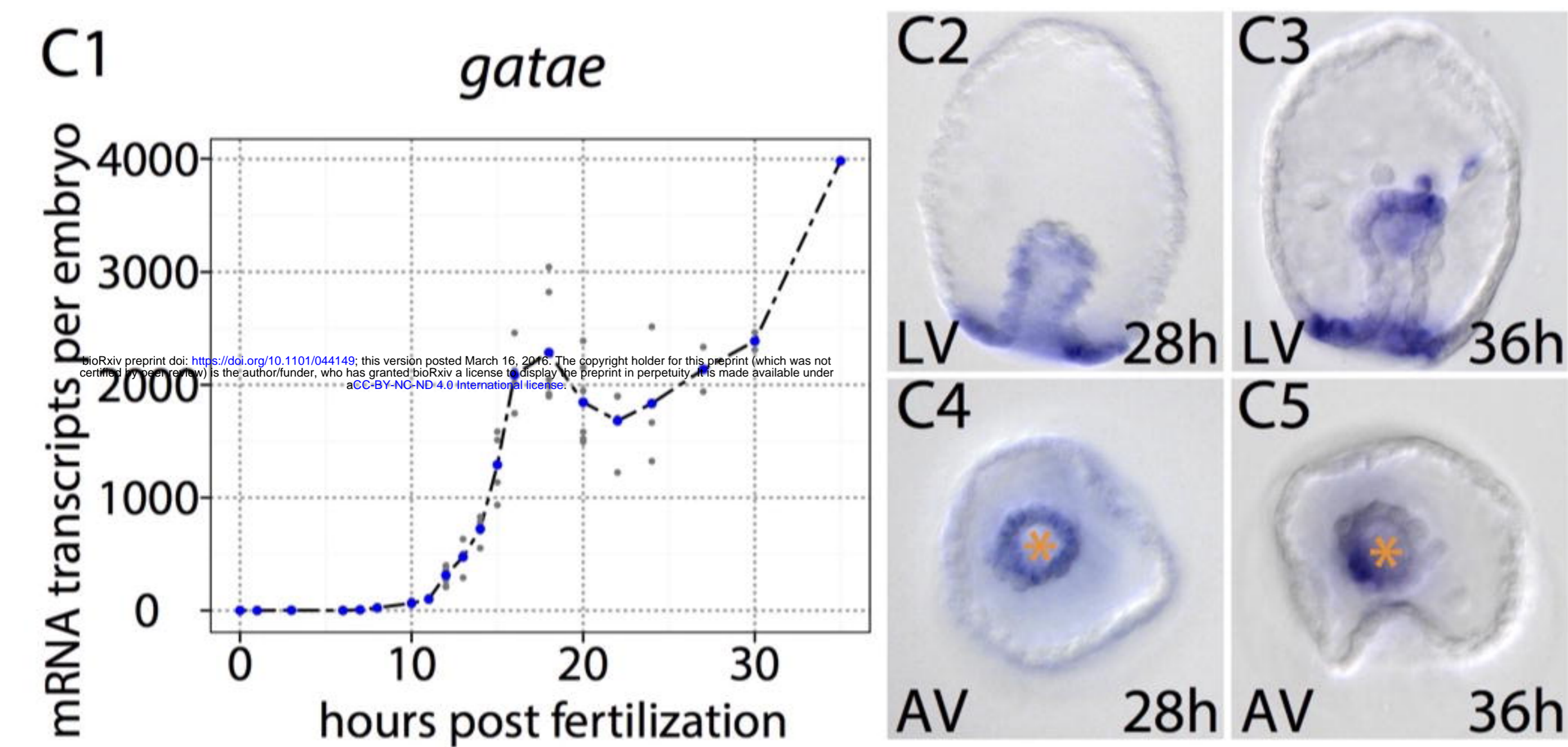
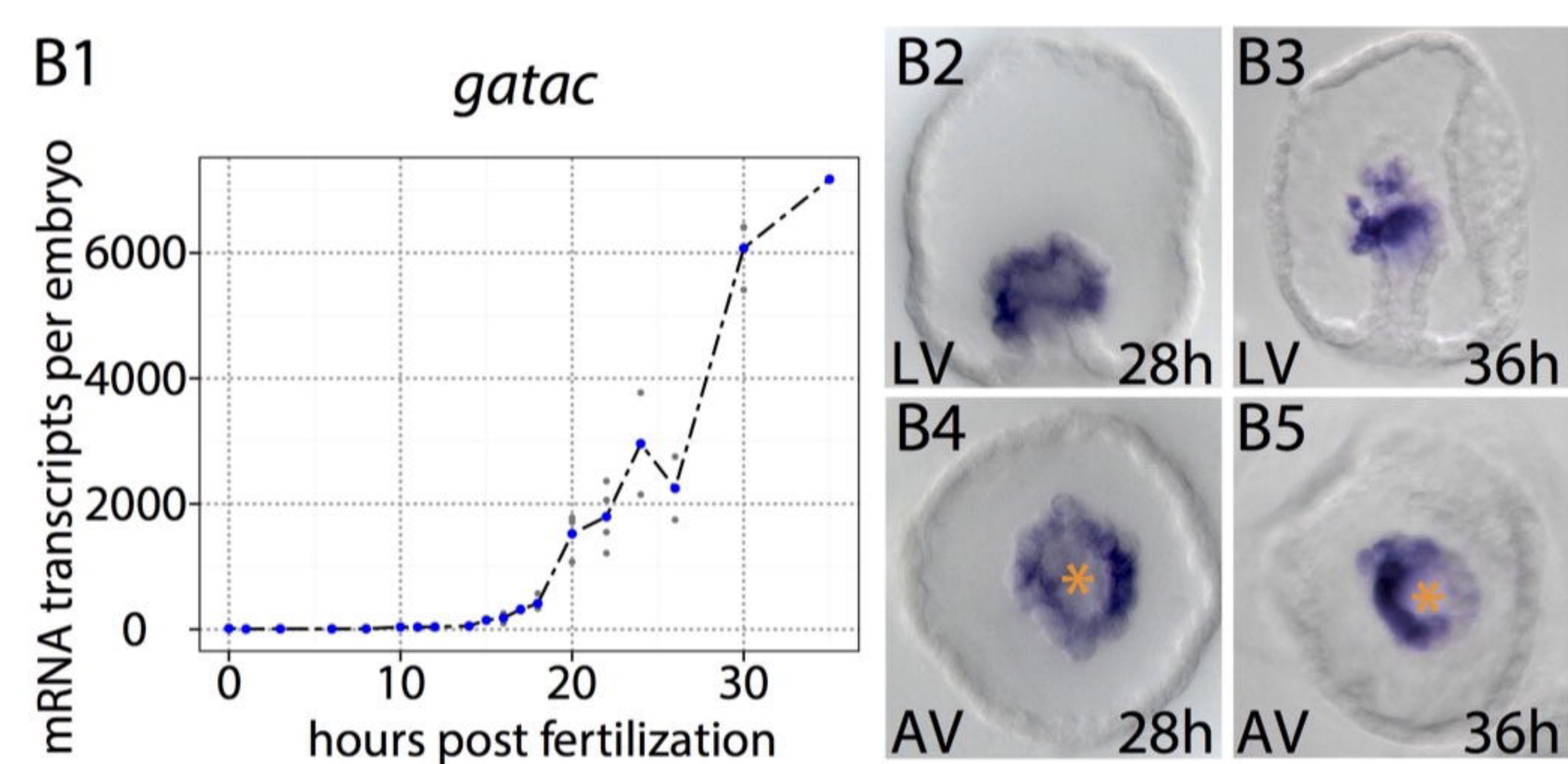
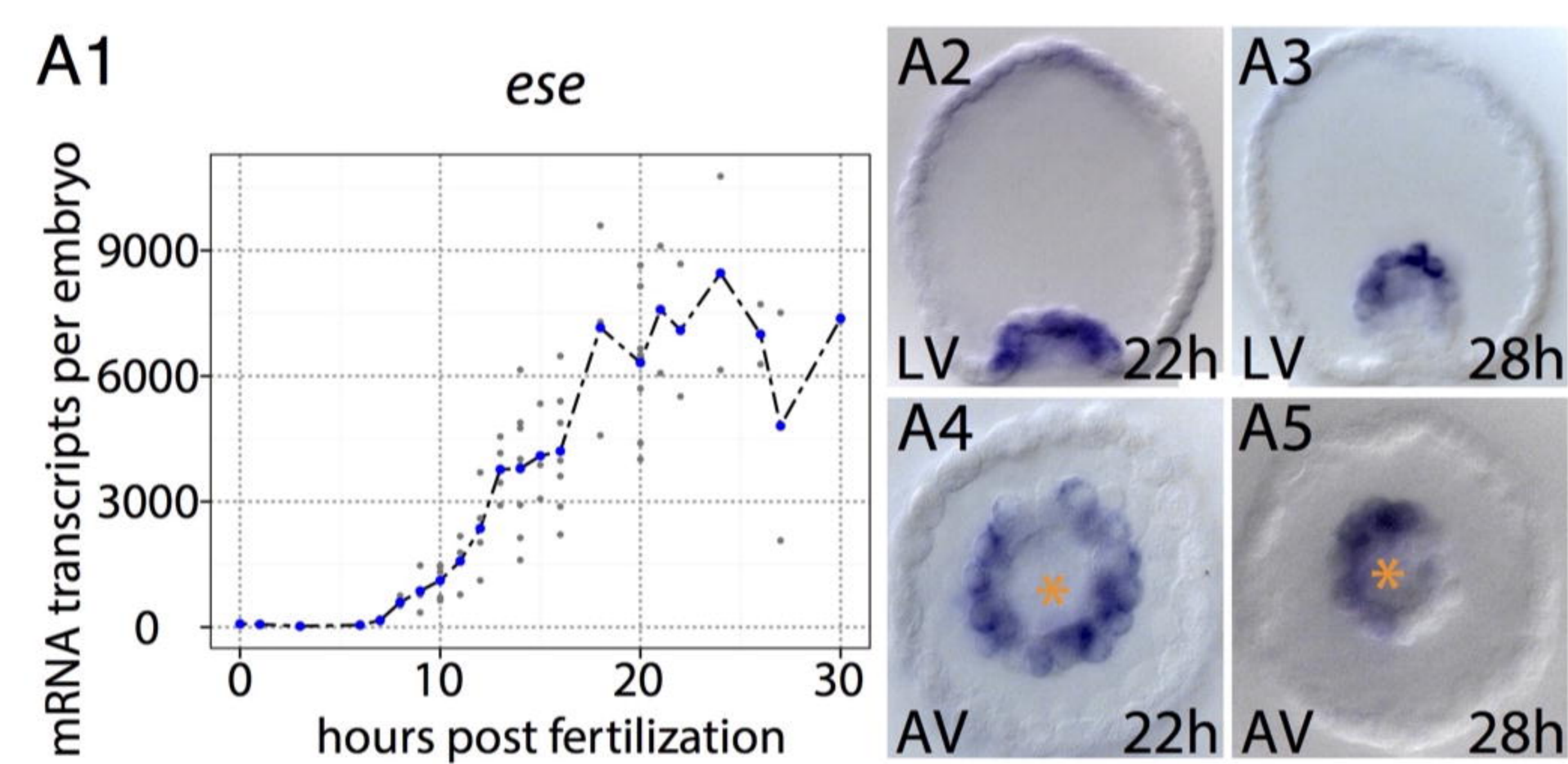
- 1 84. Gildor T, de-Leon SB-T. Comparative Study of Regulatory Circuits in Two Sea  
2 Urchin Species Reveals Tight Control of Timing and High Conservation of Expression  
3 Dynamics. *Plos Genet.* 2015;11(7):e1005435.
- 4 85. Ransick A, Davidson EH. cis-regulatory processing of Notch signaling input to  
5 the sea urchin glial cells missing gene during mesoderm specification. *Dev Biol.*  
6 2006;297(2):587-602.
- 7 86. McCauley BS, Wright EP, Exner C, Kitazawa C, Hinman VF. Development of an  
8 embryonic skeletogenic mesenchyme lineage in a sea cucumber reveals the trajectory  
9 of change for the evolution of novel structures in echinoderms. *Evodevo.* 2012;3(1):17.
- 10 87. Urben S, Nislow C, Spiegel M. The origin of skeleton forming cells in the sea  
11 urchin embryo. *Roux's Arch Dev Biol.* 1988;197:447-56.
- 12 88. Dylus DV, Czarkwiani A, Stangberg J, Ortega-Martinez O, Dupont S, Oliveri P.  
13 Large-scale gene expression study in the ophiuroid *Amphiura filiformis* provides insights  
14 into evolution of gene regulatory networks. *Evodevo.* 2016;7.
- 15 89. Wilson KA, Andrews ME, Turner FR, Raff RA. Major regulatory factors in the  
16 evolution of development: the roles of goosecoid and *Msx* in the evolution of the direct-  
17 developing sea urchin *Heliocidaris erythrogramma*. *Evolution & Development.*  
18 2005;7(5):416-28.
- 19 90. Wilson KA, Andrews ME, Raff RA. Dissociation of expression patterns of  
20 homeodomain transcription factors in the evolution of developmental mode in the sea  
21 urchins *Heliocidaris tuberculata* and *H-erythrogramma*. *Evolution & Development.*  
22 2005;7(5):401-15.
- 23 91. Raff RA, Smith MS. Axis Formation and the Rapid Evolutionary Transformation  
24 of Larval Form. *Current Topics in Developmental Biology*, Vol 86. 2009;86:163-90.
- 25 92. Emler RB. Larval Form and Metamorphosis of a Primitive Sea-Urchin, *Eucidaris-*  
26 *Thouarsi* (Echinodermata, Echinoidea, Cidaroida), with Implications for Developmental  
27 and Phylogenetic Studies. *Biological Bulletin.* 1988;174(1):4-19.
- 28 93. Bennett KC, Young CM, Emler RB. Larval Development and Metamorphosis of  
29 the Deep-Sea Cidaroid Urchin *Cidaris blakei*. *Biological Bulletin.* 2012;222(2):105-17.
- 30 94. Tu Q, Brown CT, Davidson EH, Oliveri P. Sea urchin Forkhead gene family:  
31 phylogeny and embryonic expression. *Dev Biol.* 2006;300(1):49-62.
- 32 95. Santagata S, Resh C, Hejnal A, Martindale MQ, Passamaneck YJ. Development  
33 of the larval anterior neurogenic domains of *Terebratalia transversa* (Brachiopoda)  
34 provides insights into the diversification of larval apical organs and the spiralian nervous  
35 system. *EvoDevo.* 2012;3(1):1.
- 36 96. Yu JK, Mazet F, Chen YT, Huang SW, Jung KC, Shimeld SM. The Fox genes of  
37 *Branchiostoma floridae*. *Dev Genes Evol.* 2008;218(11-12):629-38.
- 38 97. Fritzenwanker JH, Gerhart J, Freeman RM, Lowe CJ. The Fox/Forkhead  
39 transcription factor family of the hemichordate *Saccoglossus kowalevskii*. *Evodevo.*  
40 2014;5.
- 41 98. Yankura KA, Martik ML, Jennings CK, Hinman VF. Uncoupling of complex  
42 regulatory patterning during evolution of larval development in echinoderms. *Bmc*  
43 *Biology.* 2010;8.
- 44 99. Yamazaki A, Kidachi Y, Minokawa T. "Micromere" formation and expression of  
45 endomesoderm regulatory genes during embryogenesis of the primitive echinoid  
46 *Prionocidaris baculosa*. *Dev Growth Differ.* 2012;54(5):566-78.

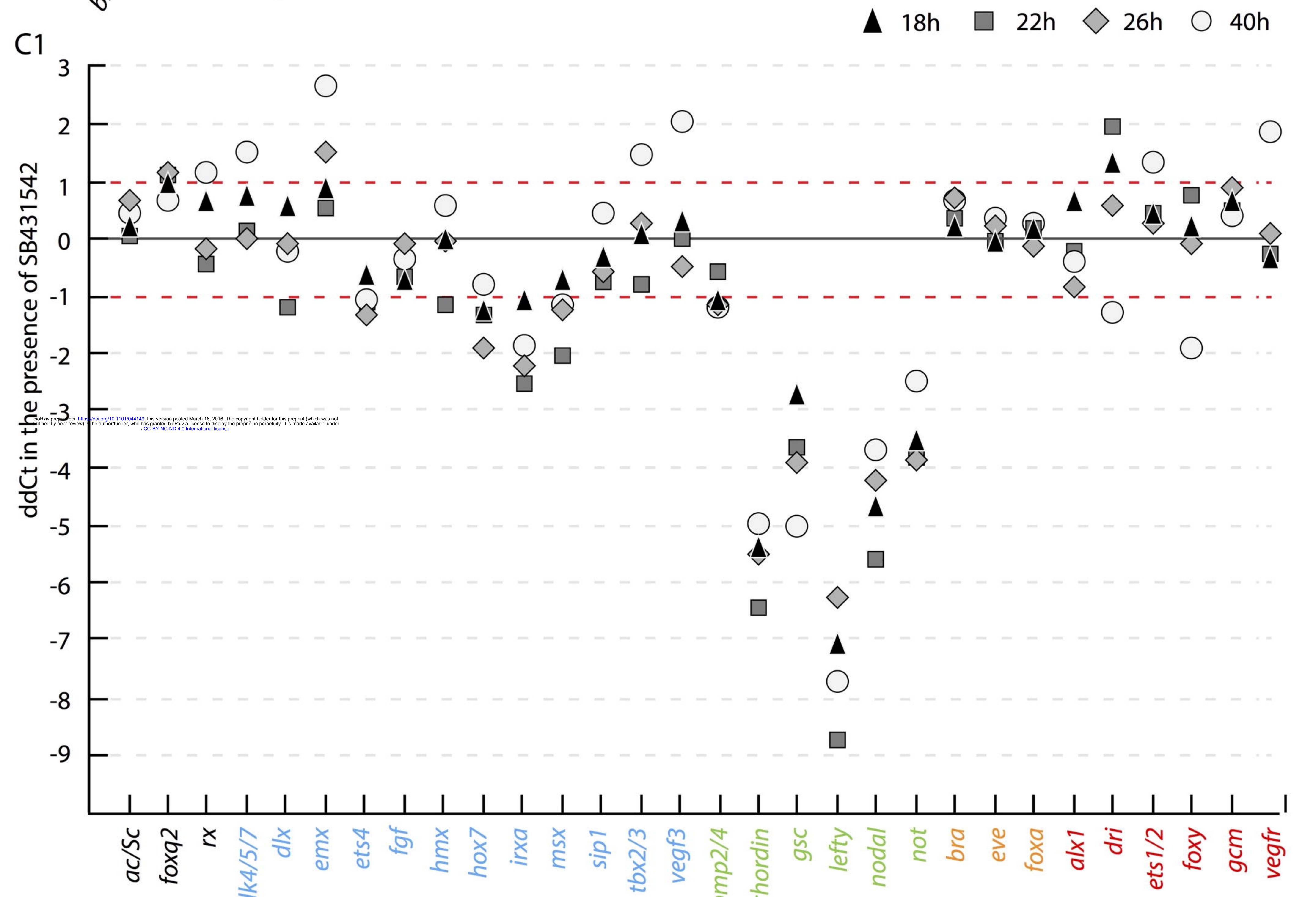
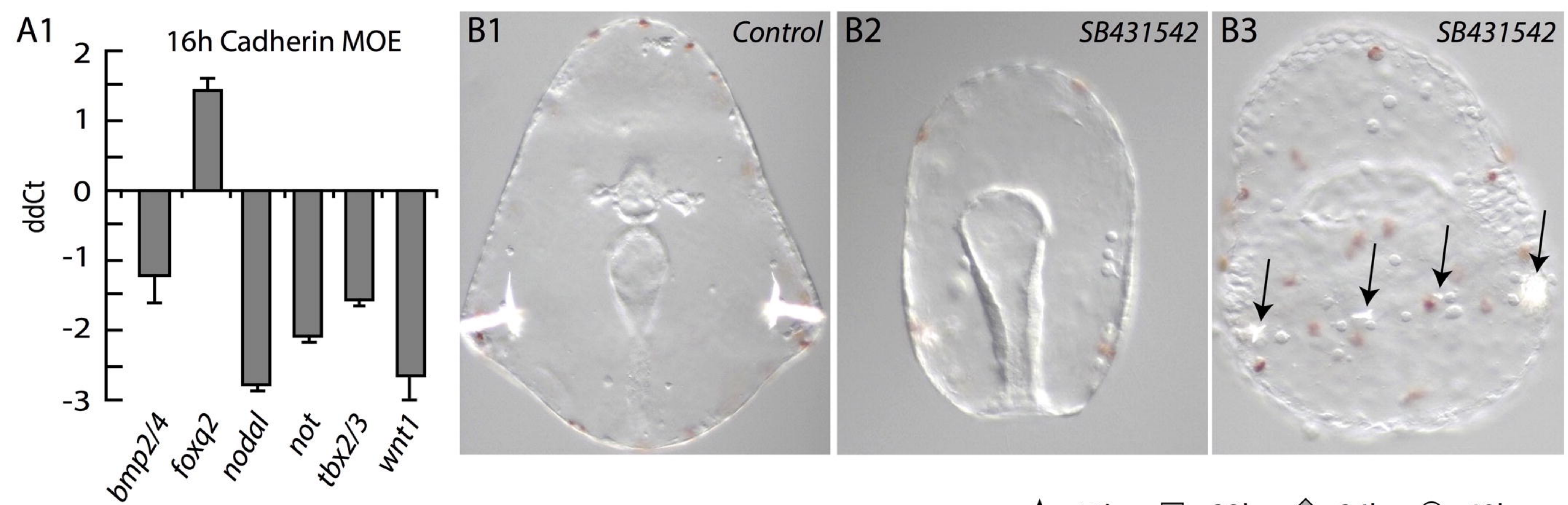


- 1 100. Levine M, Davidson EH. Gene regulatory networks for development. Proc Natl
- 2 Acad Sci U S A. 2005;102(14):4936-42.
- 3 101. Davidson EH. Evolutionary bioscience as regulatory systems biology. Dev Biol.
- 4 2011;357(1):35-40.
- 5

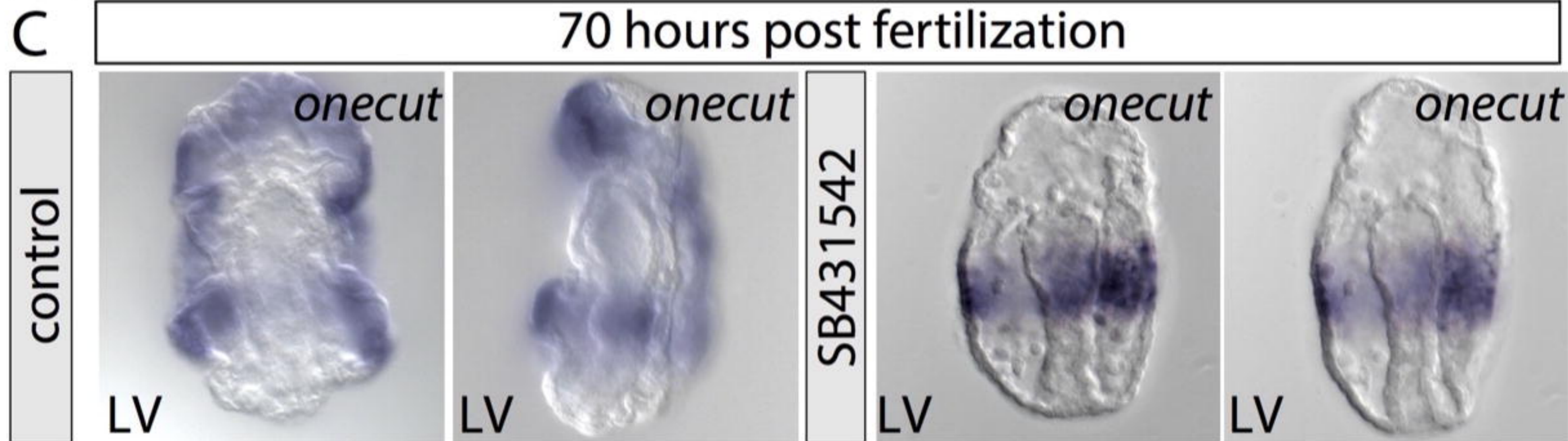
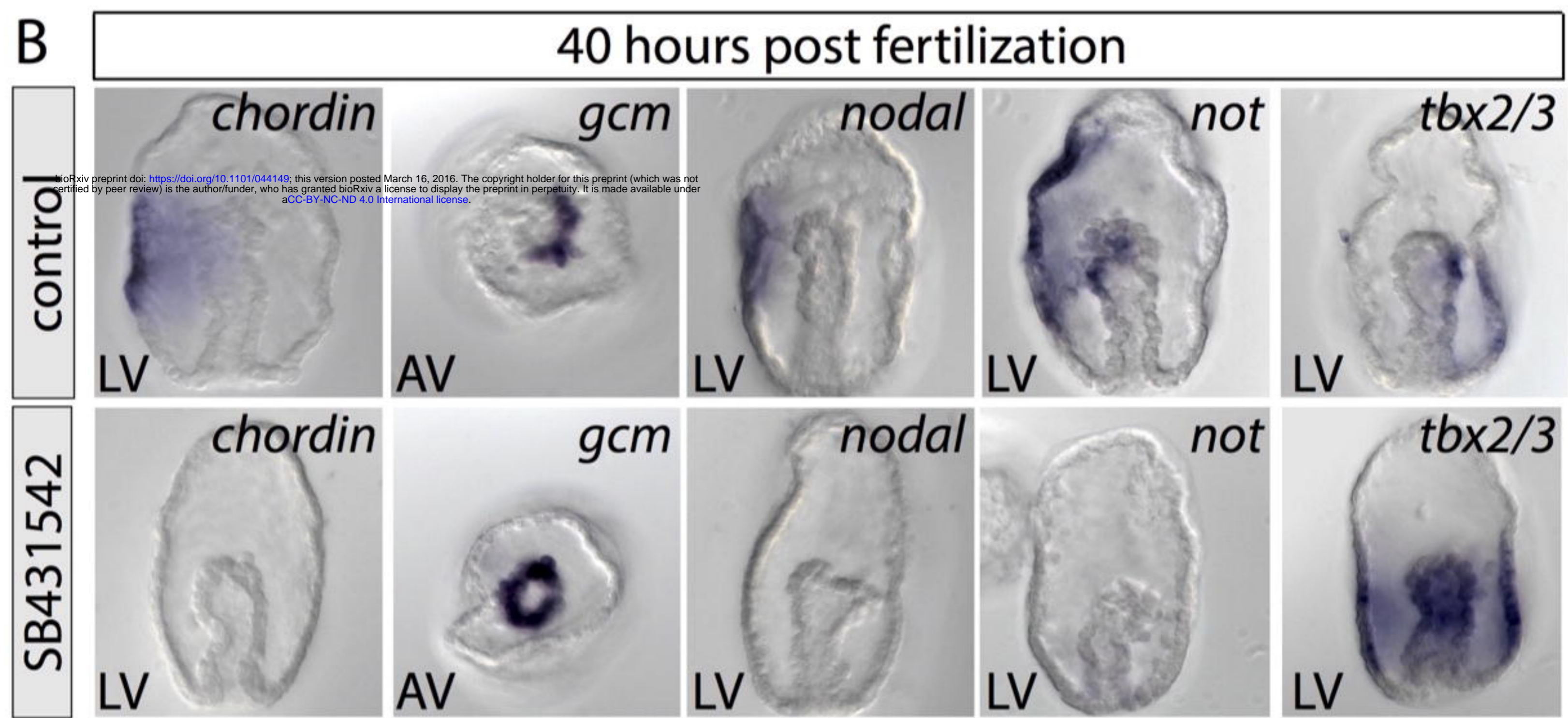




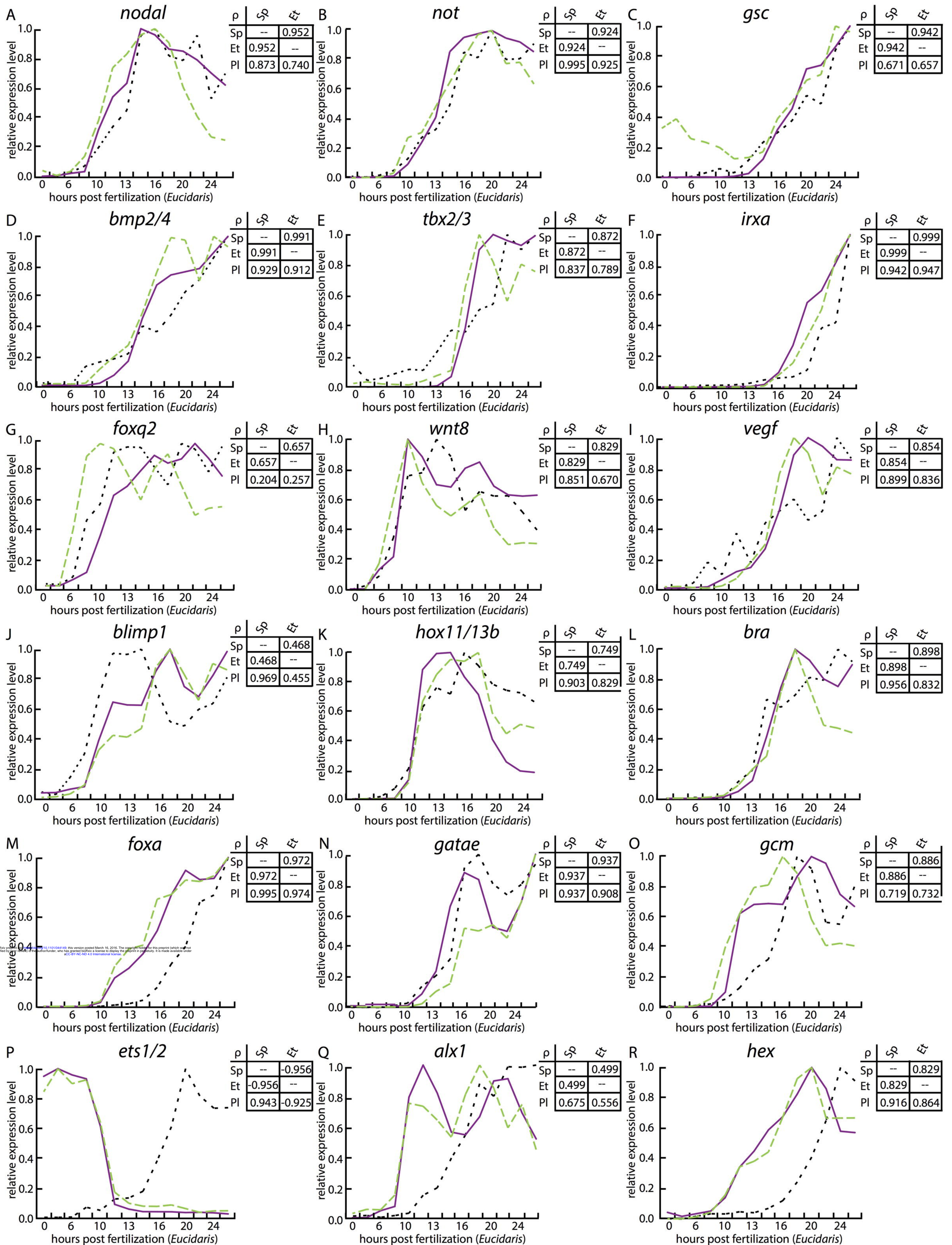


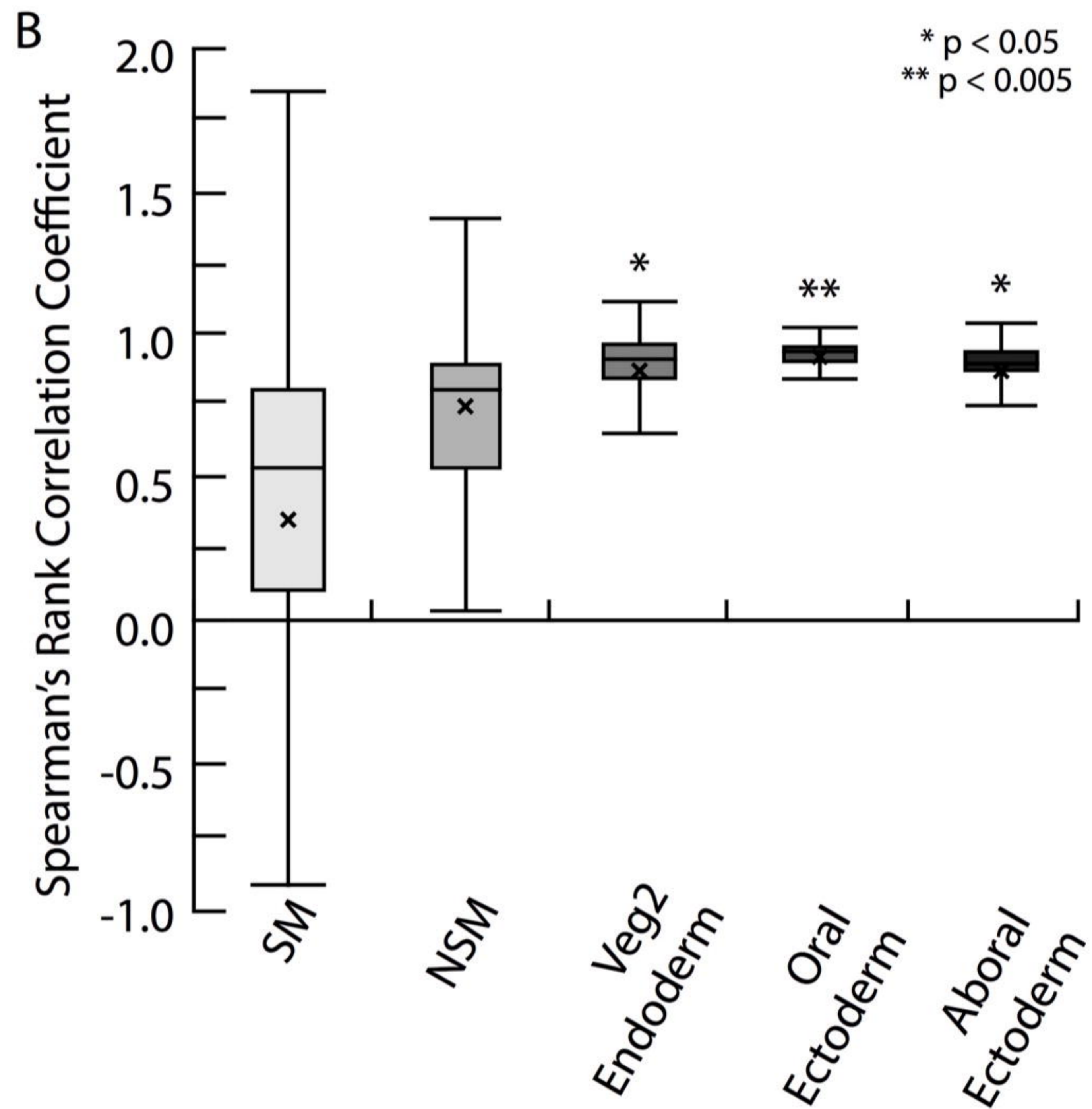
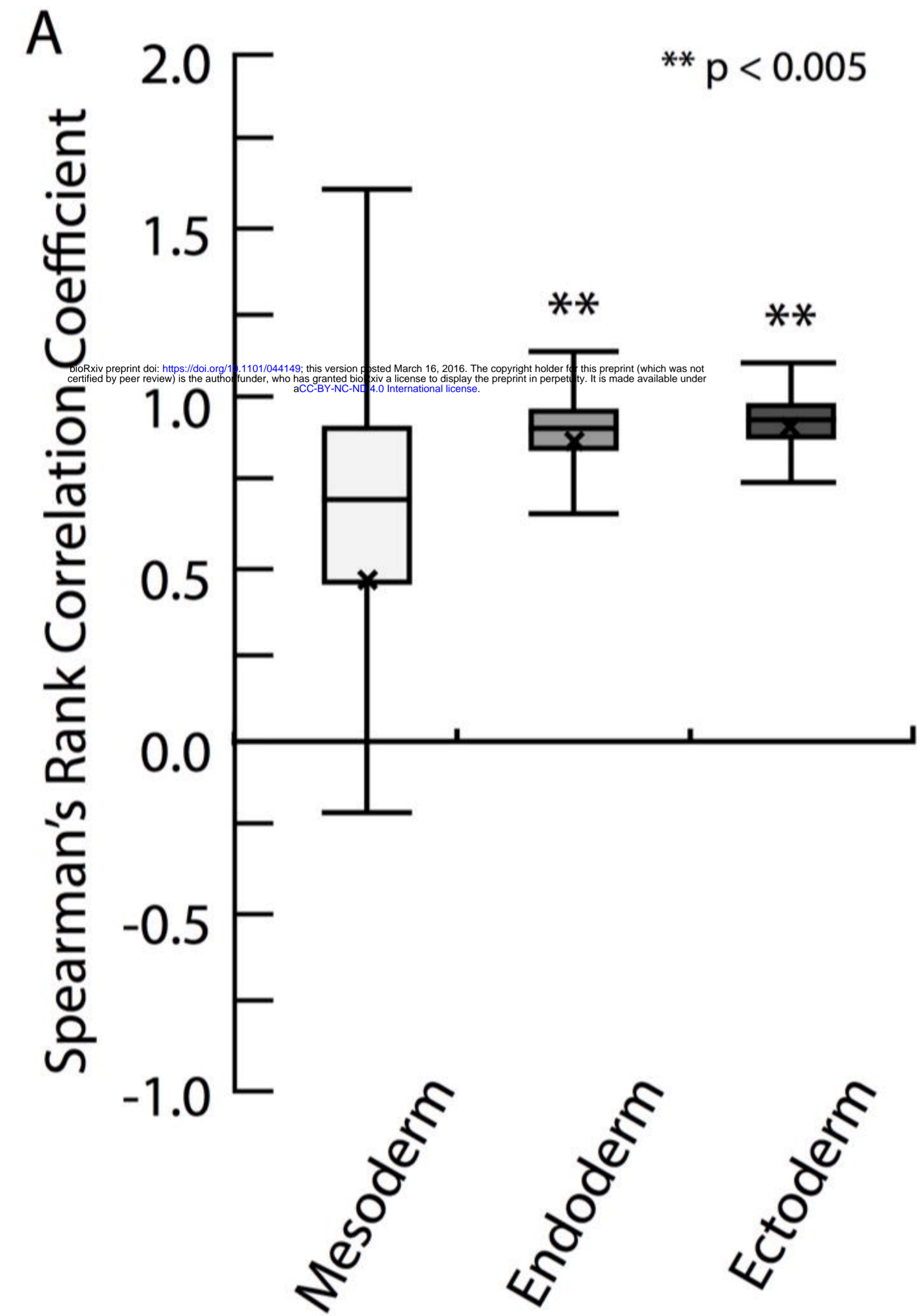


bioRxiv preprint doi: <https://doi.org/10.1101/044149>; this version posted March 16, 2016. The copyright holder for this preprint (which was not certified by peer review) is the author/funder, who has granted bioRxiv a license to display the preprint in perpetuity. It is made available under aCC-BY-NC-ND 4.0 International license.

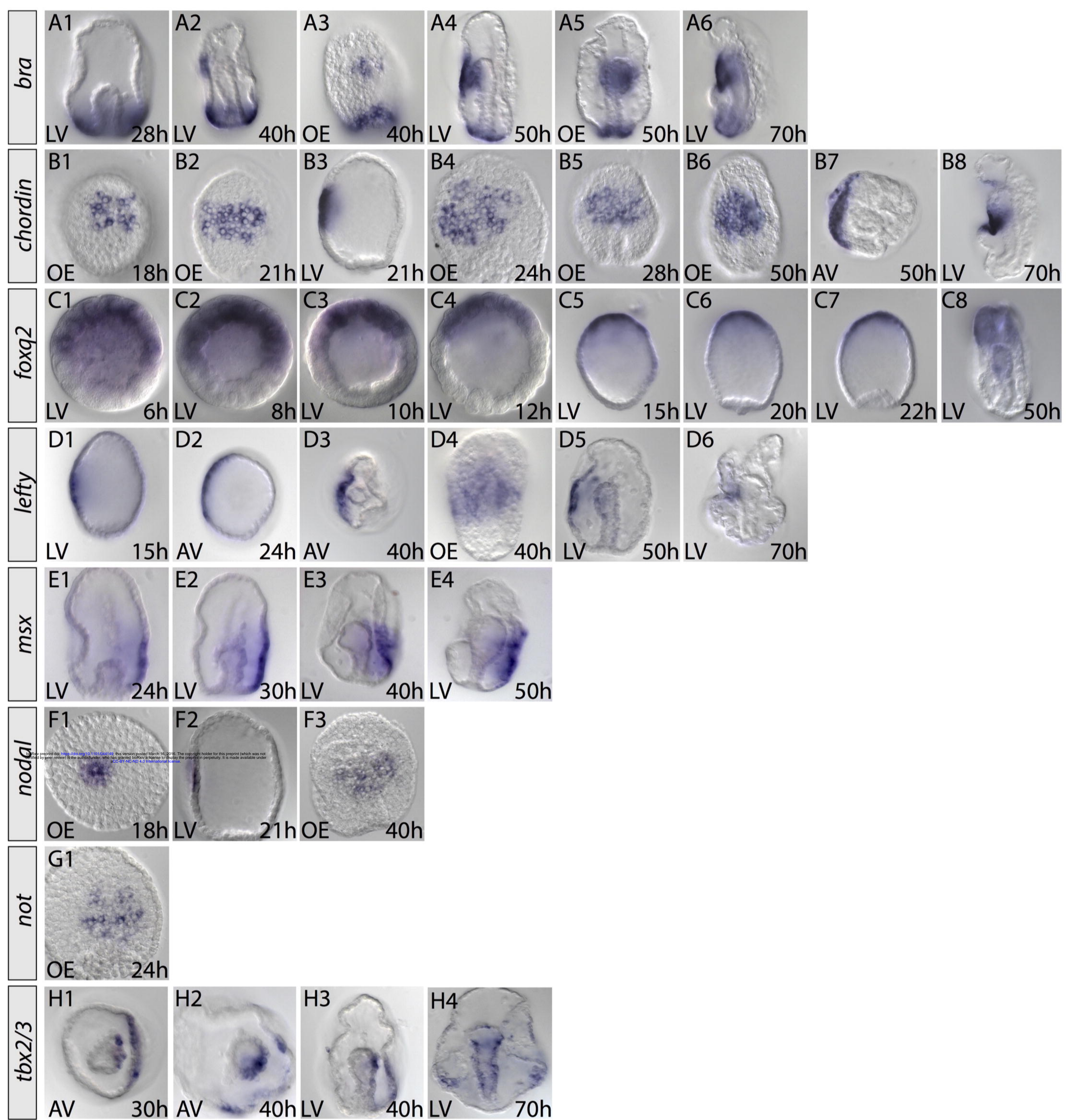


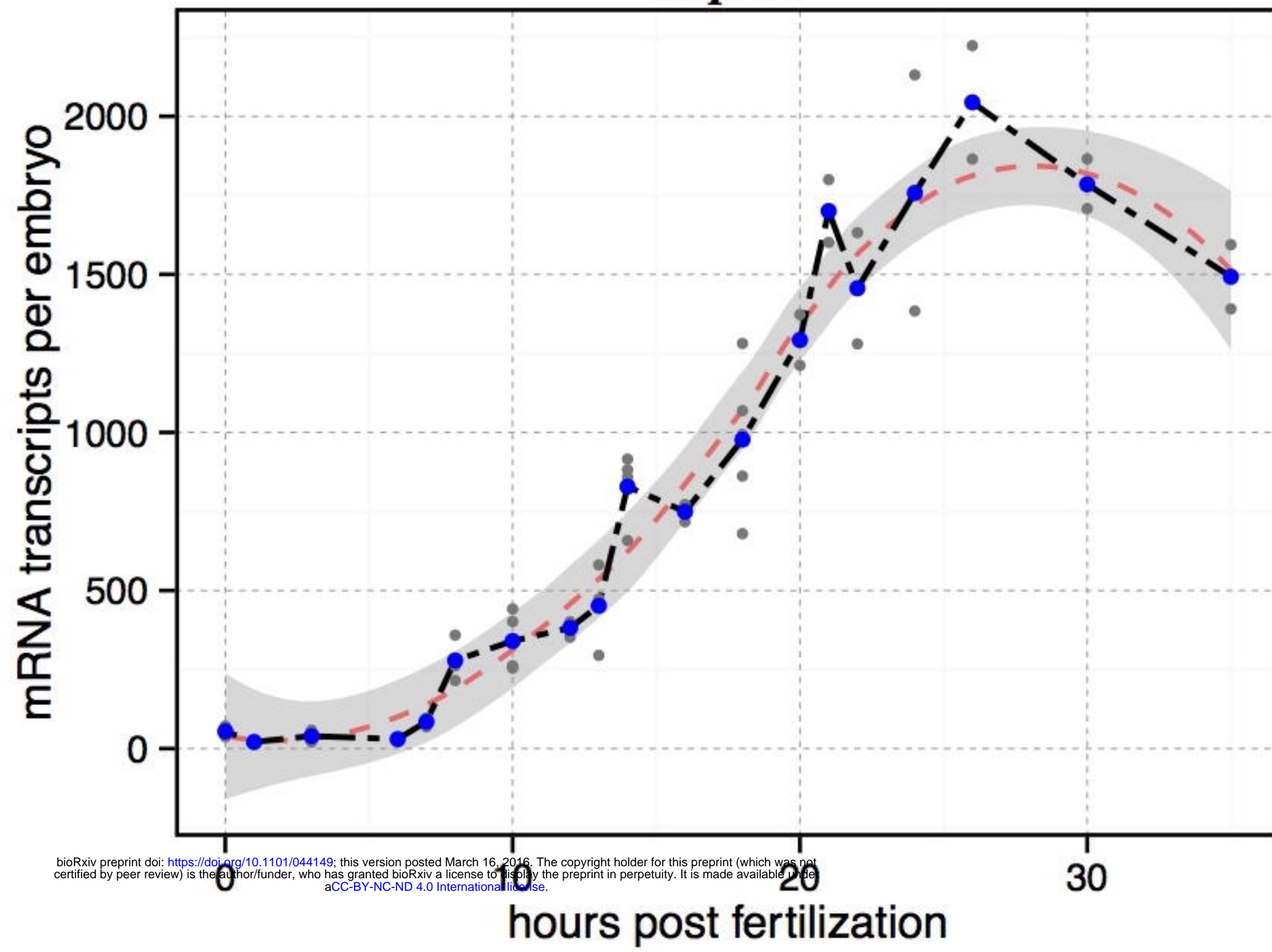
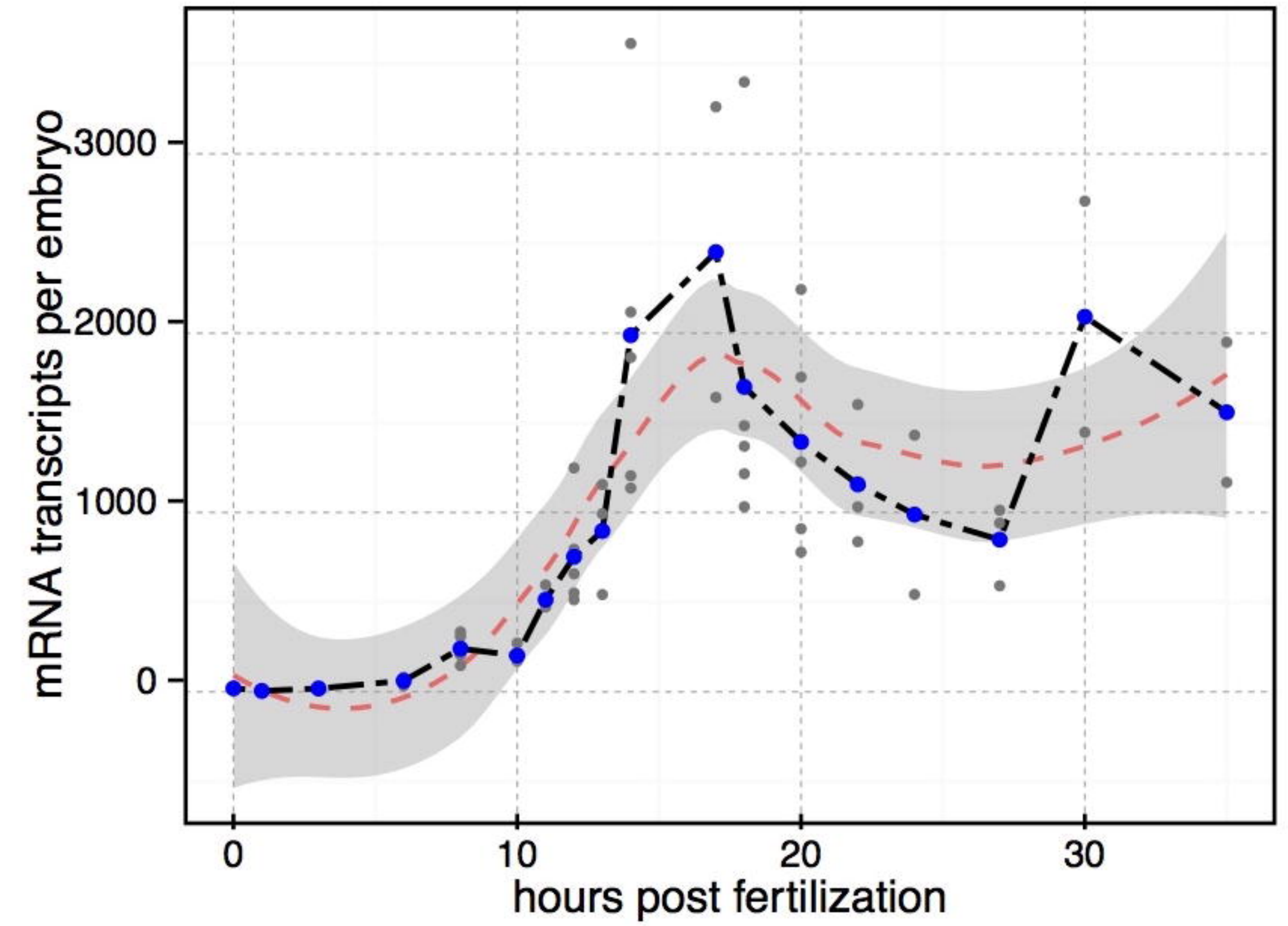
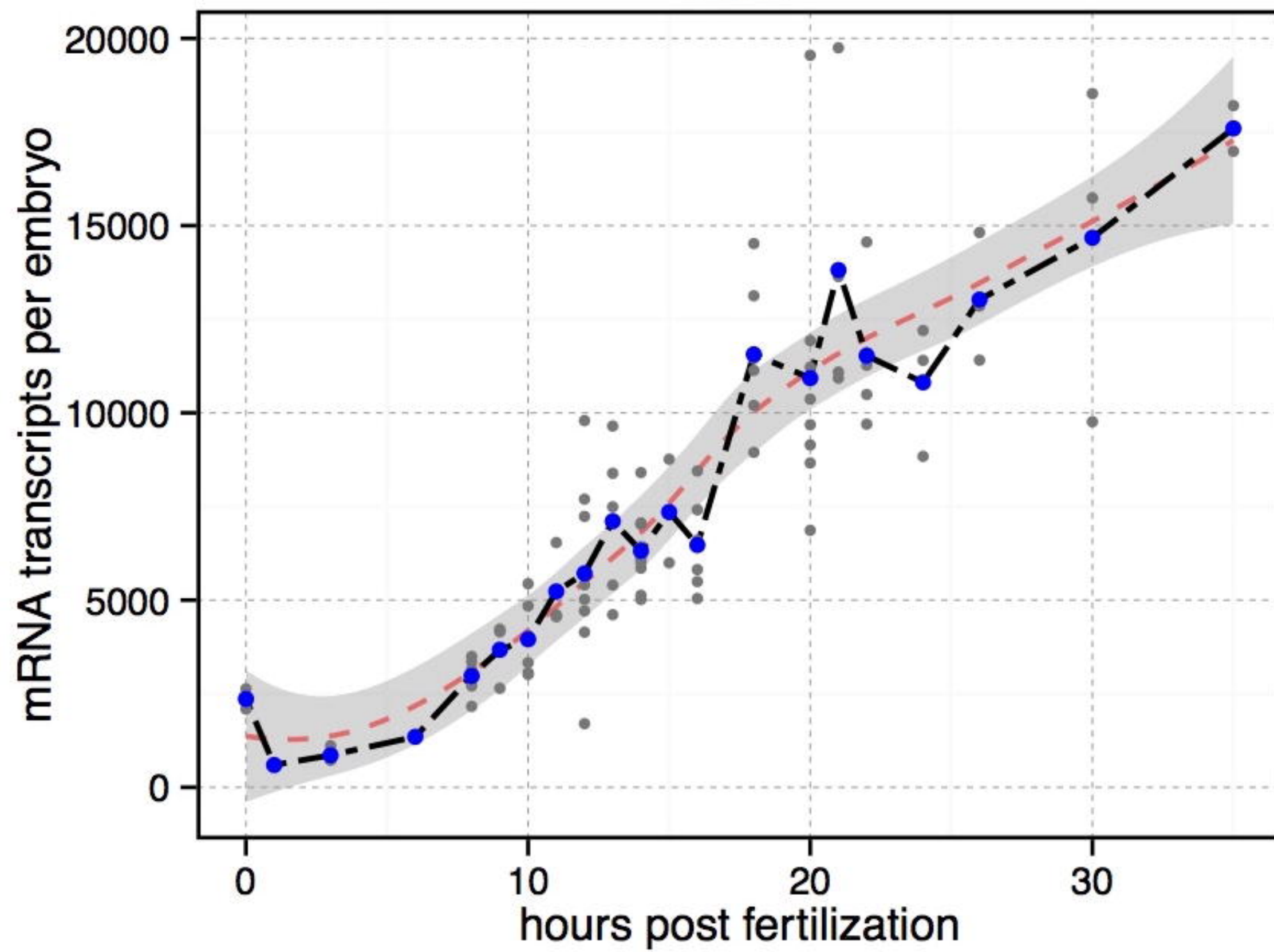
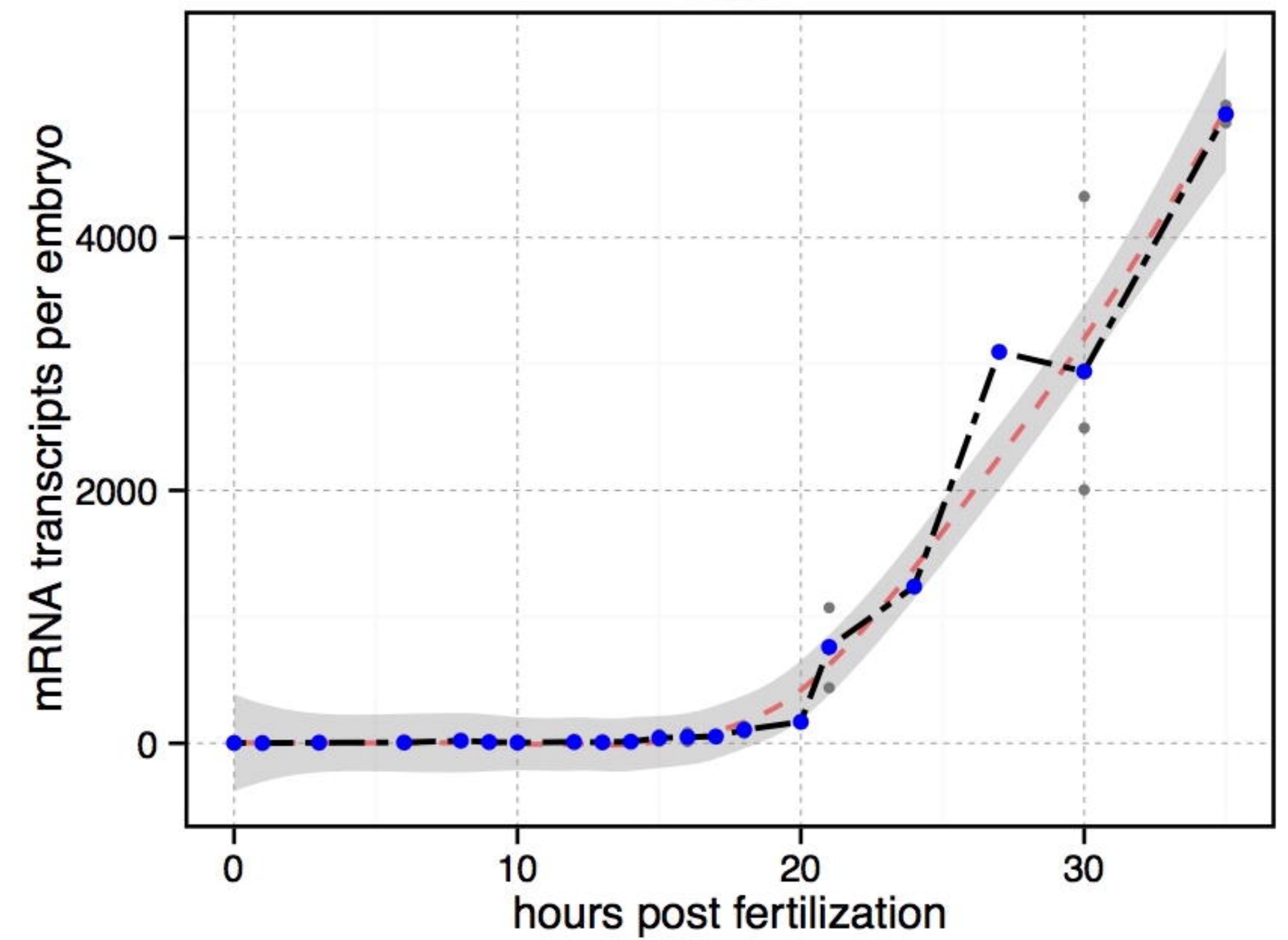
bioRxiv preprint doi: <https://doi.org/10.1101/044149>; this version posted March 16, 2016. The copyright holder for this preprint (which was not certified by peer review) is the author/funder, who has granted bioRxiv a license to display the preprint in perpetuity. It is made available under aCC-BY-NC-ND 4.0 International license.

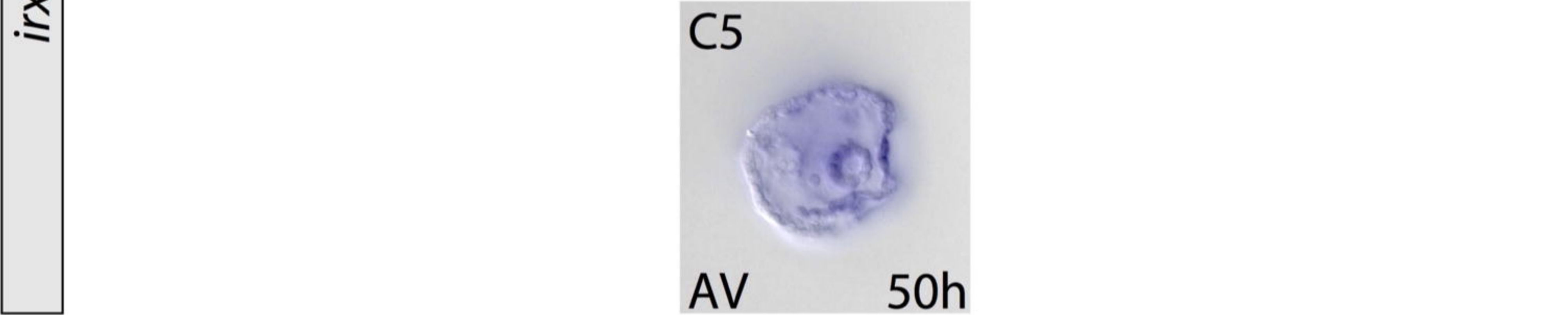
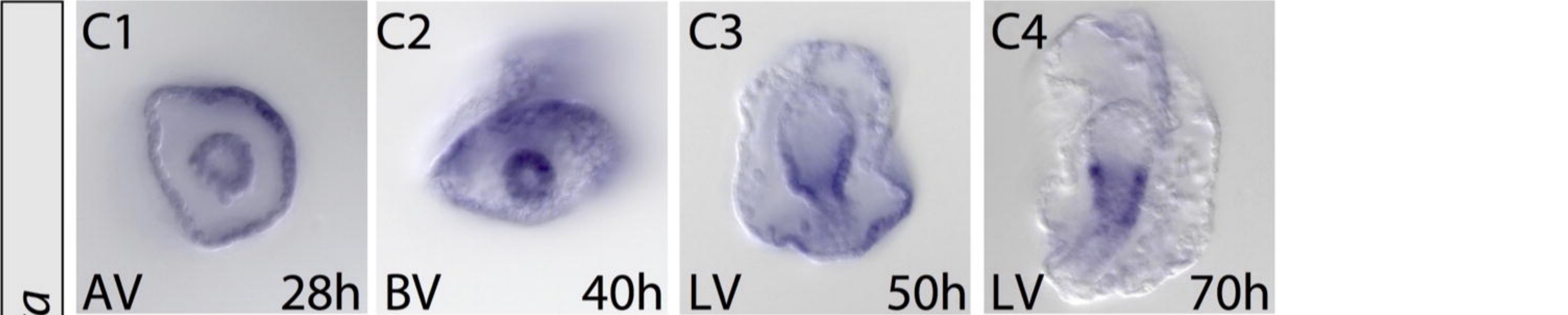
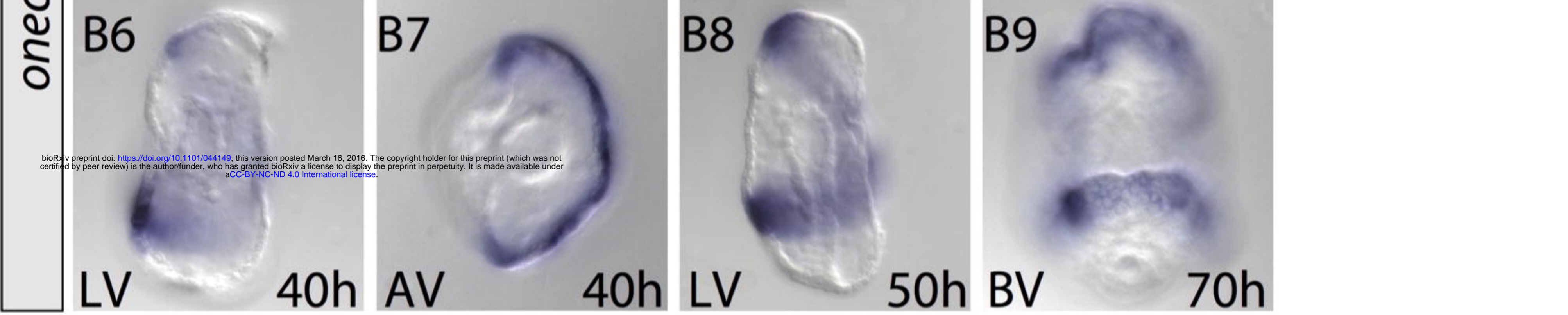
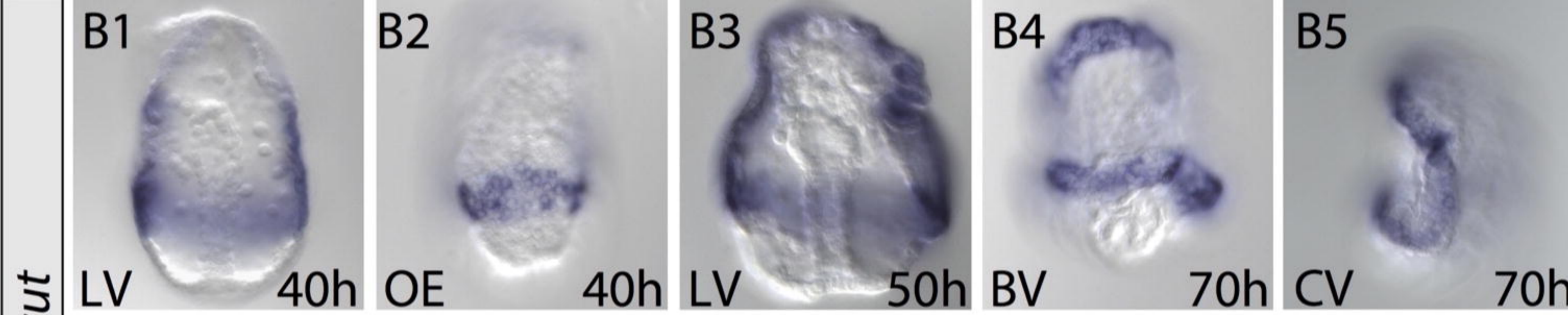
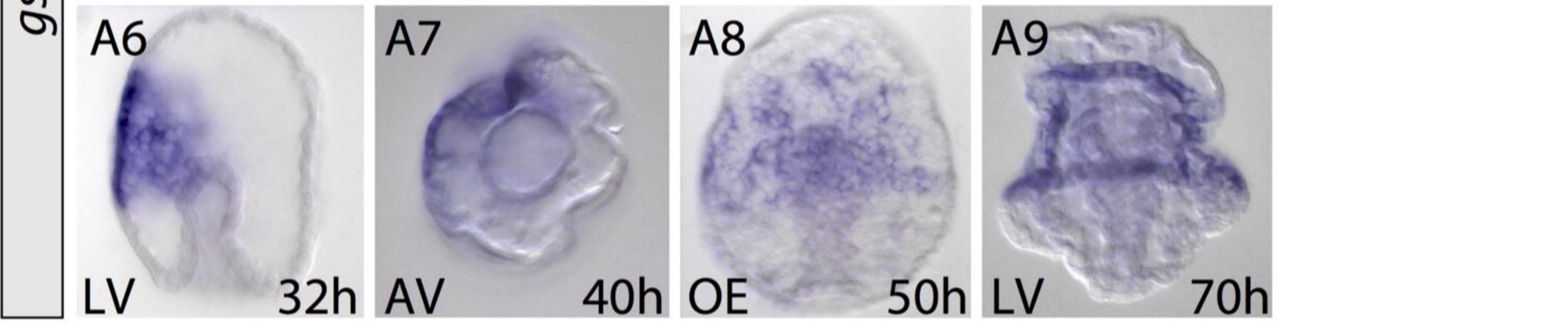
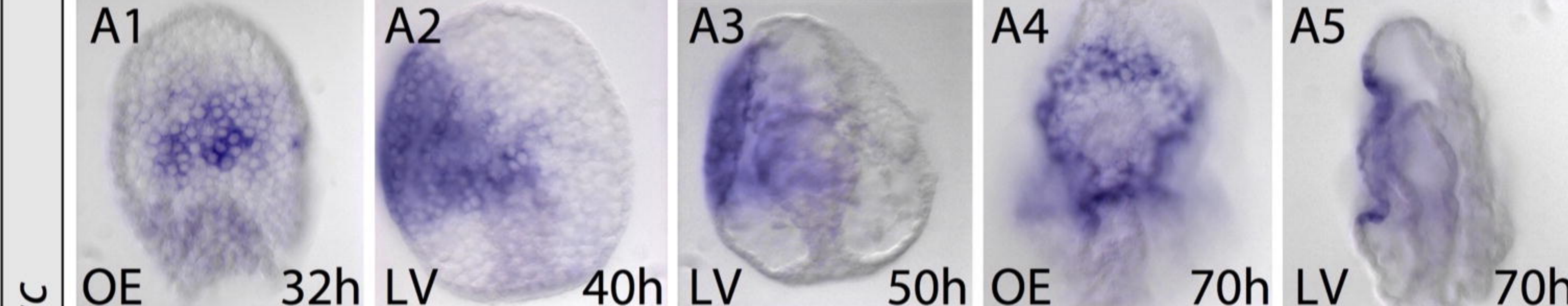








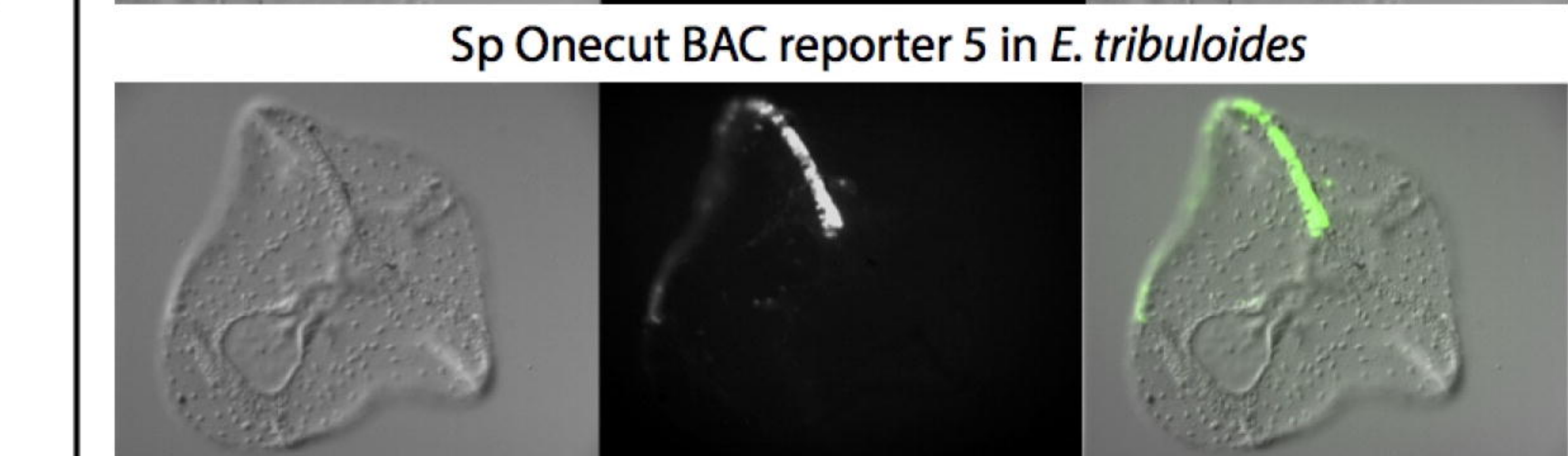
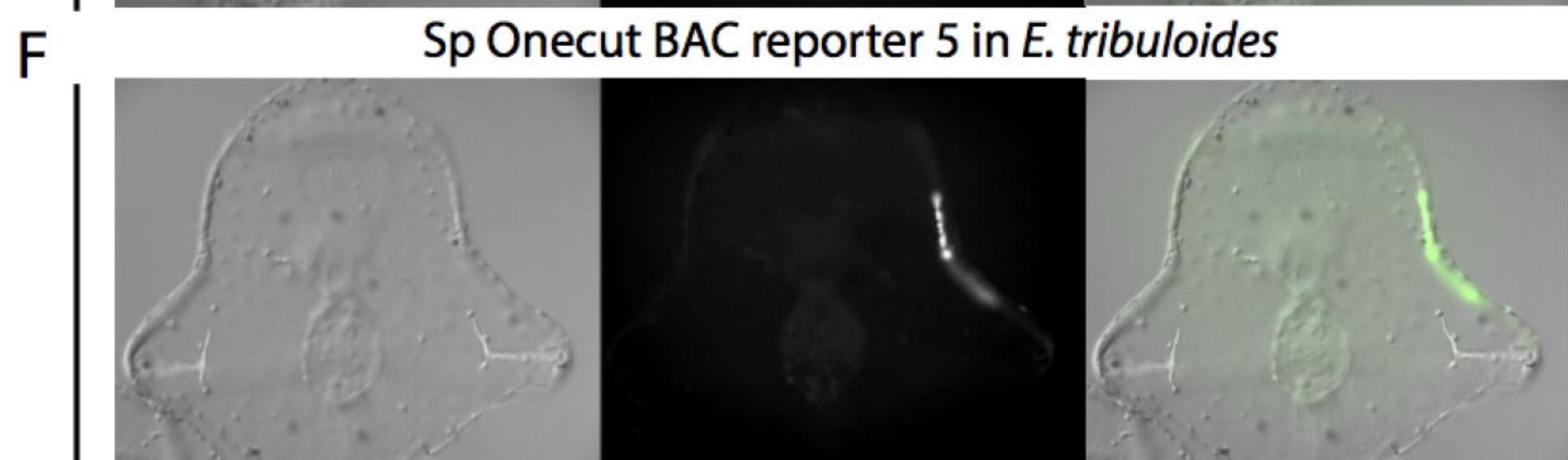
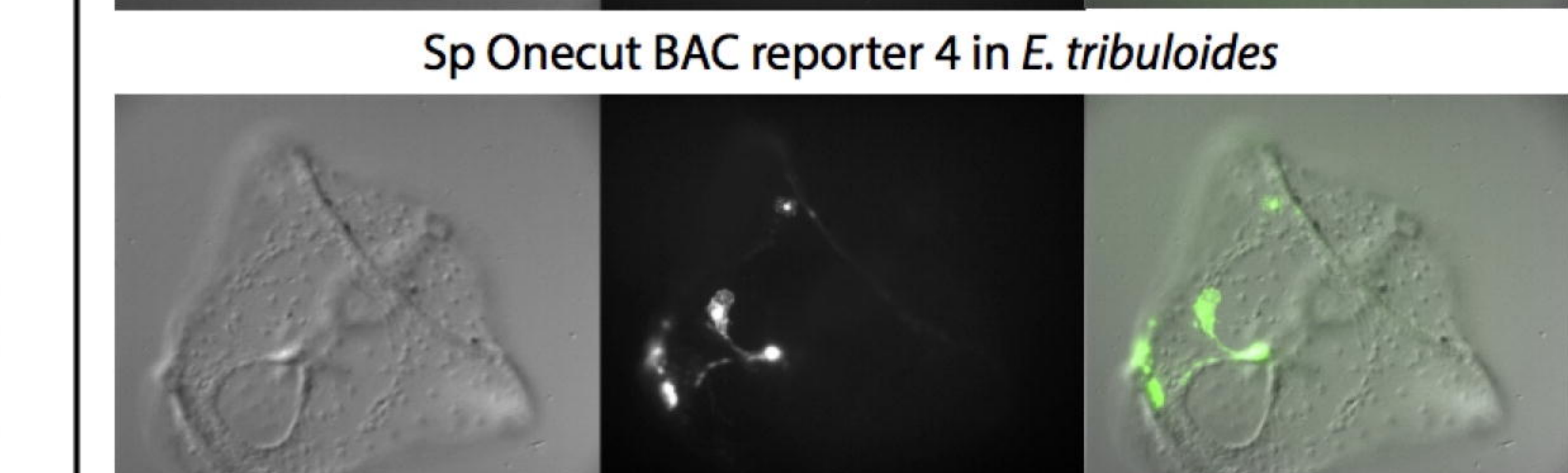
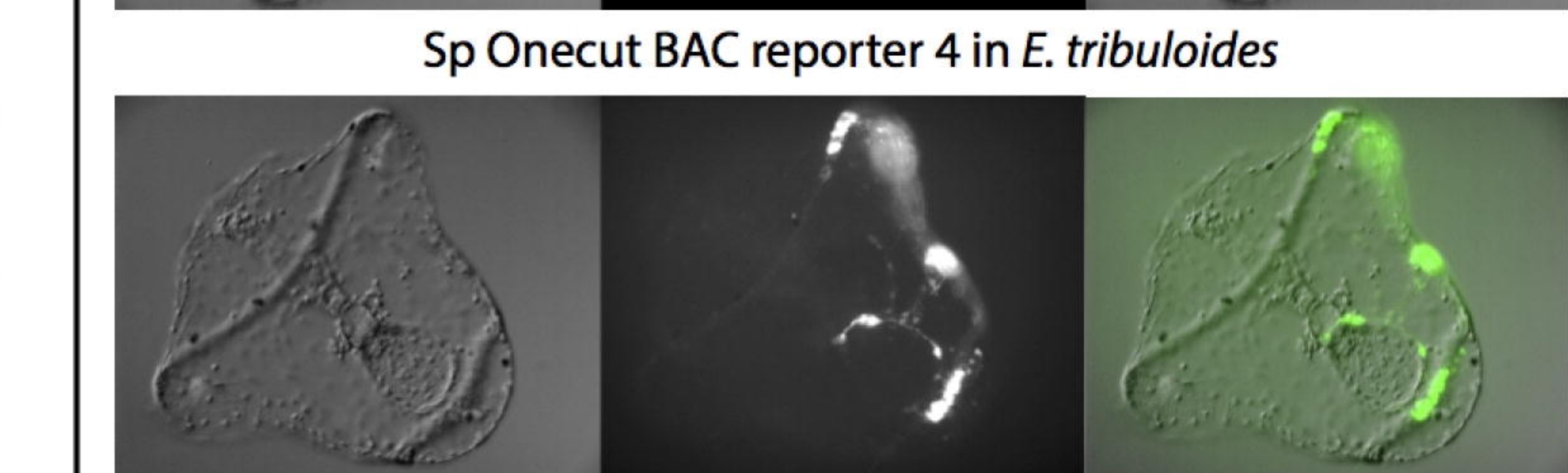
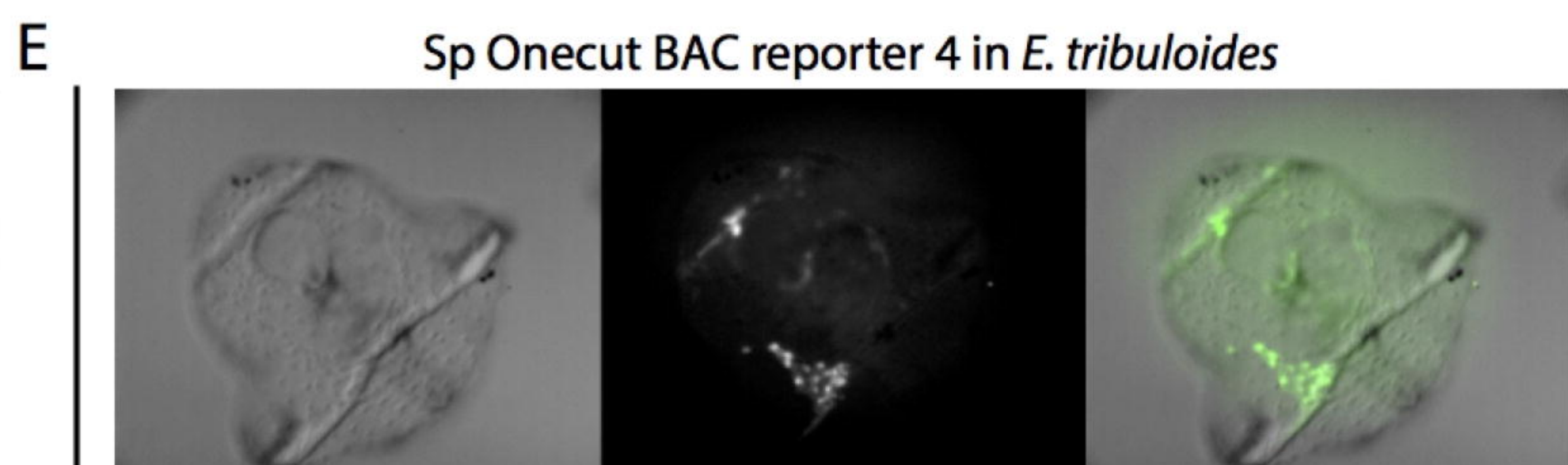
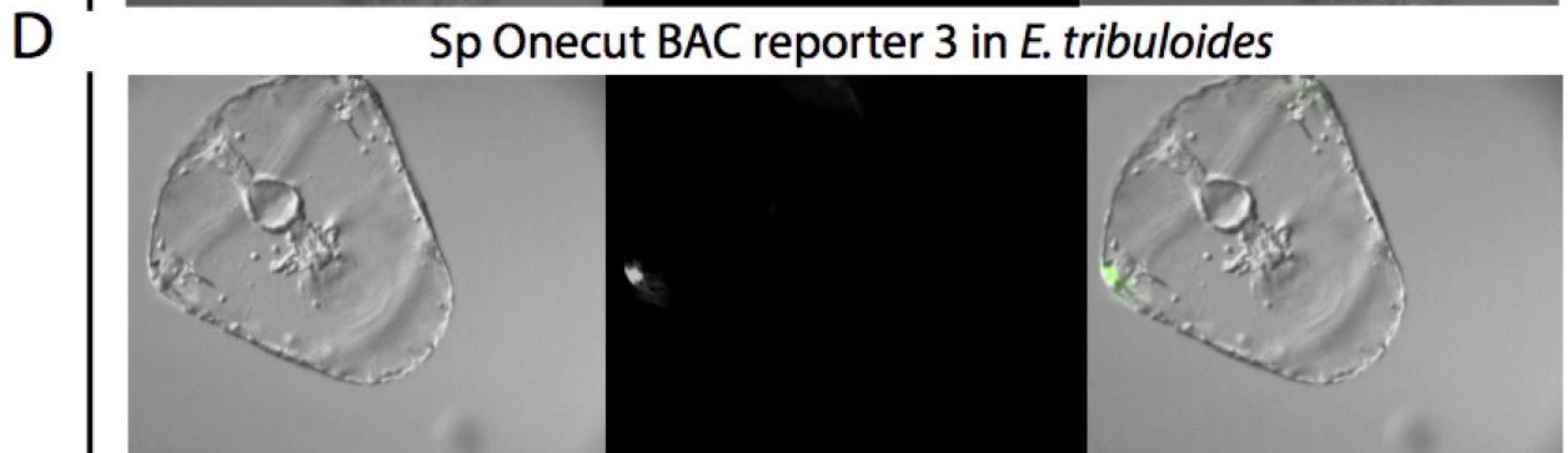
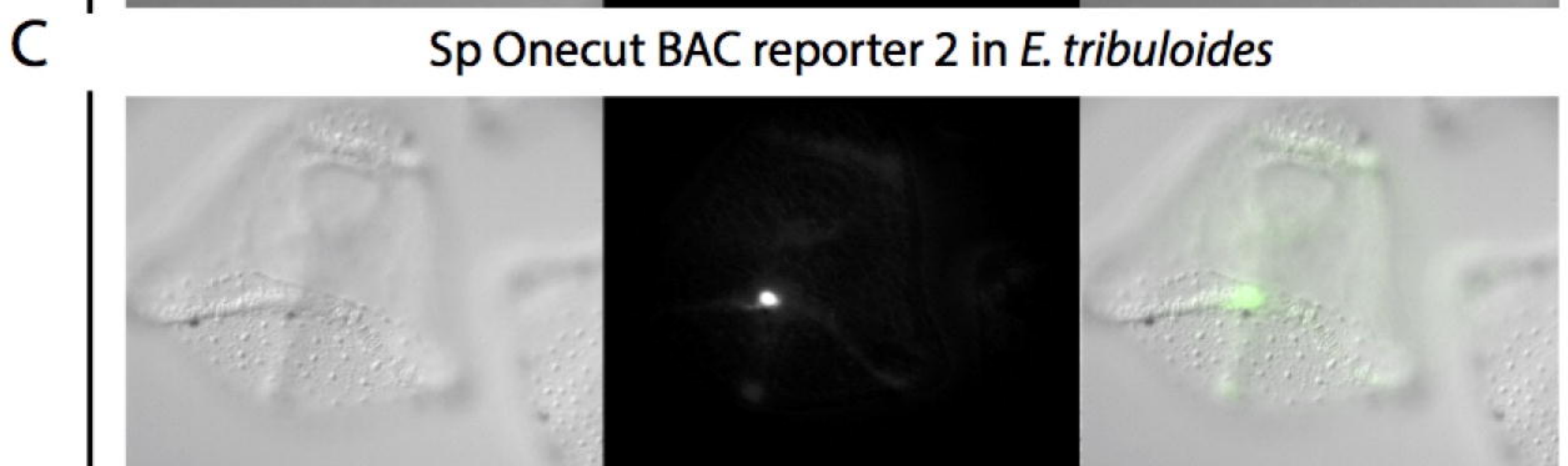
**A***bmp2/4***B***emx***C***hesc***D***msx*



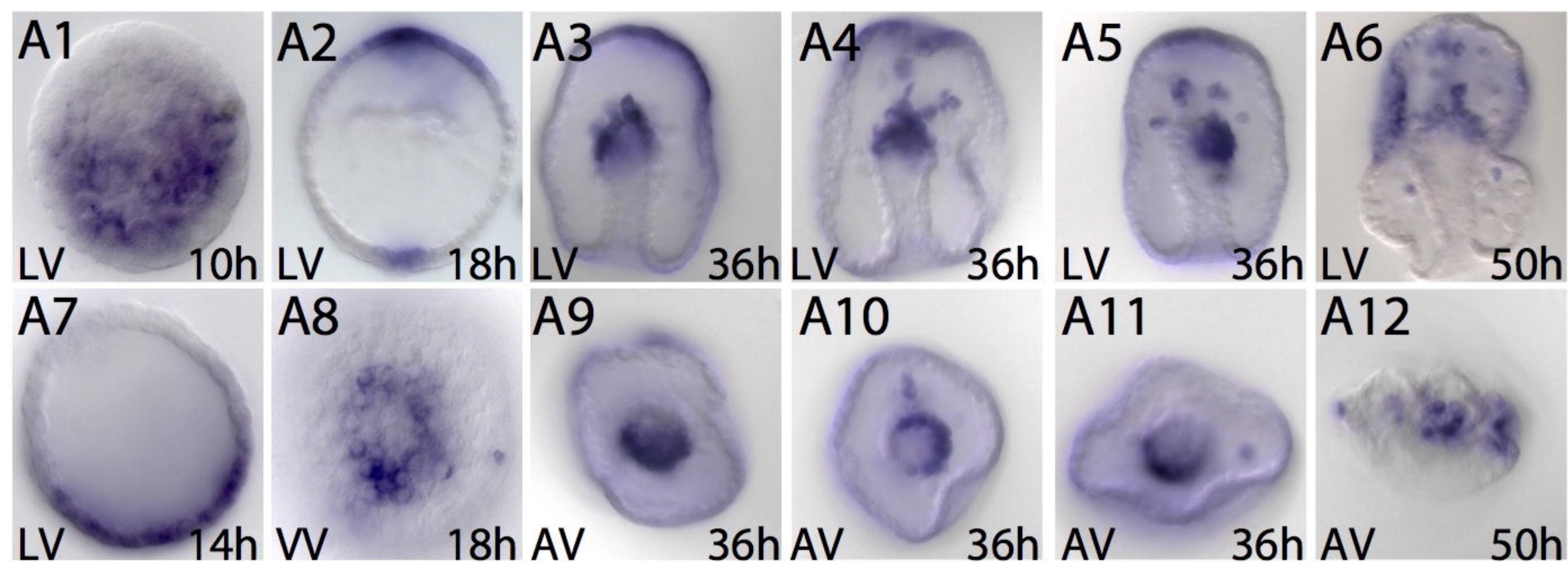
bioRxiv preprint doi: <https://doi.org/10.1101/044149>; this version posted March 16, 2016. The copyright holder for this preprint (which was not certified by peer review) is the author/funder, who has granted bioRxiv a license to display the preprint in perpetuity. It is made available under aCC-BY-NC-ND 4.0 International license.

**A**

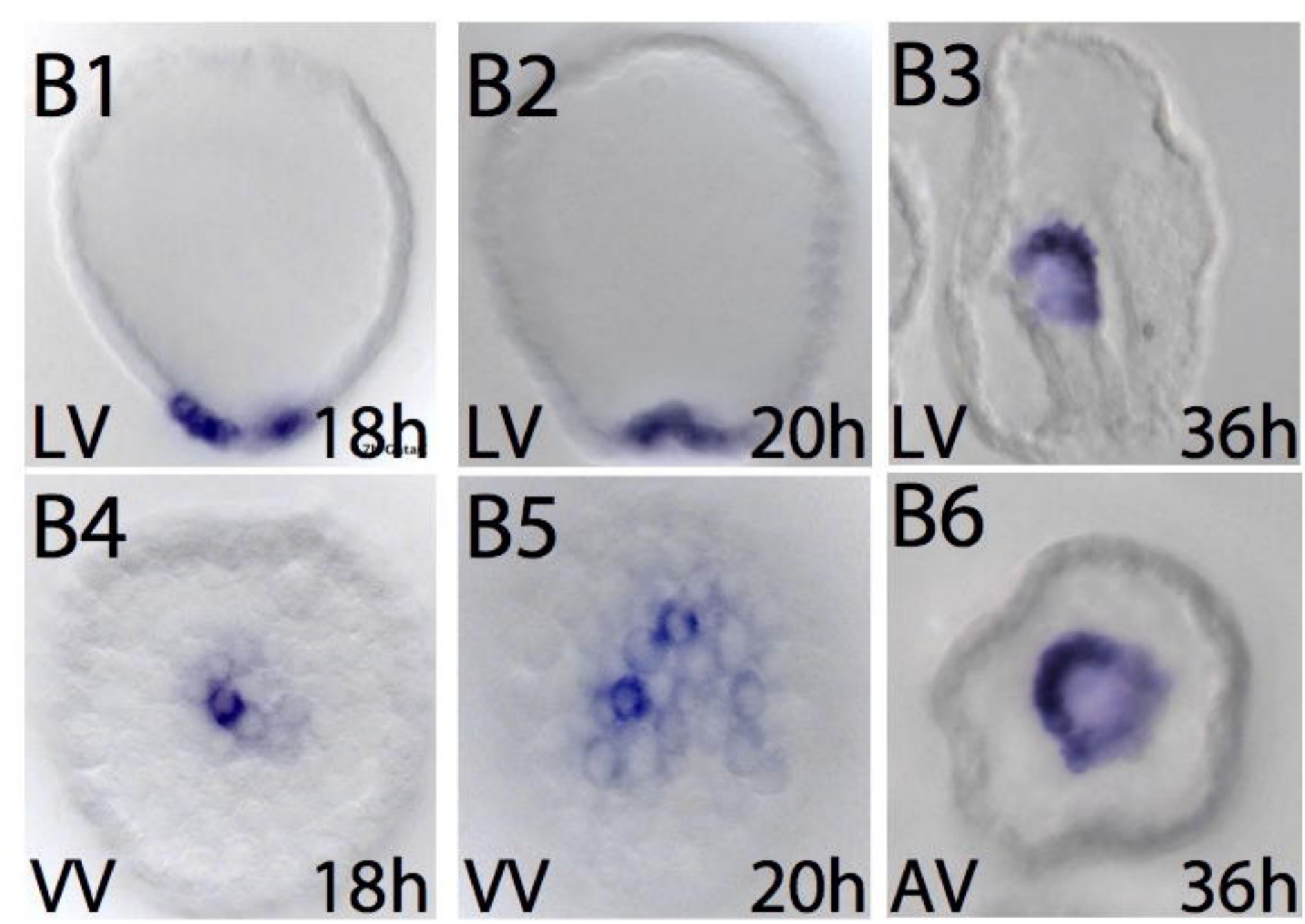
SpOnecut BAC construct*	CRM perturbation	embryos scored	Percent expressing reporter	Embryonic territory of reporter expression			
				Percent expressing in ciliary band	Percent expressing in dorsal ectoderm	Percent expressing in ventral ectoderm	Percent expressing in gut or mesenchyme
BAC Reporter 1 (B)	all CRMs	77	0.0%	0.0%	0.0%	0.0%	0.0%
BAC Reporter 2 (C)	initial activation	56	12.5%	7.1%	0.0%	0.0%	0.0%
BAC Reporter 3 (D)	post-activation maintenance	40	10.0%	7.5%	0.0%	0.0%	0.0%
BAC Reporter 4 (E)	DE & VE clearance	123	27.6%	12.2%	2.4%	10.4%	0.0%
BAC Reporter 5 (F)	none / wild-type	102	17.6%	14.7%	1.0%	0.0%	0.0%



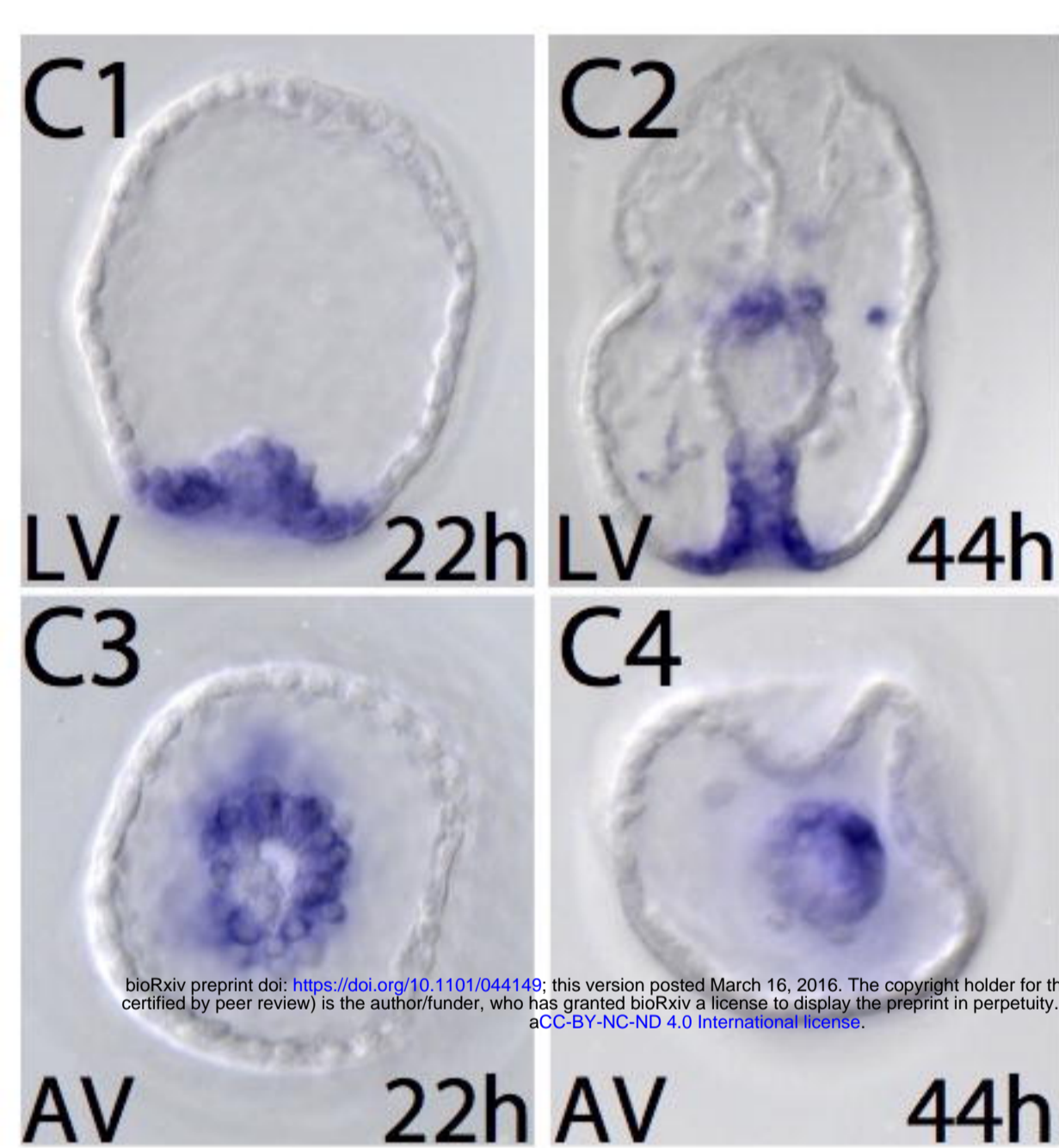
A

*ese*

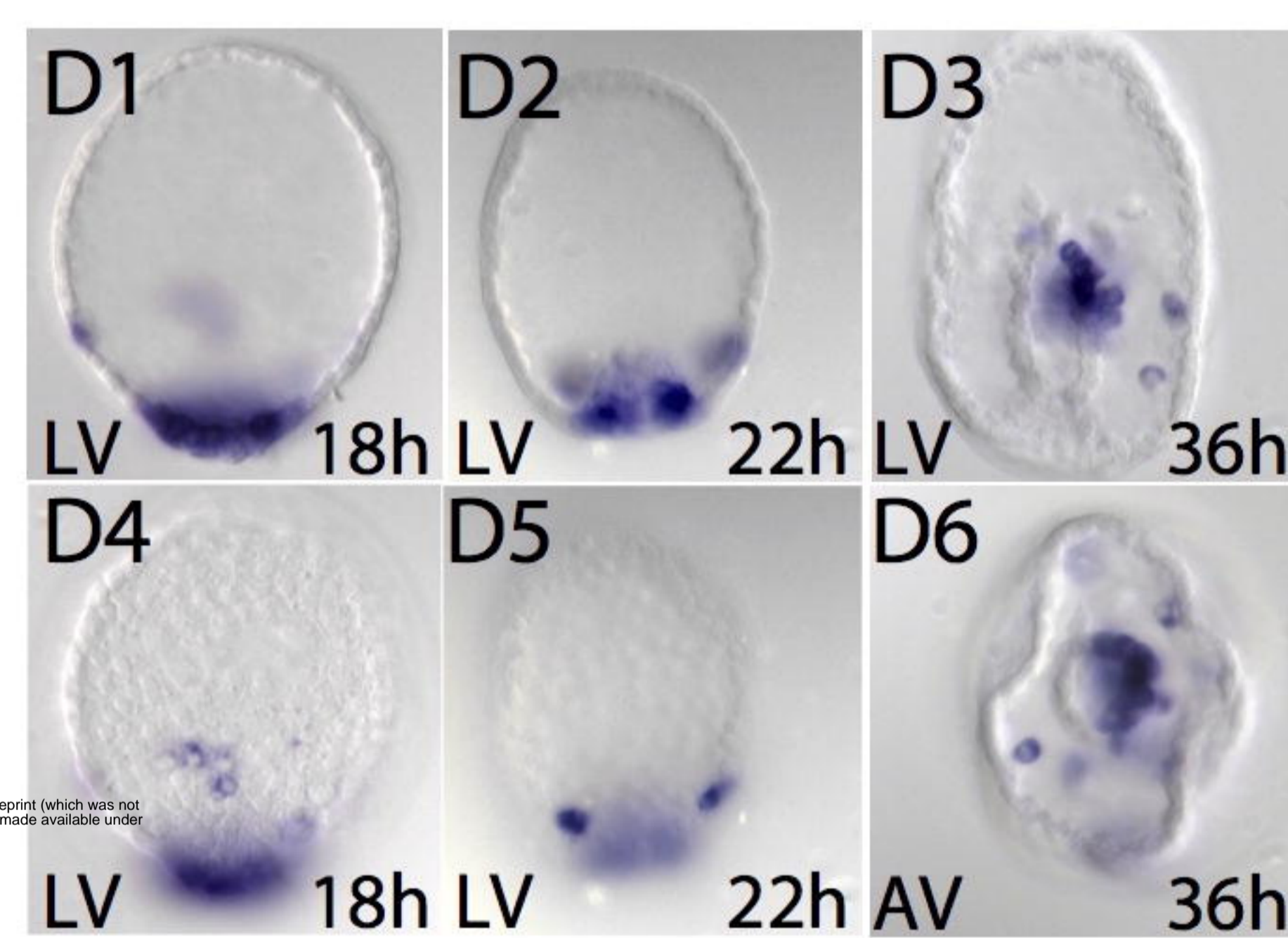
B

*gatac*

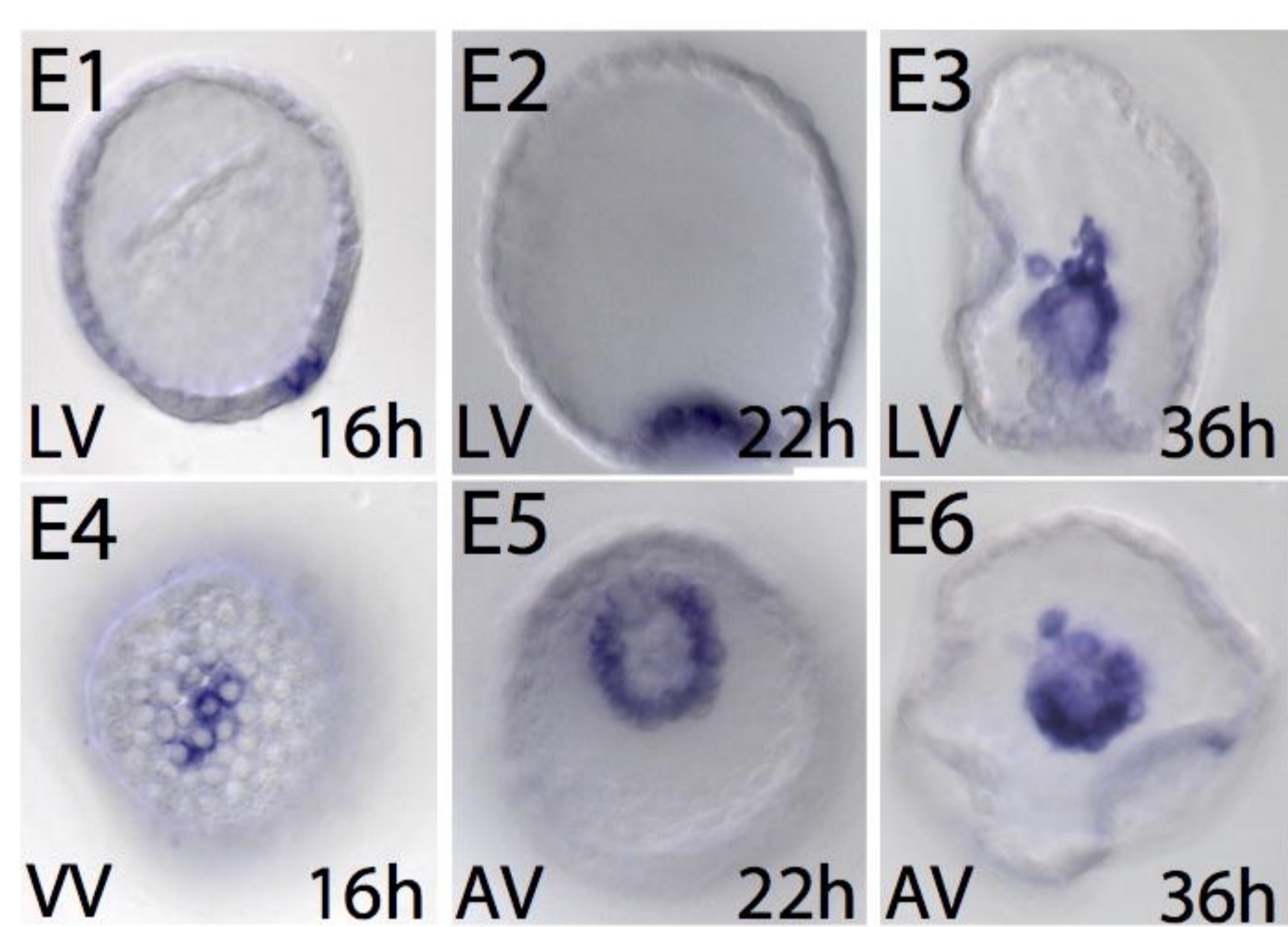
C

*gatae*

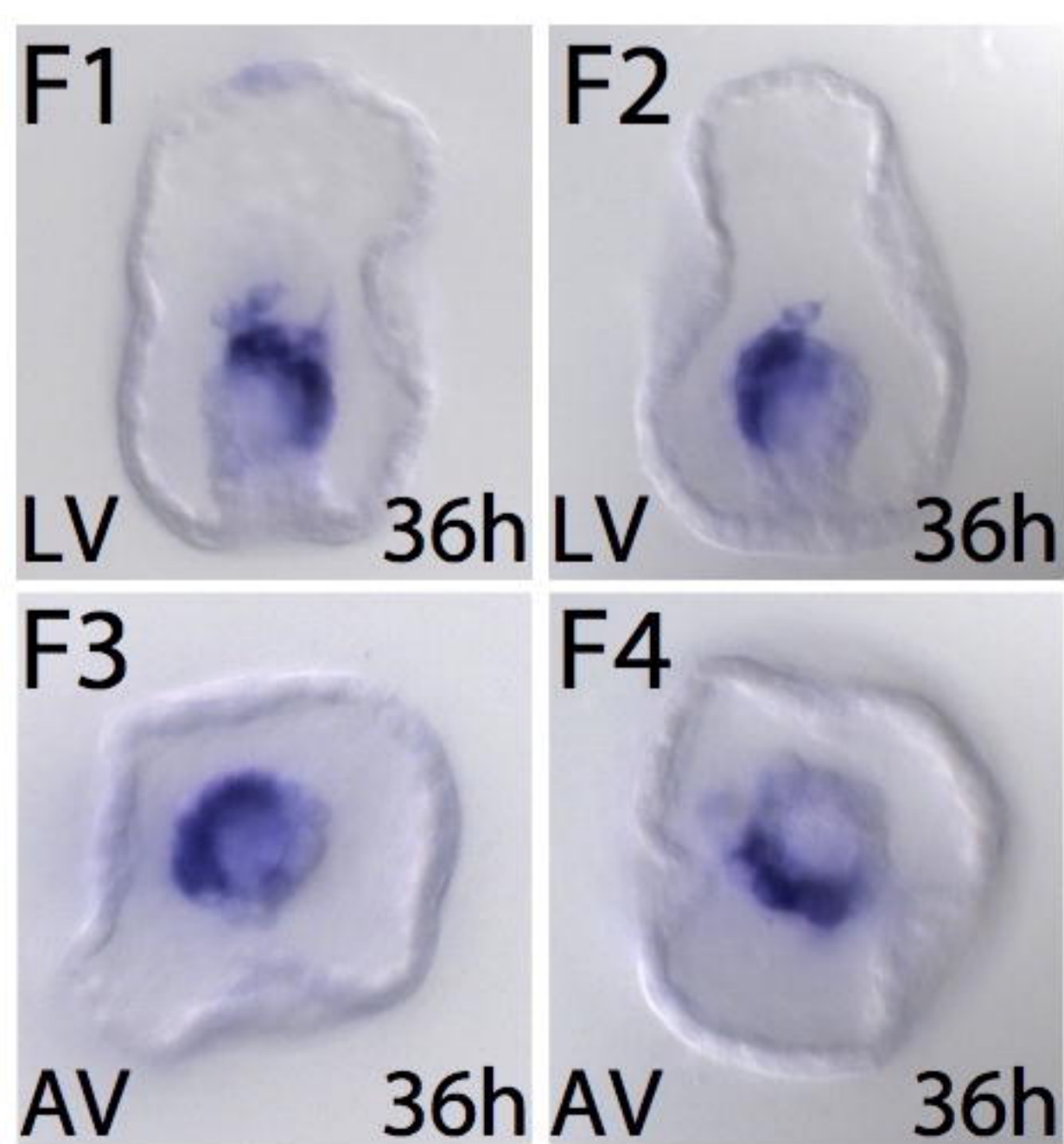
D

*gcm*

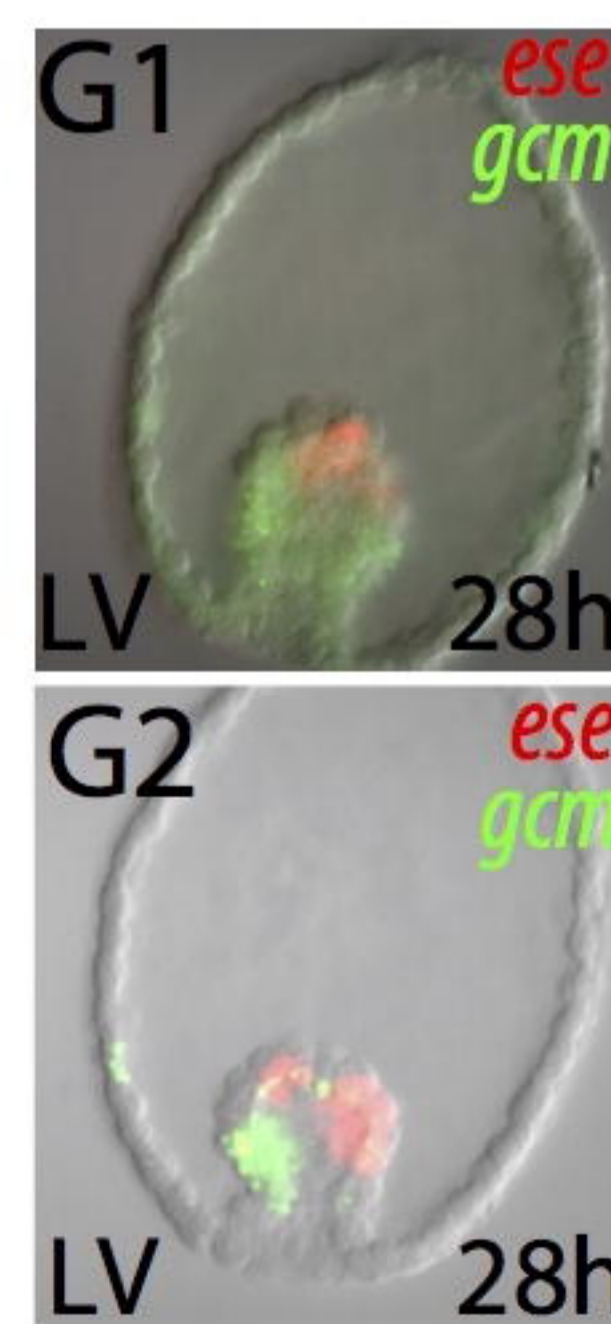
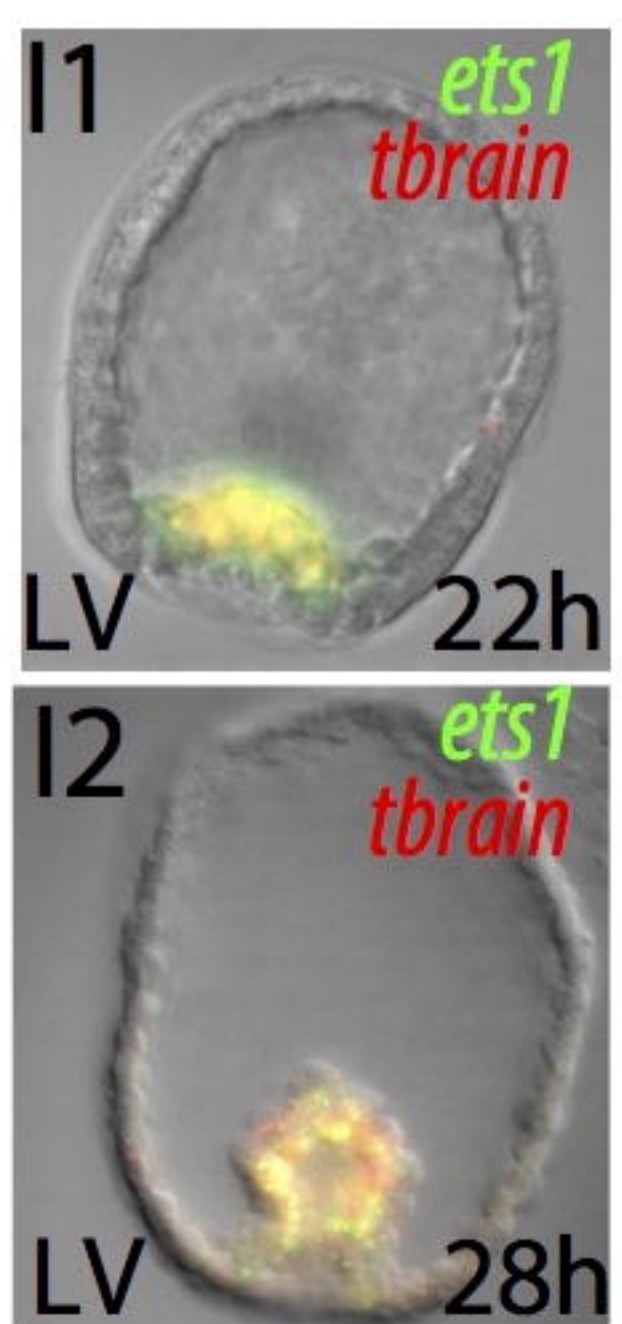
E

*prox*

F

*scl*

G

*ese/gcm*H *alx1/gcm*I *ets1/tbrain*

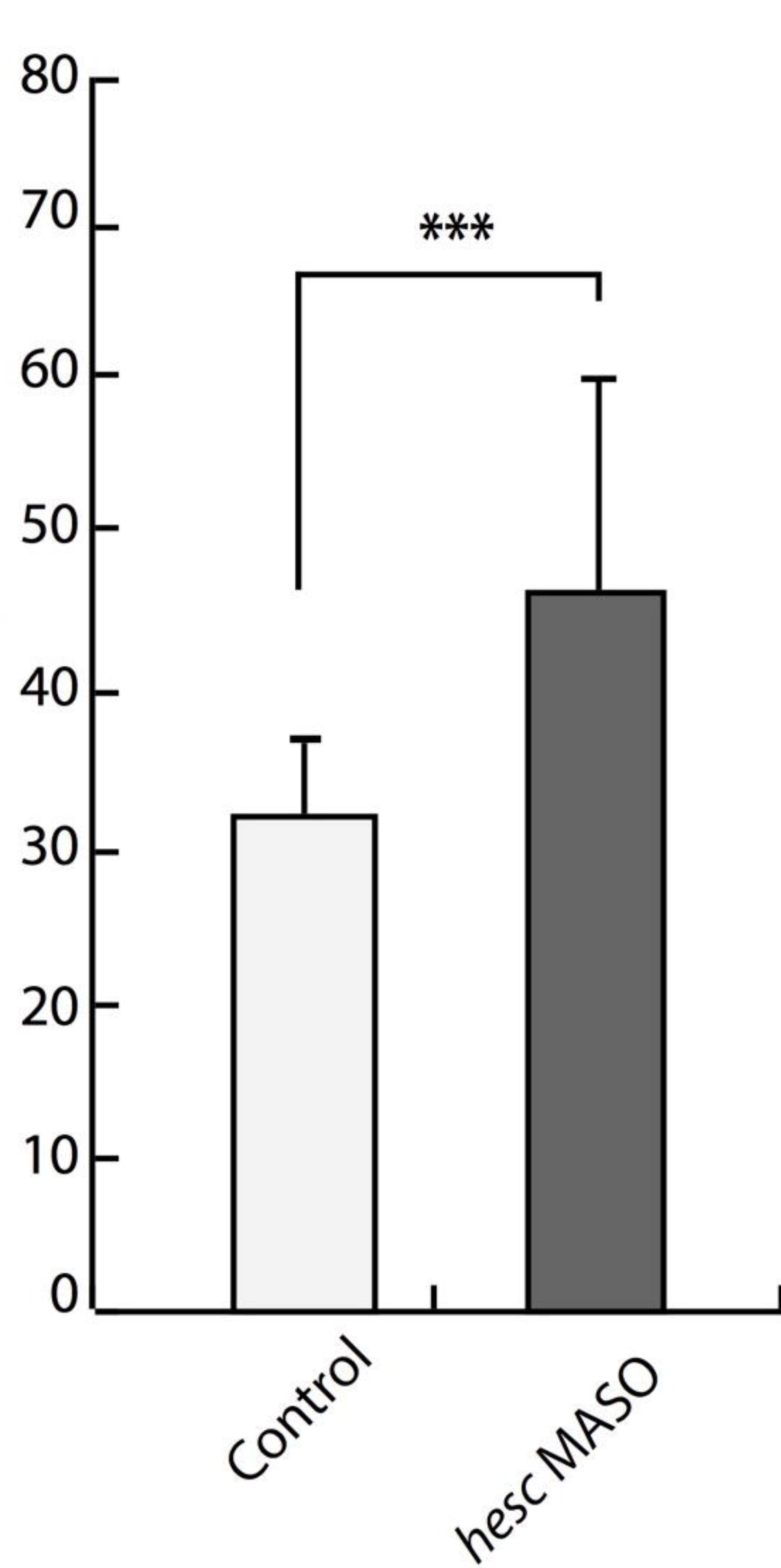
bioRxiv preprint doi: <https://doi.org/10.1101/044149>; this version posted March 16, 2016. The copyright holder for this preprint (which was not certified by peer review) is the author/funder, who has granted bioRxiv a license to display the preprint in perpetuity. It is made available under aCC-BY-NC-ND 4.0 International license.

**A** Pigment cell counts

Control	<i>hesc</i> MASO
30	61
20	24
28	65
38	38
38	69
20	50
26	52
35	40
36	42
29	49
26	72
30	48
38	46
35	27
40	29
36	44
38	36

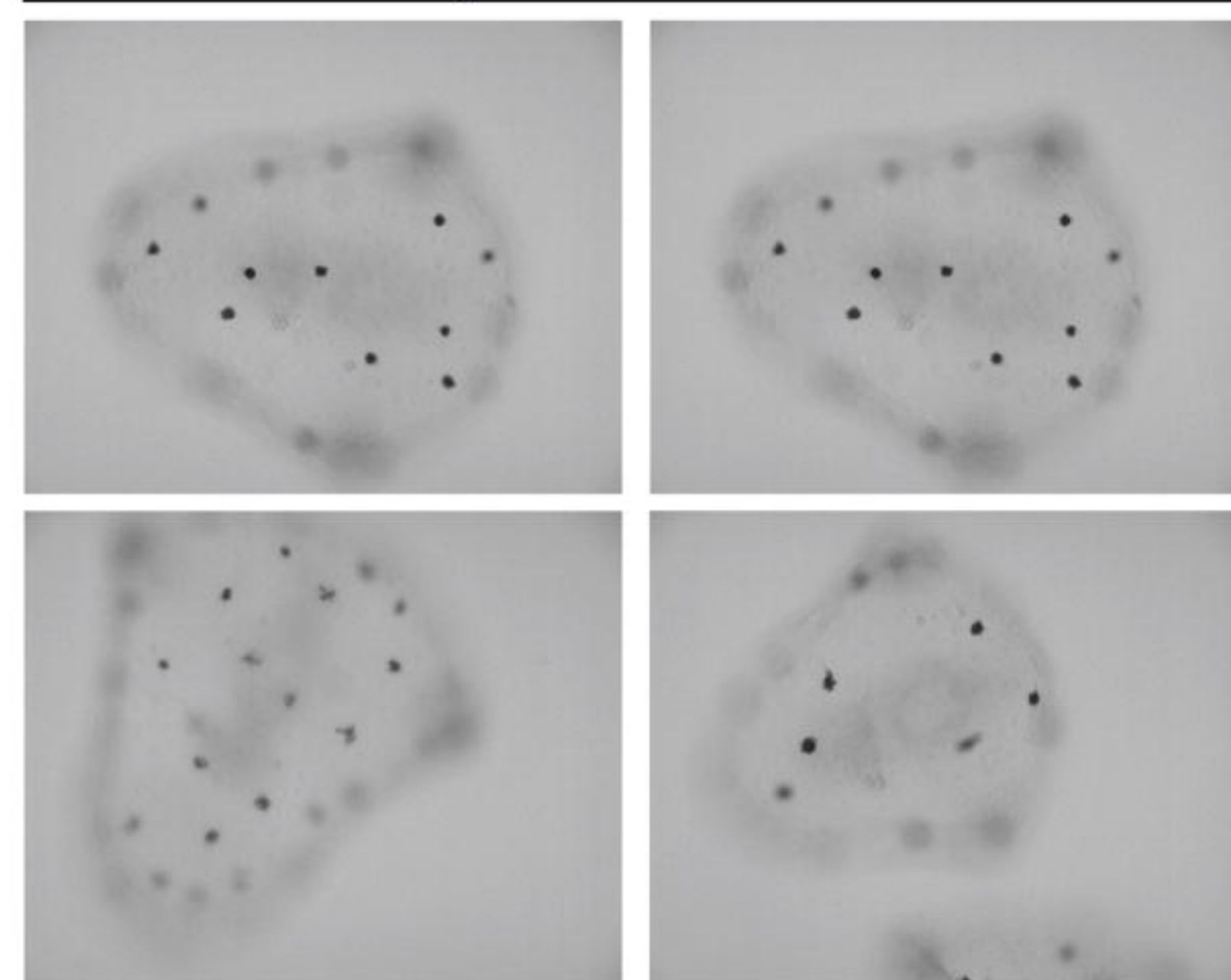
**B**

Number of pigment cells



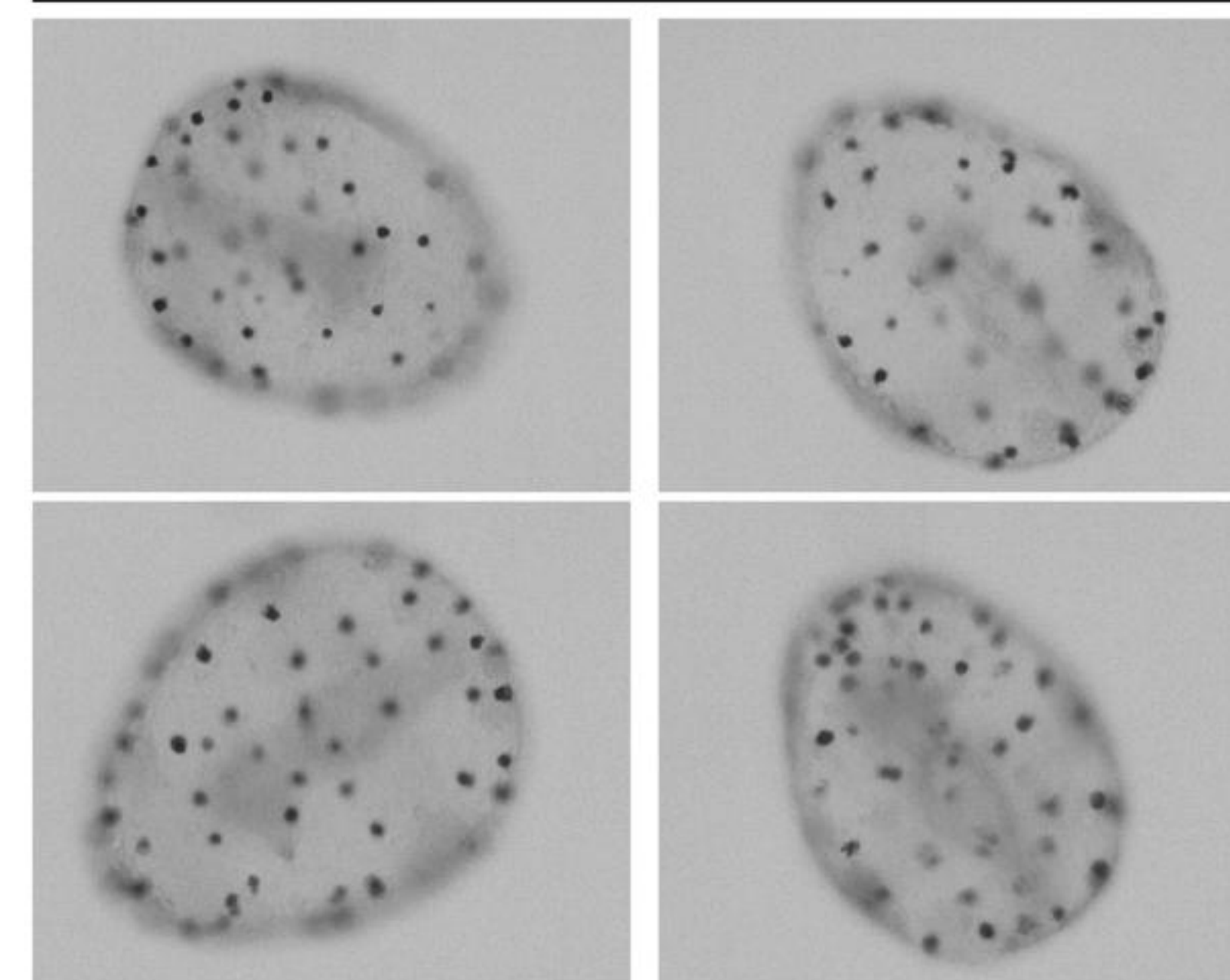
**C**

Uninjected control



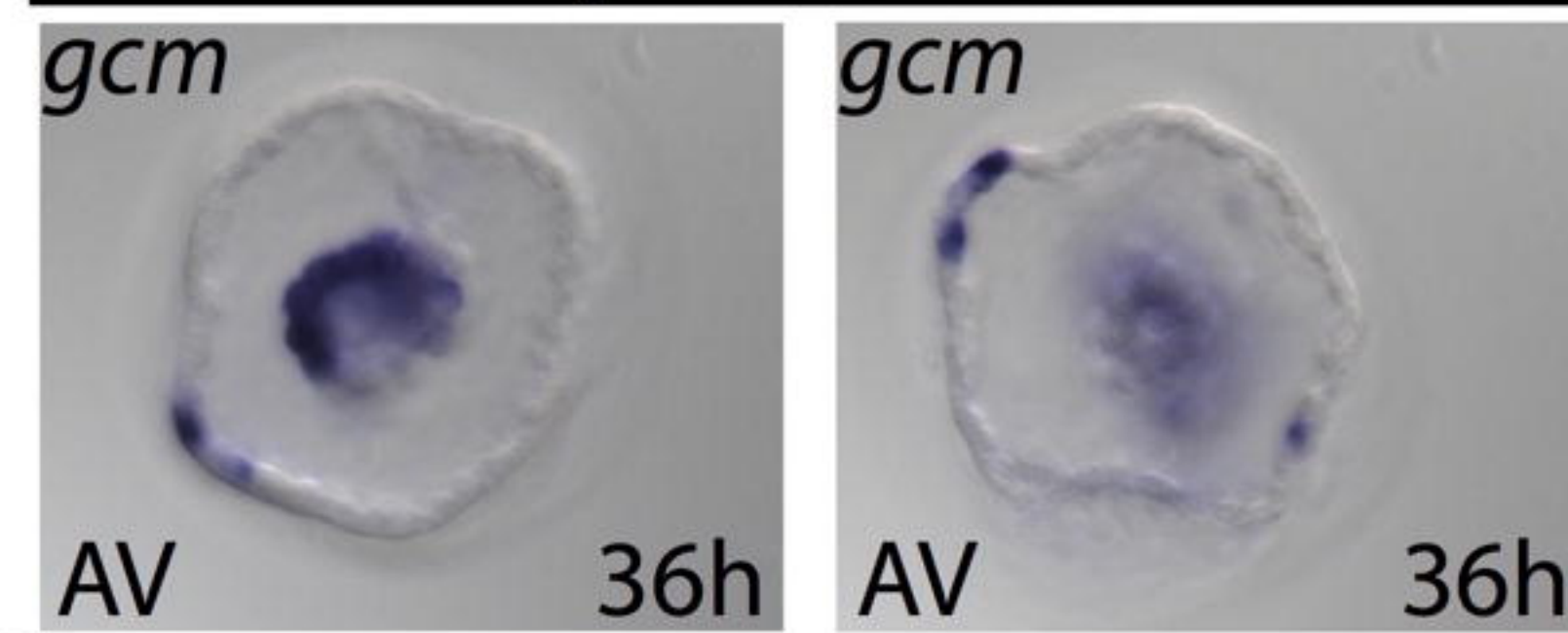
**D**

*hesc* MASO



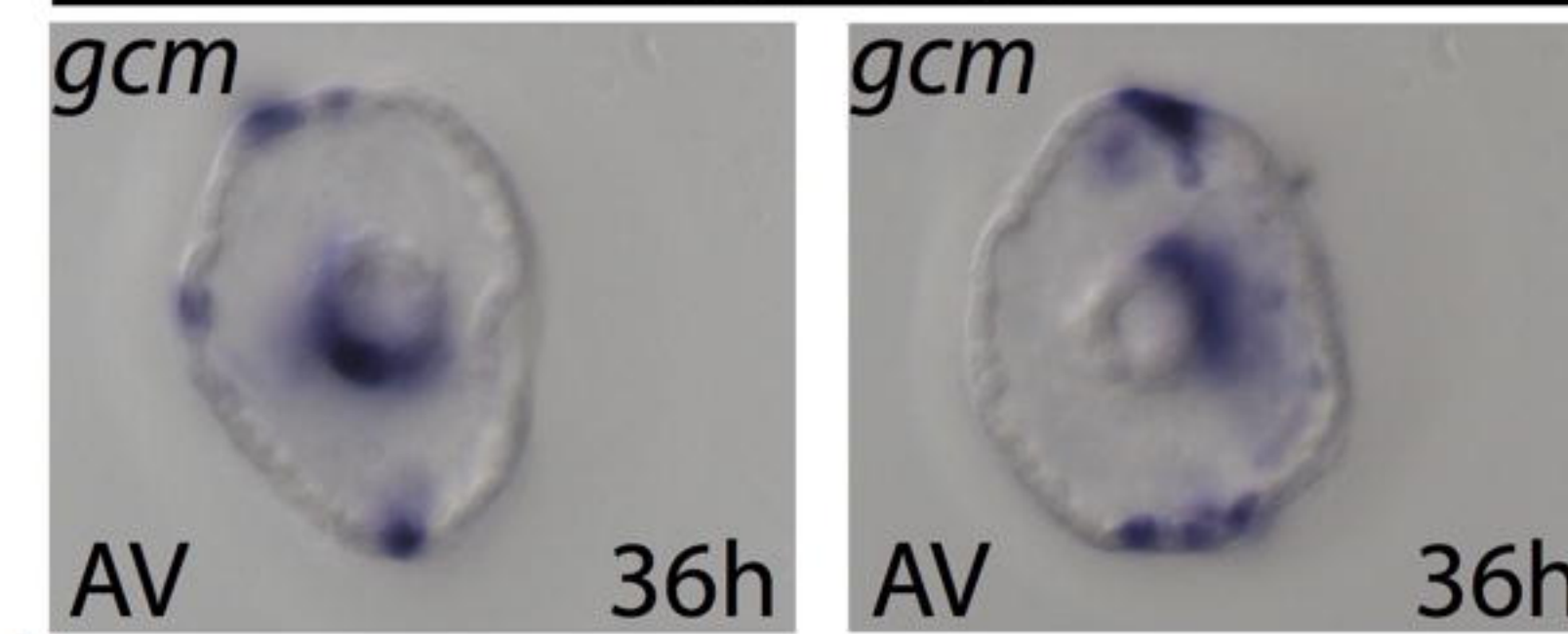
**E**

Uninjected control



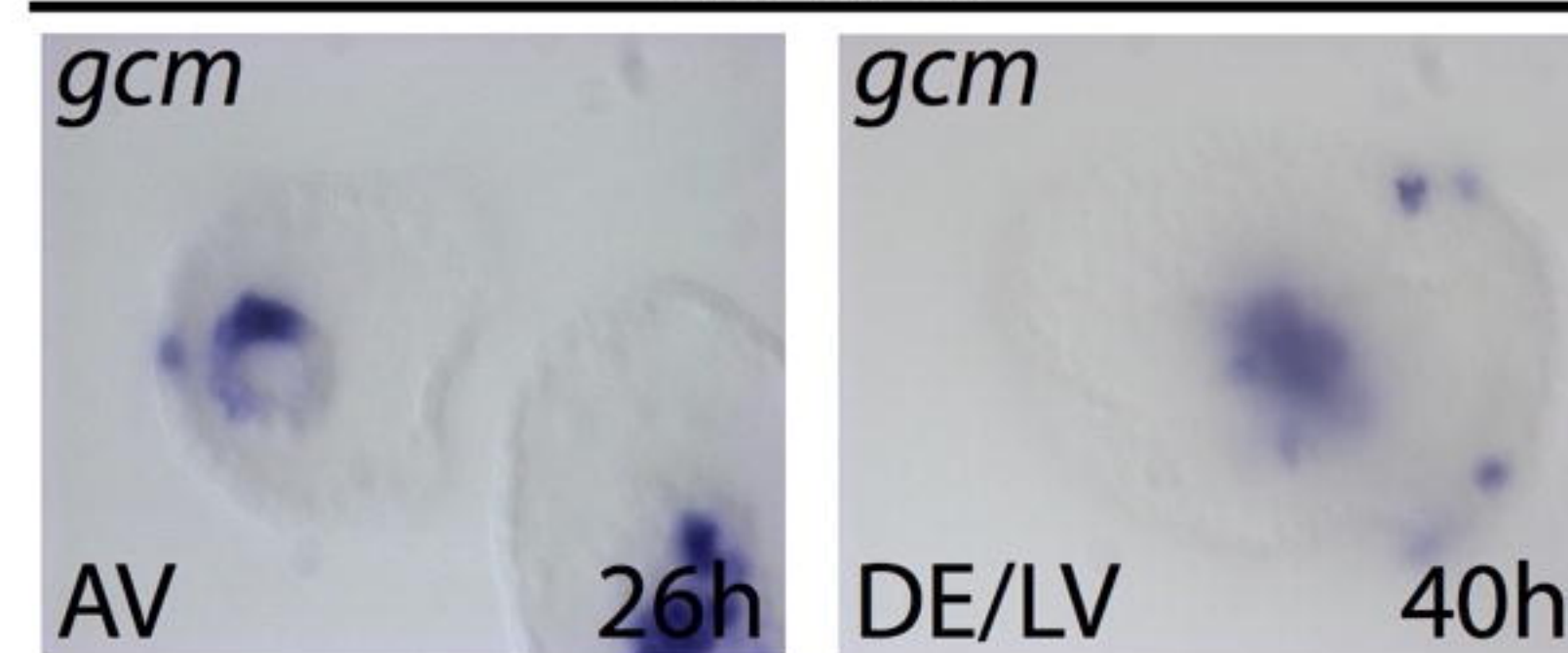
**F**

*hesc* MASO



**G**

Control



**H**

15  $\mu$ M DAPT

